SHRP-H-375

Development and Testing of a Seismic Pavement Analyzer

Soheil Nazarian
Mark R. Baker
Kevin Crain

Center for Geotechnical and
Highway Materials Research
The University of Texas at El Paso
El Paso, Texas 79968

Strategic Highway Research Program
National Research Council
Washington, DC 1993

SHRP–H–375
ISBN 0-309-05753-1
Contract H-104B
Product No.: 3019

Program Manager: *Don M. Harriott*
Project Manager: *Brian Cox*
Program Area Secretary: *Francine A. Burgess*
Production Editor: *Lynn E. Stanton*

December 1993

key words:
flexible pavements
maintenance equipment
pavement maintenance
rigid pavements
wave propagation techniques

Strategic Highway Research Program
National Academy of Sciences
2101 Constitution Avenue N.W.
Washington, DC 20418

(202) 334-3774

1.5M/NAP/1293

Acknowledgments

The research described herein was supported by the Strategic Highway Research Program (SHRP). SHRP is a unit of the National Research Council that was authorized by Section 128 of the Surface Transportation and Uniform Relocation Assistance Act of 1987.

This report results from the hard work of many individuals. Deren Yuan was one of the major researchers of this project. Olson Engineering, Inc., Dr. Richard D. Woods of the University of Michigan, and Dynatest, Inc. consulted on the project.

Throughout this project, Dr. Roger Smith of the Texas Transportation Institute was the primary consultant on pavement maintenance. Without his assistance the project could not have been completed as smoothly as it was. Bob Briggs of the Texas Department of Transportation dedicated much free time to this project.

The SHRP staff assisted in many ways. Brian Cox was the project manager, and Don Harriott and Shashikant Shah were always available for advice. The Expert Task Group offered valuable insight, continuously reminding us of the needs of a typical maintenance engineer. Mike Markow and Ken Maser were the technical consultants to SHRP. Mike Markow, with his critical views of the definitions and levels of pavement maintenance, kept the project focused. Ken Maser was a contributor to our success with his sound advice and participation in many constructive discussions.

Mari Carrillo, Cindy Edgar, Jessica Gough, and Srinavas Nori assisted in completing reports throughout this project.

Contents

List of Figures

List of Tables

Abstract

The Seismic Pavement Analyzer (SPA) is an instrument designed and constructed to monitor conditions associated with pavement deterioration. It measures such conditions as voids or loss of support under a rigid pavement, moisture infiltration in asphalt concrete pavement, fine cracking in pavements, delamination of overlays, and aging of asphalt.

The SPA detects these pavement conditions by estimating Young's and shear moduli in the pavement, base, and subgrade from the following wave propagation measurements:

1. Impact Echo;
2. Impulse Response;
3. Spectral Analysis of Surface Waves;
4. Ultrasonic Surface Wave;
5. Ultrasonic Body Wave Velocity.

The SPA records the pavement response produced by high- and low-frequency pneumatic hammers on five accelerometers and three geophones. A computer controls data acquisition, instrument control, and interpretation; measurements and interpretations are reported in both screen and database formats.

This report briefly describes the device and summarizes the usefulness of the equipment in maintenance activities. The operation of the SPA to determine different types of distress precursors is briefly illustrated. Finally, this document discusses results from several field tests. The specifications and design of different components of the device and a manual of operation are presented in a companion report.

The tests conducted during this project produced very promising results. The device was simple to use, and results were reliable and repeatable. The SPA can be commercialized with minimal hardware and software modifications.

Executive Summary

This document describes the construction of a new project-level measurement device called the Seismic Pavement Analyzer (SPA). The equipment has been designed and built to meet the needs of a pavement and maintenance engineer. The SPA is an effective tool for determining pavement distress precursors in early stages.

Five distress precursors are considered:

1. Moisture in the base layer (flexible pavement);
2. Voids or loss of support under joints (rigid pavement);
3. Overlay delamination;
4. Fine cracking; and
5. Pavement aging.

To diagnose the specified distress precursors effectively, an equivalent number of independent pavement parameters is required. This large number of parameters is measured with equipment similar to a falling weight deflectometer, but using more sophisticated computer processing and interpretation algorithms.

The potential savings to be realized are tremendous. First, having detected and measured a precursor of distress, a highway agency can resolve potential problems with preventive maintenance at a fraction of the cost of traditional maintenance or rehabilitation processes. Second, the device will enable the maintenance engineer to distinguish between maintainable sections and those that require rehabilitation. Therefore, the available maintenance funds can be directed toward maintainable projects. Third, the device can determine the effectiveness of a certain maintenance activity.

The equipment can perform several functions:

1. Analyzing in greater detail pavement conditions identified in the network-level surveys;
2. Diagnosing specific distress precursors to aid in selecting the maintenance treatment; and
3. Monitoring pavement conditions after maintenance to determine the treatment's effectiveness.

The system has been automated to make its operation quite simple. Most of the data reduction is done rapidly in the field, and the results are saved in a data base for later analysis. An on-demand graphical representation of the data collected in the field enables the engineer to identify troublesome areas within seconds of collecting the data. Finally, the diagnostic software can present the diagnosis of pavement conditions in literal pavement terms, as opposed to technical engineering terms (such as stiffness parameters).

The device has several advantages. The SPA is highly accurate in determining the present condition of the pavement. It uses methodology based on a sound theoretical background. The field testing and data reduction methodologies are compatible with the theoretical assumptions. The hardware associated with the device is relatively inexpensive. Further upgrade of the device should be inexpensive, because generally only the software will need to be updated and replaced.

The operating principle of the SPA is based on generating and detecting stress waves in a layered medium. Five testing techniques are combined. Each test and its areas of strength are summarized in table ES.1. The design and construction of the SPA are based on two general principles. First, the strength of each method should be fully utilized; and second, testing should provide enough redundancy to identify each layer that will potentially contribute to the distress of the pavement.

The major project deliverable is a prototype of the SPA. The device has travelled more than 8,000 km and has performed more than 1500 tests: it is rugged and field-worthy. So far, only minor problems have been encountered and maintaining the device has been quite simple and inexpensive. The software, which is the heart of the equipment, has been continuously improved. At this time, all components of the software relating to the operation of the device, data reduction, and data presentation perform in a satisfactory manner.
A conceptual design was developed to ensure the device's suitability for maintenance activities. Specifications were established for how precisely the test parameters must be

measured to obtain data that will be useful for detecting precursors of distress. In all cases, the SPA measures parameters at levels two to four times better than specified.

Table ES.1 - Strengths of five testing techniques used by Seismic Pavement Analyzer

Testing Technique	Strengths
Ultrasonic Body Wave	Young's Modulus of top paving layer
Ultrasonic Surface Wave	Shear modulus of top paving layer
Impulse Response	Modulus of subgrade reaction of foundation layers
Spectral Analysis of Surface Waves	Modulus of each layer Thickness of each layer Variation in modulus within each layer
Impact Echo	Thickness of paving layer or depth to delaminated layer

To determine the accuracy of the device extensive tests were conducted at a facility constructed specifically for this purpose at The University of Texas at El Paso. These tests showed that the SPA can predict known defects with reasonable accuracy.

To test the overall performance of the device under actual field conditions, seven sites were tested in two states (Texas and Georgia). Based upon these case studies, the SPA is very promising: it identified the existence of most distress precursors. However, more extensive field studies under more controlled conditions and over longer time periods are necessary to fully understand the limitations of the SPA.

Based on this three-year study it can be concluded that the SPA is a viable device for maintenance measurement. Specifically, the researchers determined that

1. in all cases, the precision and accuracy of the SPA exceeds the specified limits necessary for an effective maintenance tool;
2. the hardware is quite rugged and field-worthy;
3. the software is robust and user-friendly; and
4. in most cases, the field conditions corroborate the predicted distress precursors.

Most of the objectives of the project have been achieved. However, several aspects of the project need further work. The SPA must be used in a wide range of sites and environmental conditions to establish its limitations. These tests should be accompanied with an extensive field-testing program to ensure that the ground-truth is well known. In addition, the equipment of the next prototype should be packaged in a more rugged manner to protect different components from the elements and from road wear and tear. With minor revisions to the software and hardware, the device should be ready for commercialization in the near future.

The seismic pavement analyzer can be used effectively to enhance the results of many Strategic Highway Research Program and Federal Highway Administration (FHWA) projects. The SPA generates information about the pavement layers that describes them more completely and more accurately than any other nondestructive testing device. In the immediate future, many Long Term Pavement Performance (LTPP) projects can use the equipment for better diagnosis and more effective evaluation. In the near future the device can also be used for quality control during construction. Ultimately, the SPA can contribute to many other aspects of pavement engineering, such as design.

1

Introduction

Problem Statement

In recent years, the focus of pavement engineering has shifted from design and construction of new highways to preventive maintenance and rehabilitation of the existing highways. A highway maintenance program is usually based on a visual condition survey and, to a lesser extent, on appropriate in situ tests. By the time symptoms of deterioration are visible, major rehabilitation or reconstruction is often required. If the onset of deterioration can be measured accurately in the early stages, the problem can often be resolved or stabilized through preventive maintenance.

Strategic Highway Research Program has identified six broad elements that cause and contribute to pavement deterioration (Maser and Markow, 1990):

1. Pavement moisture;
2. Fine cracking;
3. Subsurface problems or discontinuities;
4. Voids or loss of support under rigid pavements;
5. Overlay delamination; and
6. Asphalt aging.

The University of Texas at El Paso (UTEP) and its consultants have developed a relatively inexpensive (as compared with most nondestructive testing devices) and precise device for

project-level measurements. This device, the Seismic Pavement Analyzer (SPA), will detect all the items above, except for subsurface problems and discontinuities and the potential for stripping in the asphalt concrete layer.

Objectives

The main objective of this project was to develop an inexpensive and precise device for project-level studies of maintenance needs. The specific objectives of the project were

1. to evaluate proposed pavement-measurement technologies in terms of their ability to determine

    a. if or where maintenance is needed (before maintenance activity)
    b. if the problem has been effectively remedied (after maintenance activity)

2. to develop, fabricate, and test prototype equipment to achieve the goals of the first objective

Four major features were determined necessary for effective maintenance measurements. First, the device should be sensitive enough to measure a contributing factor to a potential distress "soon enough." Second, the measurements should be accurate and comprehensive enough to identify the layer contributing to a potential distress. Third, the device should be precise enough to verify the effectiveness of maintenance processes. Finally, the device should be sophisticated enough to differentiate between a rehabilitation activity and a maintenance activity.

The SPA is a trailer-mounted nondestructive testing device. Its operating principle is based on generating and detecting stress waves in a layered medium. Several seismic testing techniques are combined:

1. Ultrasonic Body Wave;
2. Ultrasonic Surface Wave;
3. Impulse Response;
4. Spectral Analysis of Surface Waves (SASW); and
5. Impact Echo.

The design and construction of the SPA are based on two general principles. First, the area of strength of each of the five testing methods should be fully utilized. Second, testing

should provide enough redundancy to identify each layer that will potentially contribute to the distress of the pavement.

Report Organization

This report contains four major sections. The first section, Chapters 2 and 3, introduces the pavement conditions to be addressed and the measurements necessary to quantify these conditions. The second section, Chapter 4, addresses the conceptual approach to detecting the pavement conditions described in the previous sections. Chapters 5 and 6 detail the design of mechanical, electronic, and software components as well as practical aspects of each measurement technique. Finally, several case studies demonstrate the applicability and the limitations of the SPA. The report ends with a summary containing conclusions and recommendations for future developments.

2

Description of Pavement Conditions and Maintenance Activities

The maintenance activities discussed here are those that correct a localized area of deterioration, preserve the existing pavement, and reduce the rate of deterioration (e.g., corrective and preventive maintenance). Treatments that fall within this category of maintenance are included in table 2.1. In general, these treatments do not increase the structural or traffic-handling capacity of the roadway.

Table 2.1 - Treatments that are considered maintenance

Asphaltic-Concrete Roads	Portland-Cement Concrete Roads
Patching	Patching
Crack Sealing or Filling	Joint Repair
Surface Sealing (all types)	Crack and Joint Sealing
	Undersealing

Each of these activities addresses specific problems in the pavement structure. To determine when to apply a maintenance treatment and which treatment is appropriate, the maintenance engineer tries to answer several questions. Does this section of pavement need a treatment now? If not, will it need one in the near future (less than three years)? Is the problem localized, or does it cover a large area? Which treatment should be applied? Is the treatment cost effective?

This chapter considers each pavement condition, the basic life-extension treatment, and the methods the maintenance engineer normally uses to determine whether and when to apply such treatments.

Pavement Conditions

Moisture in the Foundation

The types of distress caused by moisture-related problems in the foundation layers (in advanced stages) are summarized by Carpenter, et al. (1981). Typically, the softening of one or more of the foundation layers and the degradation of material quality in terms of stiffness and strength are the initial manifestations of excess moisture within the pavement system. Field studies (Cedergren, 1974) have shown that wheel loads on saturated sections are many times more damaging than those on dry sections.

Moisture under Joints

The deterioration of foundation layers exposed to moisture in a rigid pavement is similar to that in a flexible pavement. The types of moisture-related distress to be expected in rigid pavements are also summarized by Carpenter, et al. (1981). Erodible foundation materials under a slab will deteriorate when subjected to load. The existence of moisture significantly increases the rate of deterioration. In this case, the foundation layer will either become softer or a void will develop under the concrete slab. Slab curling (bending or warping) will contribute to the deterioration.

Voids or Loss of Support

The presence of voids or loss of support underneath a slab is detrimental because as stress increases the fatigue life of the pavement decreases, and there may be faulting of joints. Important factors in this process are discussed by Torres and McCullough (1983). The

larger the void or the thinner the slab, the lower the support and the shorter the life of the pavement.

Overlay Delamination

The process and significance of overlay delamination is well known. The degree of interfacial bonding influences the state of stress within the overlay. Interfacial bonding has been identified as the most significant factor affecting overlay performance (Ameri-Gaznon and Little, 1988). When delaminated, the overlay acts independently of the rest of the pavement system, allowing excessive movement at the bottom of the overlay relative to the top, where the wheel load is in contact with the pavement. As a result, large tensile strains develop at the bottom of the overlay.

Fine Cracking

Cracks often begin as hairline cracks that allow little water into the structure. Although they are a discontinuity in the pavement structure, they are not generally a problem until they become wide enough to allow water to enter into the structure. If allowed to deteriorate, they become wider and develop spalling at the surface, allowing much more water to enter. Furthermore, the intrusion of an incompressible during a cold period creates high compressive forces on the crack or joint face during warmer periods, creating spalling. The cracks may also contribute to the aging process of asphalt on the crack face, accelerating crack deterioration.

Pavement Aging

The aging process in the field is complex. Several independent investigations (Tia et al.; 1988; Von Quintus et al., 1991; Goodrich, 1988) indicate that the modulus of the asphalt increases with time (aging). Aging should be considered in two stages, short-term and long-term (Bell, 1989). Short-term aging occurs during construction, while the mix is hot. Such aging is mainly due to a loss of volatile components in the asphalt. Long-term aging occurs after the mixture is in place, and is primarily attributed to progressive oxidation of the material in the field.

Maintenance Activities

Patching

Patching is the repair of localized areas of low strength or other types of deterioration. Patching can address every possible type of deterioration, if the damage is localized. Such distress can occur in any pavement layer, leading to a localized failure observable on the surface. Loss of strength can be caused by a change in the material properties or localized differences in construction and original materials. It can also be due to loss of support caused by erosion or degradation of supporting layers.

Maintenance engineers generally do not test to determine if patching is required. They simply begin applying patches when the deterioration affects the pavement surface to the point that driving becomes hazardous. The key question that a maintenance engineer needs to address in testing is whether patching will effectively resolve the problem. If the problem is widespread, a comprehensive rehabilitation treatment will be more cost effective than patching.

Crack and Joint Sealing

Many of the materials used in pavement construction have moisture-sensitive stiffness. As the moisture content of unbound granular materials and soils increases, their stiffness decreases. Moisture leads to the degradation of asphalt concrete due to stripping, aging, weathering, and raveling. Free water under portland cement slabs can develop very high pressures, eroding the base and subbase materials, or leading to loss of support. Crack and joint sealing to reduce the influx of moisture from the surface into the pavement structure.

The maintenance engineer will generally use the observable condition of the crack and joints to determine if crack and joint sealing is appropriate. Many maintenance engineers will not seal a crack until it is greater than 5 mm wide. If the amount of weakening resulting from moisture at the joints and cracks could be determined, that information could help determine when crack and joint sealing is needed to reduce the infiltration of moisture.

Surface Seals

Surface seals generally extend the life of pavements by improving the surface friction of the pavement, by reducing weathering and raveling, or by reducing the infiltration of moisture

into the pavement structure. Surface friction is not considered in this project; weathering and raveling are basically the result of asphalt concrete aging.

The maintenance engineer normally looks for signs of weathering and raveling or for the presence of a network of fine cracks that can be sealed with the surface seal. If the presence and level of aging could be determined, the degradation of asphalt because of aging could be prevented or reduced. If the degradation of paving materials because of abnormal moisture levels in the asphalt and supporting layers or fine cracking could be determined, the need to place a seal to reduce infiltration of water into the structure could be evaluated.

Undersealing

Undersealing is the process of filling voids under portland cement concrete pavements with a grout of cementatious material in order to reestablish support under the slab. The movement and loss of fine-grained materials creates voids, normally on the leave side of the joint or crack. This leads to faulting of the joint or crack. The loss of support also increases the stress in the portland cement concrete pavement near the corners, leading to corner breaks.

In some cases, the base material is degraded but not ejected. This can create a thin layer of very soft material under the joint. A loss of support is then present without a true void. In such a case, undersealing generally cannot displace the deteriorated materials sufficiently to reestablish full support.

The maintenance engineer normally looks for the presence of pumping, faulting, and corner breaks to determine that voids are present and to determine if undersealing is appropriate. In some instances, nondestructive testing devices (such as falling weight deflectometer and Dynaflect) or manual methods (such as dropping a BB) are used for this task. Measurements to determine the loss of support, the presence of voids, and the size of voids are needed to determine if voids are developing and if undersealing should be considered to reestablish support.

3

Developing Specifications for Measurement

It is extremely important to measure the precursors of distress in the early stages. Below a certain measurement level, a change in the distress-triggering parameters results in insignificant changes in the condition or serviceability of the pavement. However, if the precursors of distress are identified "too late," reconstruction or rehabilitation may be more appropriate. This section will discuss the characteristics and quantities of changes in pavement parameters that signal the early stages of distress.

The remaining life of a pavement is controlled by the complex interaction of several factors such as traffic, pavement structure, drainage, road geometry, climate, and economy. In recent years several algorithms have been developed to predict the type and rate of deterioration and to suggest alternative maintenance strategies at appropriate time intervals. A good example is the Texas Flexible Pavement System (TFPS) (Uzan and Smith, 1988 and Rhode et al., 1990). In ideal conditions, one can adhere to these "theoretical" maintenance schedules. Often, however, pavements experience distress prematurely or maintenance activities are ineffective. This document suggests a process to define the levels of accuracy and precision required for maintenance-measuring equipment.

Moisture in Foundation Layers (Asphalt-Concrete Pavements)

Cracking and moisture in the foundation are considered together because of the strong interaction that exists between them. The paving layer of a new pavement is usually impervious, and cracks are scarce or nonexistent. In this stage, most of the damage to the

pavement is the result of traffic or environment, and moisture infiltrates either from the shoulders or from the water table. As soon as cracks develop, moisture may penetrate from the surface. If the surface layer is primarily a wearing course and the majority of the structure is in the base, the infiltration of moisture and the existence of cracks are not of great concern so long as the base and subgrade materials do not lose their integrity because of exposure to moisture.

Factors that should be considered (excluding political and economic factors) are the climatic parameters (such as the amount and seasonal distribution of rainfall), the drainage properties of the base and subgrade materials, the structural properties of the asphalt concrete, base, subgrade, and their seasonal variations, and the nature and seasonal distribution of traffic (Markow, 1982). TFPS considers the effects and interactions of these parameters in a comprehensive fashion. The amount and seasonal distribution of the rainfall are modeled from the historical data from each county in the State of Texas. Based upon these climatic models, the properties of each layer are regularly modified and updated.

The parameters that are considered include moisture, temperature, and distress type. The TFPS program does not consider the transient and dynamic nature of change in moisture or modulus with time. Considering the most basic principles of geotechnical engineering, the transient and dynamic nature of change in moisture is of little practical use in predicting maintenance life. A material that becomes saturated and unsaturated over a short time period is a well-drained material and has high permeability. The strength and stiffness of such a material (and as a result, the remaining life of a pavement constructed with or over such a material) is not significantly affected by change in moisture. On the other hand, in a material that does not exhibit large fluctuation in moisture over short periods (i.e., a material with low permeability), the change in equilibrium base moisture may significantly affect its modulus and remaining life.

A shortcoming of TFPS, as applied to maintenance problems, is that it does not model the accumulation of damage resulting from change in equilibrium base moisture or modulus. The simple process used to model the accumulation of damage with time is described below.

Conceptual Approach

A conceptual model depicting the variation in cracking with traffic is shown in figure 3.1. Depending on the severity of cracks, four levels of maintenance or rehabilitation activities are indicated. Within Level 1, the pavement is in satisfactory condition and no maintenance is needed other than occasional localized maintenance. In Level 2, the pavement section

needs preventive maintenance (i.e., surface sealing and crack sealing). In the more severe Level 3, overall maintenance or rehabilitation activity should be undertaken (i.e., thin overlay or localized repair with surface sealing). Finally, in Level 4, the pavement has to be completely rehabilitated or reconstructed.

Assuming that all measurements are made when the pavement is in the "no maintenance" level, the goal is to predict if and when the pavement will approach Levels 2, 3, or 4. Therefore, relatively long-term behavior of the pavement has to be predicted.

Computer models such as TFPS consider the long-term effects of seasonal variation of modulus and moisture content on the propagation of cracks. However, these models fail to consider the effects of reduction in moduli above and beyond those anticipated because of seasonal variations. Markow (1982) has developed models that fully consider the interaction of such parameters. However, such models require many assumptions describing the interrelation between different values. We approached the problem from a different angle.

Shown in figure 3.2 are the relationships between cracking and the number of equivalent single axle loads (ESAL) for two different moduli (M_1 and M_2) of base. Assume that at a given number of ESAL, n_1, the modulus decreases from M_1 to M_2. As indicated before, n_1 is located in the "no maintenance" zone of figure 3.1. From point n_1 on, the remaining life curve will follow a conceptual curve M_{21}. The TFPS cannot develop this curve. However, the upper and lower bounds can be reasonably defined. First, it is intuitive that the curve has to be bound between the M_1 and M_2 curves. Secondly, the slope of the curve at any given time should be bound between the slope of curves M_{2U} and M_{2L}. Curve M_{2U} is determined by a linear transformation of curve M_2 in the y-direction equal to ΔM $[M_2(n_1)-M_1(n_1)]$. This implies that the progression of distress is more heavily influenced by time (traffic). Curve M_{2L} corresponds to a linear transformation of curve M_2 in the x-direction equal to Δn $(n'_1 - n_1)$, which indicates that the progress of distress is more heavily influenced by the extent of cracks. This procedure is adequate for small levels of distress (such as those used in this study); for extensive cracking, this model may yield erroneous results. We will assume that curve M_{21} is located halfway between curves M_{2U} and M_{2L}.

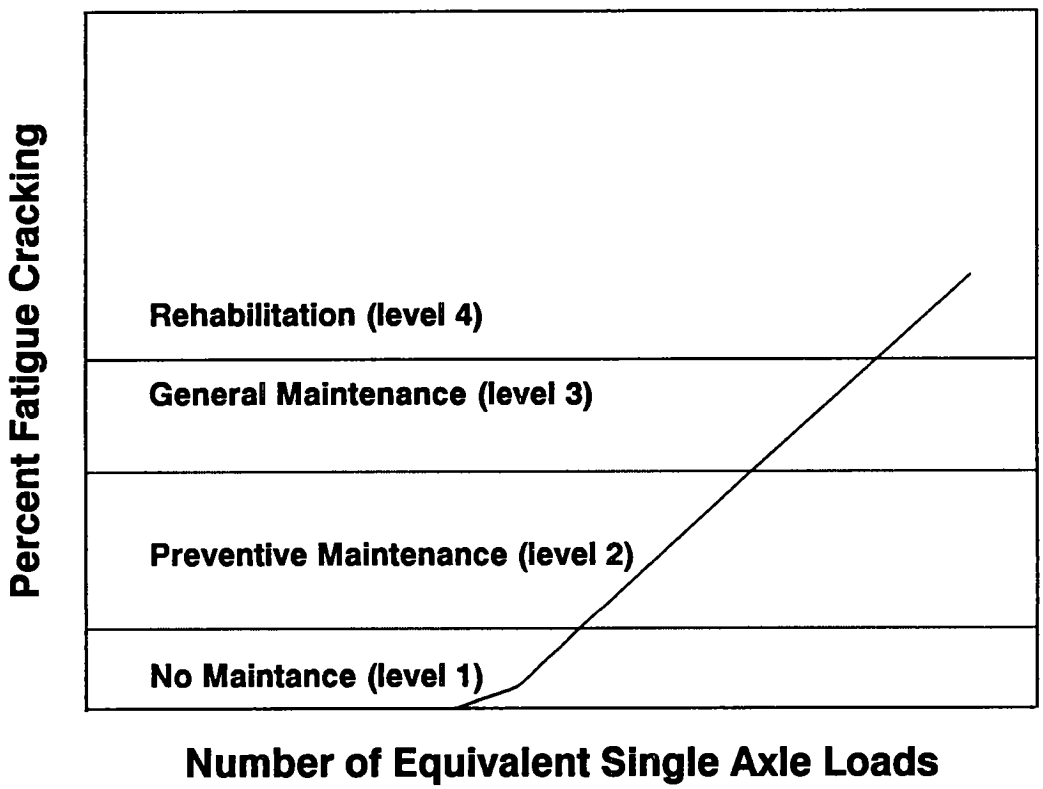

Figure 3.1 - Conceptual variation in distress with traffic

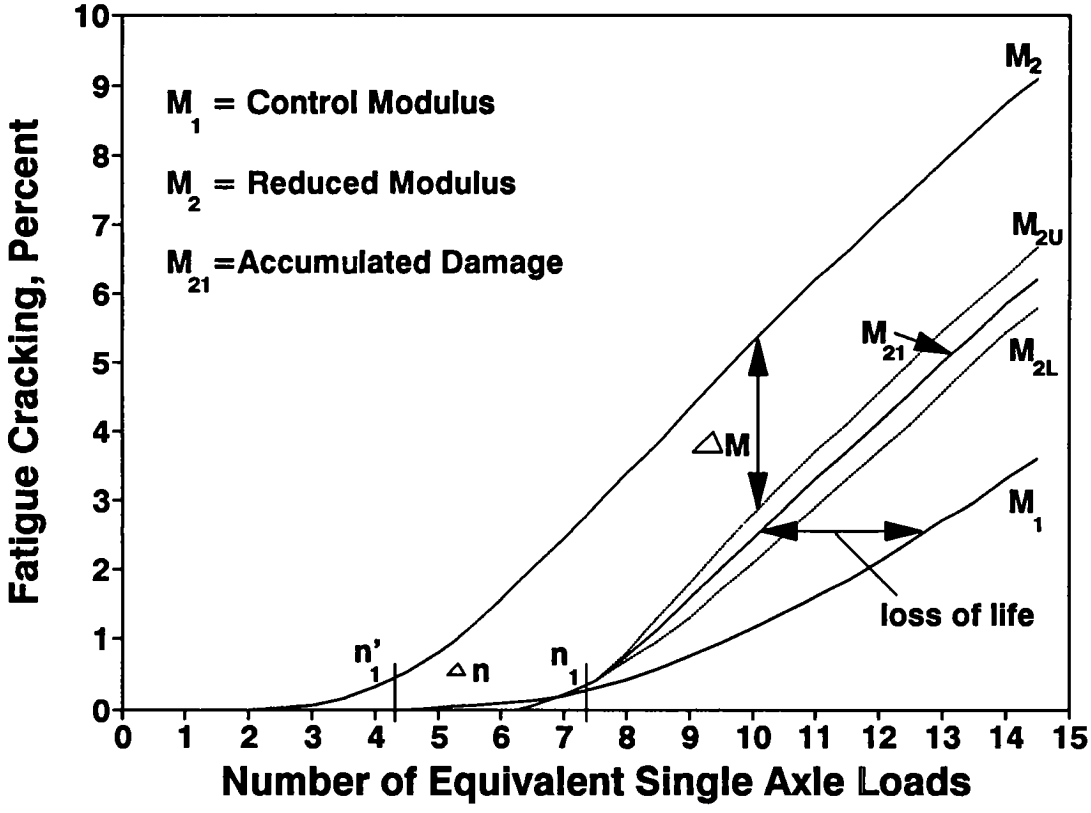

Figure 3.2 - Conceptual development of accumulative damage model for softened base layer

Two types of measurement should be considered—relative and absolute. In relative tests, the pavement is tested shortly after completion of the project and then periodically retested. Let us assume that at a given time, a reduction in modulus from M_1 to M_2 is detected. If the difference between curves M_1 and M_{21} (see figure 3.2) is not significant, one can conclude that the change in modulus from M_1 to M_2 is not of concern. With such a small variation in modulus, if the precursor of stress is not detected in a timely manner, the remaining life of pavement is only slightly affected. Conversely, if the change in modulus from M_1 to M_2 results in a large deviation between curves M_1 and M_{21}, maintenance has to be scheduled earlier. This is the preferred approach for monitoring new pavements. The same line of reasoning can also be used to determine the effectiveness of a maintenance activity. The only difference is that, significant increase in or stabilization of modulus values with time is of interest.

For absolute measurements, the pavement is tested at a given point for the first time. The only information available is probably the traffic history and the pavement structure. In this case, the information should be used to determine the appropriate level of integrity of the pavement. The disadvantage of this method is that a precise model may not be available.

Practical Approach

In this section, we attempt to establish the level of accuracy necessary for measuring moduli of base for maintenance purposes. The modulus of the base and its change with time can be measured with finite accuracy. Therefore, the change in the distress precursor below a certain level cannot be detected. We will investigate the impact that such a level will have on the remaining life of the pavement.

Given the conceptual approach described above, many qualitative levels have to be defined. In the following section, the upper limits of "no maintenance," "preventive maintenance," and "overall maintenance" (shown in figure 3.1) are arbitrarily set at 2 percent, 5 percent, and 20 percent. In practice, the maintenance engineer selects these levels based upon experience and the available budget.

The percent cracking in a typical pavement as a function of the number of ESAL, as determined by TFPS, is shown in figure 3.3. The pavement consists of 125 mm of AC layer with a modulus of 3.5 GPa (at 21°C), 300 mm of base with a modulus of 210 MPa, over a granular subgrade with a modulus of 70 MPa. This pavement section will be the control pavement in the rest of this section. The pavement is assumed to be in Beaumont, Texas, corresponding to a wet climate with a high water table. The 20-year traffic design was

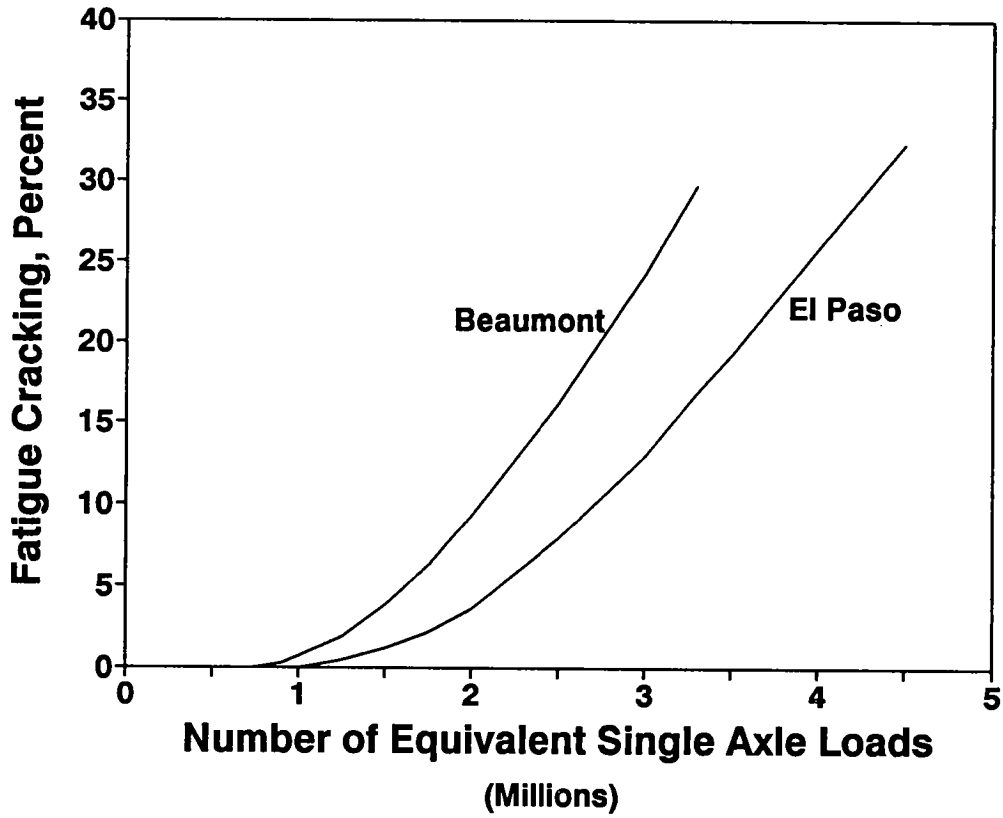

Figure 3.3 - Variation in fatigue cracking with traffic for a typical AC pavement

assumed to be 5 million ESAL. The same curve is shown for an identical pavement in an extremely different climatic condition: El Paso, Texas (water table over 100 m deep, average annual rainfall of 20 cm). The pavement in Beaumont experiences distress faster than that in El Paso. This can be attributed to damaging factors associated with the interaction between the extent of cracks and the level of precipitation. The traffic and pavement structure were identical for both climatic regions.

The variation in fatigue cracking as a function of the number of ESAL for the control section in Beaumont is shown again in figure 3.4. This figure also shows curves for cases in which the modulus of base is initially 10 to 50 percent less than the control section. Using the procedure depicted in figure 3.2, figure 3.4 can be modified to develop a damage curve for the modulus of base reduced by 10 to 40 percent due to a change in the equilibrium moisture at a given time. We arbitrarily and conservatively assume that the change in equilibrium moisture (and as a result the modulus) occurs as soon as the percent cracking of the control pavement section deviates from zero. This point is clearly marked on the figure. In practice, this is determined by regularly testing the pavement.

In the next step, the degree of change in the measured modulus is determined. The maintenance engineer must determine

1. Whether any type of maintenance will be necessary within the next three years.
2. Whether maintenance will be localized or overall.

Given an acceptable level of cracking before maintenance (differed maintenance) and the number of years from the date when measurements were carried out, the degree of change in the modulus of base is shown in table 3.1.

Table 3.1 - Degree of change in modulus necessary for detecting moisture in base

Acceptable Fatigue* Cracking (Percent)	Required Change in Base Modulus (Percent)		
	Year 1	Year 2	Year 3
5	>50	25	10
10	>50	45	30
15	>50	>50	42
20	>50	>50	>50

*Acceptable level of cracks resulting from differed maintenance. See text for explanation.

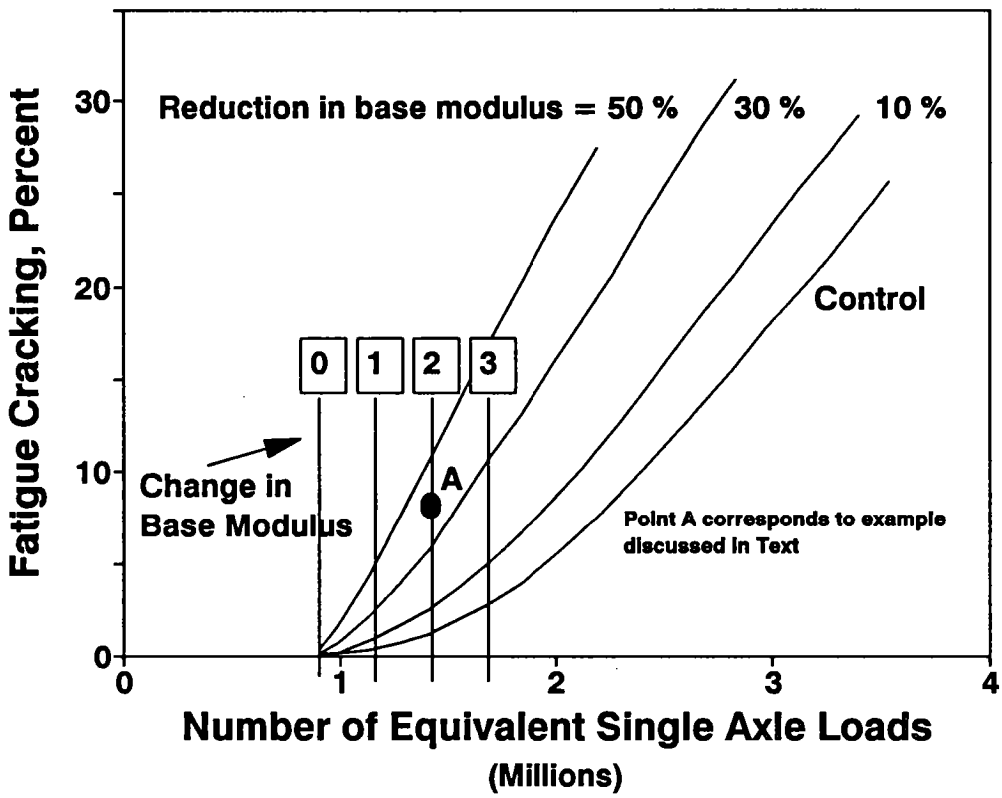

Figure 3.4 - Accumulative damage medel for a typical AC pavement with softened base layer

The acceptable level of cracking before maintenance requires further explanation. Every highway agency would prefer to maintain roads as soon as any distress is evident. Realistically, priorities for maintenance have to be based on financial constraints. Therefore, some roads will crack before they are maintained. The level of cracking that an agency can tolerate is called acceptable cracking. Acceptable cracking close to zero is desirable and should be selected if no budgetary constraints exist.

The values reported in table 3.1 are obtained from figure 3.4. Shown on the figure is the point when a reduction in modulus occurs. Also shown are three other vertical lines marked Year 1, Year 2, and Year 3. These three lines correspond to the three years of scheduling mentioned above. The values shown in table 3.1 are derived from the intersection of each of these time lines with the appropriate percent cracking. As an example, point A, corresponding to an acceptable level of cracking of 10 percent at year 2, is marked on figure 3.4. This value is roughly equal to 45 percent.

Practically speaking, precision better than 10 to 15 percent is sufficient for a typical pavement. It will be shown later that the SPA can achieve this accuracy. The same procedure was followed for the El Paso data, and the levels of accuracy shown above were achieved.

The advantage of this algorithm is that for each climatic region, for each acceptable level of maintenance, and for each economically feasible level of differed maintenance, the required level of measurement accuracy can be determined.

Void or Loss of Support (Portland Cement Concrete)

The mechanism involved in loss of support at the edge of a PCC pavement is experimentally described by Dempsey (1982) and is detailed theoretically by Raad (1982). The Laboratoire Central des Ponts et Chaussees (1979) recommend considering the interaction among traffic, climate, subbase materials, and joint load transfer. They presented these values in a three-dimensional space to provide a qualitative model for determining the interactive parameters that should be considered.

Based on this model, the critical parameter is the horizontal extent of loss of support. To utilize the damage model, the increase in tensile stresses was determined as a function of loss of support. These stresses were adapted from the work of Darter (1977), who utilized a finite element program to determine the tensile stresses as a function of the extent of loss of

support and the thermal gradient. In the next step, the fatigue life of the pavement was estimated. Smith, et al. (1990) suggest that the fatigue life, N, can be determined from

$$\log_{10} N = 2.13 \, (1 / SR)^{1.2} \tag{3.1}$$

Parameter SR is the stress ratio, defined as the ratio of the tensile stress measured to a 28-day modulus of rupture. Furthermore, they proposed that the percent cracking, P, as a function of traffic, n, can be conservatively determined from

$$P = 1 / \{ 0.01 + 0.03 * [20^{-\log (n/N)}] \} \tag{3.2}$$

Once again, the simplified damage accumulation methodology described above was used to develop deviation in behavior as a function of cracking. The levels of change in loss of support were again determined as reported in table 3.2.

Table 3.2 - Degree of change in voids necessary for detecting loss of support

Acceptable Cracking (Percent)	Required Change in Loss of Support (mm)		
	Year 1	Year 2	Year 3
5	600	300	150
10	>600	>600	600
15	>600	>600	>600
20	>600	>600	>600

Foundation Softening (Portland Cement Concrete)

Another possible precursor of distress in concrete slabs is the softening of the subgrade layer without voids actually developing. The same methodology used to model the loss of support was used to determine the increase in tensile stress as a function of reduction in the modulus of subgrade reaction. Based on this relationship, acceptable levels of accuracy were once again developed, as shown in table 3.3. In most cases a level of change higher than 30 to 40 percent is required.

Delamination of Overlays

In this case, actual damage is detected. Current maintenance activities are not appropriate for correcting these defects, unless the delamination occurs over a very limited area. Even then, only those areas that break loose are repaired with patching. Therefore, from a maintenance point of view, the value of detecting this type of distress precursor is limited. The primary concern is knowing the extent of delamination. If the delamination is extensive, the maintenance personnel will schedule rehabilitation rather than patching. This will assist the engineer in charge of maintenance to allocate funds more effectively.

Table 3.3 - Degree of change in subgrade modulus necessary for detecting foundation softening

Acceptable Cracking (Percent)	Required Change in Modulus of Subgrade (Percent)		
	Year 1	Year 2	Year 3
5	40	30	20
10	>40	>40	40
15	>40	>40	>40
20	>40	>40	>40

Fine Cracking

The reduction in the remaining life of the pavement as a function of the reduction in the effective stiffness of a cracked paving layer is of little concern. However, the fact that the cracks allow water to penetrate more readily into other layers and accelerate the rate of damage is quite important. This aspect of damage because of cracks was discussed in the previous section.

Aging of Asphalt Layer

As indicated before, the process of aging in the early stages is not well understood. Several research studies are analyzing this process.

4

Principles of Measurements

This chapter describes the measurement of distress precursors in particular pavement components, as summarized in table 4.1. The method of determining each distress precursor is described below.

Moisture in Base

The impulse-response method presumes that the paving material becomes less rigid (more flexible) as its water content increases. This is true for most paving materials, except concrete and some stabilized foundation layers. High flexibility of these materials indicates the need for maintenance.

Similarly, as the water content increases in the foundation layers, the materials become less stiff. By measuring the shear wave velocity profile of a given site using the Spectral Analysis of Surface Waves (SASW) method, one can determine the location and the amount of decrease in moduli of different layers in the pavement.

Fine Cracking

The impulse-response method presumes that a cracked section of pavement is less rigid than an intact one. The limitation of this method is that the crack has to propagate through the thickness of the paving layer.

Table 4.1 - Levels and nature of measurements for each distress precursor

Distress Precursor	Test	Quantity Measured	Pavement Component Evaluated
Moisture in Base	Impulse Response	Change in flexibility due to change in moisture content	Overall pavement system
	Spectral Analysis of Surface Waves (SASW)	Change in Young's modulus due to change in moisture content	Base, subbase and subgrade
Fine Cracking	Impulse Response	Reduction in rigidity of the paving layer due to cracks	Overall pavement system
	Body Wave Velocity	Delay in travel time of compressional wave because of longer travel path and lower rigidity	Paving layer
Voids or Loss of Support	Impulse Response	Significant increase in flexibility of slab due to lack of support under the slab	Supporting layer
	Impact Echo	Return (resonant frequency) associated with the thickness of slab	Upper layer (asphalt or concrete)

Table 4.1, cont. - Levels and nature of measurements for each distress precursor

Distress Precursor	Test	Quantity Measured	Pavement Component Evaluated
Overlay Delamination	Impulse Response	Significant increase in flexibility of overlay due to lack of support under the overlay	Overall pavement system
	Impact Echo	Return (resonant) frequency associated with the thickness of overlay	Overlay
Aging	Ultrasonic SASW	Shear wave velocity of AC layer	AC layer
	Body Wave Velocity	Poisson's ratio, by measuring compression wave Velocity of AC layer and combining with shear wave velocity	AC layer

The ultrasonic-body-wave method can determine the existence of cracks, even if they have not extended through the thickness of the layer. In this method, stress wave energy is generated at one point and detected at several other points. Any cracks in the material located between the source and the receiver will delay the direct propagation of waves and will reduce the amplitude associated with the arriving wave. Differentiation between a strong material containing cracks and a weak material is not possible at this time.

Voids or Loss of Support

A void beneath or within a slab results in increased flexibility of the slab. Therefore, measuring the flexibility of the slab at different locations using the impulse-response method can pinpoint the voids or loss of support.

The impact echo method distinguishes between overlay delamination and voids beneath or within the slab. The method, a special case of ultrasonic-body-wave propagation, can also determine the depth to the reflector.

Overlay Delamination

The impulse response and the impact echo are the prime methods for determining the location and existence of delamination. The theoretical and experimental aspects of using these two tests for detecting overlay delamination are identical to those used for locating voids and loss of support. The only differences are the nature and location of the interface. For delamination, the void occurs at the interface of two layers and the delaminated layer is located closer to surface.

Pavement Aging

An aging asphalt layer becomes stiffer and more brittle. By measuring shear wave velocity and Poisson's ratio, one can determine the effect of aging on the behavior of the asphalt layer. The shear modulus increases and Poisson's ratio decreases as the layer ages. The ultrasonic SASW method can determine the shear wave velocity of the asphalt layer. Direct compression wave propagation can determine the compression wave velocity. Knowing the shear and compression wave velocities, one can determine Poisson's ratio of the material. The methodology for characterizing aging has not been developed in this project. Two projects, Strategic Highway Research Program A-003 and Asphalt Aggregate Mixture Analysis System (Von Quintus, et al., 1991), are studying this phenomena.

5

Seismic Pavement Analyzer Overview

Effective measurement of pavement conditions that are precursors to distress requires measuring a large number of pavement properties. As the distress precursors identified in previous sections are not directly measurable physical properties, several physical property measurements must be made to diagnose the precursors.

This chapter gives an overview of these measurements and their interpretation for diagnosing distress precursors. Three subsequent sections deal with measurement procedures, data analysis techniques, and data interpretation techniques.

Measurement Procedure

Diagnosis of distress precursors is based on measuring mechanical properties and thicknesses of each of the pavement system layers. The Seismic Pavement Analyzer (SPA) lowers transducers and sources to the pavement and digitally records surface deformations induced by a large pneumatic hammer which generates low-frequency vibrations, and a small pneumatic hammer which generates high-frequency vibrations (see figure 5.1).

This transducer frame is mounted on a trailer that can be towed behind a vehicle and is similar in size and concept to a Falling Weight Deflectometer (FWD) (see figure 5.2). The SPA differs from the FWD in that more and higher frequency transducers are used, and more sophisticated interpretation techniques are applied.

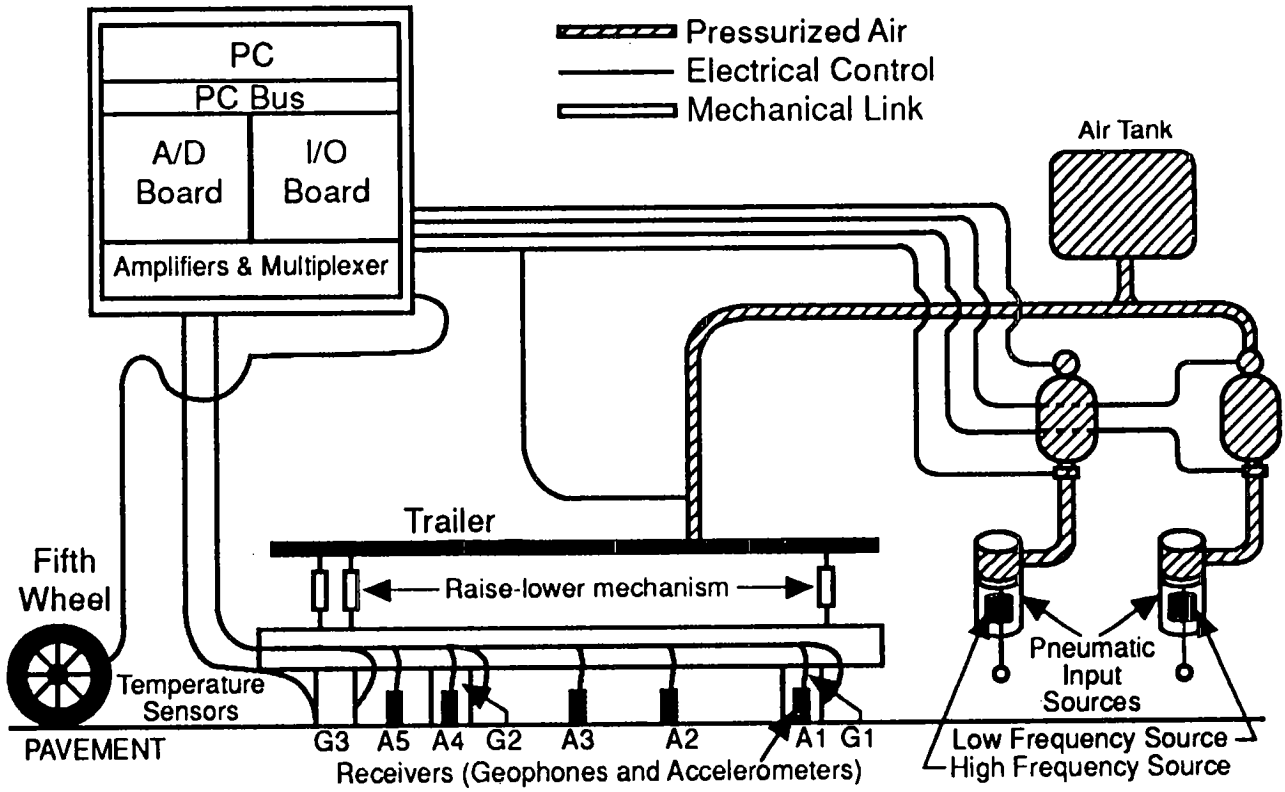

Figure 5.1 - Schematic of Seismic Pavement Analyzer

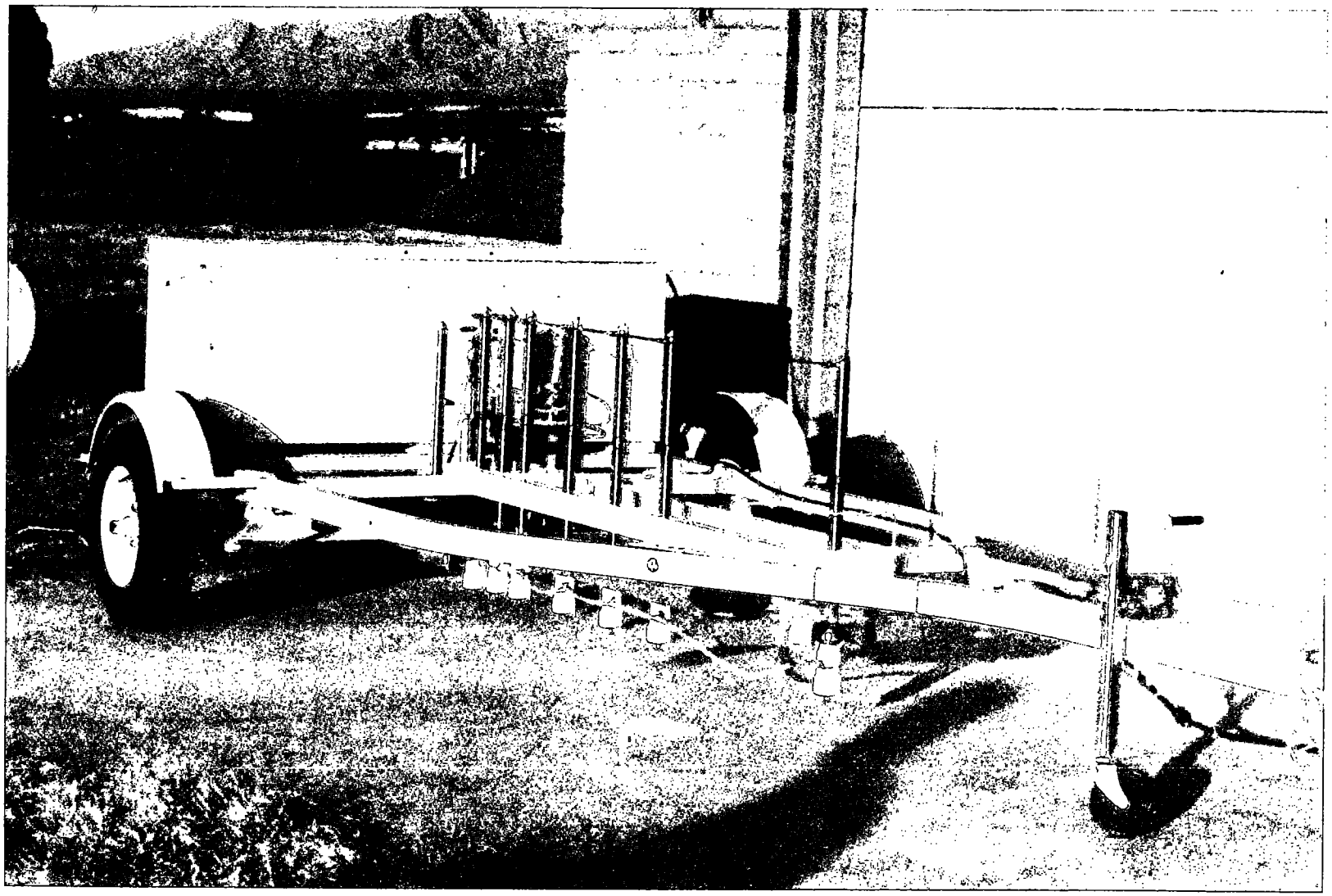

Figure 5.2 - View of Seismic Pavement Analyzer

The SPA is controlled by an operator at a computer connected to the trailer by a cable. The computer may be run from the cab of the truck towing the SPA or from various locations around the SPA.

All measurements are spot measurements; that is, the device has to be towed and situated at a specific point before measurements can be made. A complete testing cycle at one point takes less than one minute. A complete testing cycle includes situating at the site, lowering the sources and receivers, making measurements, and withdrawing the equipment. During this one minute, most of the data reduction is also executed.

Nontechnical factors affecting the performance of the SPA are summarized in table 5.1. Safe operation of the device requires traffic control. The level of traffic control necessary is equivalent to that needed to operate an FWD. The skill level of the operator depends on the operation mode of the device. The SPA has two major levels of operation, operation mode and research mode. A conscientious technician with a high school diploma or a degree from a two-year technical college is needed for the operation mode. It is estimated that one or two weeks of training through videotape and the assistance of a maintenance engineer is also necessary. A research engineer with a background in pavements and wave propagation should operate the SPA in research mode.

The appropriate spacing of measurements depends on the intended use. For maintenance, a procedure similar to that of the FWD can be used. However, for high-precision diagnostics, tests should be carried out every 0.3 m to 30 m, depending on the nature of distress. The lower limit of 0.3-m spacing is suitable for precision mapping of delaminated areas or loss of support under portland cement concrete. The upper limit of 30 m is suitable for determining the general variation in the condition of pavement. For rigid pavements, test spacing depends on the joint spacing. Typically the two joints and at least the middle of the slab should be tested. For research purposes, the frequency of measurement should be based on the goals of the research.

An extensive field study (Nazarian et al., 1991) has determined the effects of temperature on the results of different tests. This study concluded that testing rigid pavements at ambient temperatures in excess of 35°C is not feasible. For flexible pavements, the temperature should not exceed 50°C. At such high temperatures, the asphalt concrete layer is too viscous and coupling of energy to it is difficult. To minimize the effects of fluctuation in the moisture level due to precipitation, the equipment should not be used until one day after significant precipitation. As described in Chapter 3, the short-term transient change in moisture is not of any practical interest in maintenance activities.

The cost of operating the device is estimated as 20 cents per point, plus $10 per hour. This estimate is based upon the cost of operating the FWD as reported by one of the states.

Table 5.1 - Nontechnical factors affecting the performance of Seismic Pavement Analyzer

Item	Remarks	
Measurement Speed	One minute per point	
Traffic Control Required	Similar to that used for FWD testing	
Skill Level of Operator	Operation Mode:	A qualified technician
	Research Mode:	A research engineer
Frequency of Measurement	Routine Maintenance:	Similar to the procedure used with FWD
	Diagnostics:	Every 0.3 to 30 m depending on the project
	Research:	Determined case by case
Necessary Ambient Condition	Concrete: Ambient temperature not to exceed 35°C	
	Asphalt : Ambient temperature not to exceed 50°C	
Operating Cost per Measurement	20 cents per point, plus $10 per hour	

Data Analysis

The SPA collects three levels of data. The first level is raw data. These are the waveforms generated by hammer impacts and collected by the transducers. The second level is processed data. These are pavement layer properties derived from the raw data through established theoretical models. The third level is interpreted data. These are diagnoses of pavement distress precursors from data processed through models. These models will be improved and upgraded as further field data is available. Processed data will be archived, with the

interpretations, so that the user or manufacturer can test and upgrade the interpretation models.

The raw data (waveforms) collected from the hammer impacts are processed immediately and are not saved for archival unless specifically requested. Each of the eight vibration sensors records three impacts. The storage requirements for saving these raw data are large (up to 0.4 megabytes per sample). The SPA can save these data for troubleshooting or research on enhanced processing techniques.

Processed data are the result of calculations performed on the raw data and are independent estimates of the physical properties of the pavement system. These calculated properties are archived for all measurements. Table 5.2 lists the pavement properties estimated from the raw data. Young's modulus is estimated from compressional velocity measurements in the AC or PCC and from mechanical impedance in the base. The shear modulus is estimated from surface wave velocity dispersion. Thicknesses are estimated with the impact echo in the paving layer and with surface wave dispersion in the pavement and base. Damping is estimated from the impulse-response method.

Table 5.2 - Pavement properties estimated by the Seismic Pavement Analyzer

Pavement Component	Parameter Measured				
	Young's Modulus	Shear Modulus	Thickness	Damping	Other
Paving Layer	yes	yes	yes	no	Temperature
Base	yes	yes	yes*	no	
Subgrade	no	yes	no	yes	

*Thickness estimate of base depends on shear modulus contrast with subgrade.

Interpreted data are diagnoses of distress precursors. Table 5.3 lists the seven distress types to be diagnosed from the physical property measurements listed in table 5.2. The "Candidate for Rehabilitation" category is included in the pavement and base layers for conditions where failure appears to be imminent and maintenance or rehabilitation should have already occurred.

Table 5.3 - Distress precursor interpretations from pavement properties

Paving Layer Distress Precursors
Fine cracking
Aging
Delamination
Candidate for rehabilitation
Base Distress Precursors
Void under pavement
Softening of slab under pavement
Moisture change in base
Candidate for rehabilitation

Data Interpretation

The interpretation technique assumes that the distress precursors to be identified are specific to a given pavement layer or are essentially independent of the presence of other distress precursors. Aging, fine cracking, overlay delamination, and voids are directly observable physical conditions unrelated to a failure model. Moisture in the base and under joints is strongly related to a failure model, but infiltration paths may be highly localized and not seen in the measurements.

Presuming independence of the distress precursors permits a layer-by-layer diagnosis, since the SPA measurements (table 5.2) are also layer specific. Aging of asphalt is diagnosed through an increase in brittleness, apparent in Young's and shear moduli; delamination is apparent in thickness and echo size. Fine cracking in pavement is diagnosed through a strong reduction in the shear modulus, relative to a reduction in Young's modulus. In the base, voids and moisture both reduce moduli, while voids present a relatively undamped system compared to the presence of moisture.

Distress precursors are interpreted with a hypothesis-testing approach, relative to the design parameters for the pavement system. For instance, if fine cracking exists, then Young's and shear moduli in the pavement will fall within a specified range of values that are a fraction of the ideal stiffness for the concrete type used. If measurement points fall outside these ranges for known distress types, distances from the measurement points to the region will be used to weight the probability that the hypothesis is true.

Description of Measurement Technologies

Impulse-Response (IR) Method

Two parameters are obtained with the IR method—the shear modulus of subgrade and the damping ratio of the system. These two parameters characterize the existence of several distress precursors. In general, the modulus of subgrade can be used to delineate between good and poor support. The damping ratio can distinguish between the loss of support or weak support. The two parameters are extracted from the flexibility spectrum measured in the field. An extensive theoretical and field study (Reddy, 1992) shows that except for thin layers (less than 75 mm) and soft paving layers (i.e., flexible pavements), the modulus obtained by the IR method is a good representation of the shear modulus of subgrade, and the stiffness of the paving layers would influence the results insignificantly. In other cases, the properties of the pavement layers (AC and base) affect the outcome in such a manner that the modulus obtained from the IR test should be considered an overall modulus.

The IR tests use the low-frequency source and geophone G1 (see figure 5.1). The pavement is impacted to couple stress wave energy in the surface layer. At the interface of the surface layer and the base layer, a portion of this energy is transmitted to the bottom layers, and the remainder is reflected back into the surface layer. The imparted energy is measured with a load cell. The response of the pavement, in terms of particle velocity, is monitored with the geophone and then numerically converted to displacement. The load and displacement time-histories are simultaneously recorded and are transformed to the frequency domain using a Fast-Fourier Transform algorithm. The ratio of the displacement and load (termed flexibility) at each frequency is then determined.

For analysis purposes, the pavement is modeled as a single-degree-of-freedom (SDOF) system. Three parameters are required to describe such a system—natural frequency, damping ratio, and gain factor. The last two can be replaced by the static amplitude and the peak amplitude. These three parameters are collectively called the modal parameters of the system. The natural frequency and gain factor are used to determine the modulus of subgrade. The damping ratio is used directly.

To determine the modal parameters, a curve is fitted to the flexibility spectrum according to an elaborate curve-fitting algorithm that uses the coherence function as a weighing function (Richardson and Formenti, 1982). The poles, zeros, and gain factor obtained from the curve-fitting are easily converted to modal parameters. From these parameters, the modulus

of subgrade is determined. The shear modulus of subgrade, G, is calculated from (Dobry and Gazetas, 1986)

$$G = (1 - \nu) / [2L\, A_o\, I_s\, S_z] \tag{5.1}$$

where

ν = Poisson's ratio of subgrade
L = length of slab, and
A_o = static flexibility of slab (flexibility at f = 0).

The shape factor, S_z, has been developed by Dobry and Gazetas (1986). The value of S_z is equal to 0.80 for a long flexible pavement.

I_s (Reddy, 1992) is a parameter which considers the effect of an increase in flexibility near the edges and corners of a slab. Parameter I_s is a function of the length and width of the slab, as well as the coordinates of the impact point relative to one corner. Depending on the size of the slab and the point of impact, the value of I_s can be as high as 6.

The damping ratio, which typically varies between 0 to 100 percent, is an indicator of the degree of the slab's resistance to movement. A slab that is in contact with the subgrade or contains a water-saturated void demonstrates a highly damped behavior and has a damping ratio of greater than 70 percent. A slab containing an edge void would demonstrate a damping ratio in the order of 10 to 40 percent. A loss of support located in the middle of the slab will have a damping of 30 to 60 percent.

Spectral-Analysis-of-Surface-Waves (SASW) Method

The Spectral-Analysis-of-Surface-Waves (SASW) method was mainly developed by Nazarian and Stokoe (1989). SASW is a seismic method that can determine shear modulus profiles of pavement sections nondestructively.

The key point in the SASW method is the measurement of the dispersive nature of surface waves. A complete investigation of a site with the SASW method consists of collecting data, determining the experimental dispersion curve, and determining the stiffness profile (inversion process).

The set-up used for the SASW tests is depicted in Figure 5.1. All accelerometers and geophones are active. The transfer function and coherence function between pairs of receivers are determined during the data collection.

A computer algorithm utilizes the phase information of the cross power spectra and the coherence functions from several receiver spacings to determine a representative dispersion curve in an automated fashion (Nazarian and Desai, 1993).

The last step is to determine the elastic modulus of different layers, given the dispersion curve. A recently developed automated inversion process (Yuan and Nazarian, 1993) determines the stiffness profile of the pavement section.

Ultrasonic-Surface-Wave Method

The ultrasonic-surface-wave method is an offshoot of the SASW method. The major distinction between these two methods is that in the ultrasonic-surface-wave method the properties of the top paving layer can be easily and directly determined without a complex inversion algorithm. To implement the method, the high-frequency source and accelerometers A1 and A2 (see figure 5.1) are utilized.

Up to a wavelength approximately equal to the thickness of the uppermost layer, the velocity of propagation is independent of wavelength. Therefore, if one simply generates high-frequency (short-wavelength) waves, and if one assumes that the properties of the uppermost layer are uniform, the shear modulus of the top layer, G, can be determined from

$$G = \rho\,[(1.13 - 0.16)\,\nu\,V_{ph}]^2 \qquad (5.2)$$

where

V_{ph} = velocity of surface waves
ρ = mass density
ν = Poisson's ratio.

The thickness of the surface layer can be estimated by determining the wavelength above which the surface wave velocity is constant.

The methodology can be simplified even further. If one assumes that the properties of the uppermost layer are uniform, the modulus of the top layer, G, can be determined from

$$G = \rho\,[(1.13 - 0.16\nu)\,(\,m/360D)]^2 \qquad (5.3)$$

Parameter m (deg/Hz) is the least-squares fit slope of the phase of the transfer function in the high-frequency range.

Ultrasonic Compression Wave Velocity Measurement

Once the compression wave velocity of a material is known, its Young's modulus can be readily determined. The same set-up used to perform the SASW tests can be used to measure compression wave velocity of the upper layer of pavement.

Miller and Pursey (1955) found that when the surface of a medium is impacted, the generated stress waves propagate mostly with Rayleigh wave energy and, to a lesser extent, with shear and compression wave energy. As such, the body wave energy present in a seismic record generated using the set-up shown in figure 5.1 is very small; for all practical purposes it does not contaminate the SASW results. However, compression waves travel faster than any other type of seismic wave and are detected first on seismic records.

An automated technique for determining the arrival of compression waves has been developed. Times of first arrival of compression waves are measured by triggering on an amplitude range within a time window (Willis and Toksoz, 1983).

Impact-Echo Method

The impact-echo method can effectively locate defects, voids, cracks, and zones of deterioration within concrete. The method has been thoroughly studied and effectively used on many projects by researchers at the National Institute of Standards and Technology. In a comprehensive theoretical and experimental study, Sansalone and Carino (1986) considered the effects of type of impact source, distance from impact point to receiver, type of receiving transducers, and depth of reflecting interfaces.

The high-frequency source and accelerometer A1 are used, and possibly A2 as well (see figure 5.1). Once the compression wave velocity of concrete, V_p, is known, the depth-to-reflector, T, can be determined from (Sansalone and Carino, 1986)

$$T = V_p / 2f \tag{5.4}$$

where f is the resonant (return) frequency obtained by transforming the deformation record into the frequency domain.

6

Description of the Device

The Seismic Pavement Analyzer (SPA) consists of two hardware subsystems and three software subsystems. The first hardware subsystem consists of the mechanical components, including the transducers, sources, and their mountings; the second hardware subsystem consists of the electronic components, including signal conditioning, data acquisition, and controls. The three software subsystems are data acquisition, data interpretation, and database management. These components are described below. This chapter describes only the basic functions of the different components of the device. More technical information is provided in a companion report.

Hardware Subsystems

Mechanical Components

The SPA was shown in figure 5.2. The device includes a two-wheel trailer, a box at the rear holding pneumatic and electronic controls, and a transducer mounting bar holding the geophone and accelerometer pneumatic cylinders.

The transducer mounting consists of a 17-mm channel, mounted to the body of the trailer with pneumatic springs. The springs isolate the transducer mounting from the trailer and source vibrations and also allow several centimeters of vertical adjustment for pavement topography.

Individual spring-return air cylinders raise and lower the transducers to the pavement. With this design, significant pavement topography is accommodated with a uniform transducer coupling force, and less noise is coupled from the trailer to the transducers.

The geophone and accelerometer transducer holders, as shown in figure 6.1, protect the transducers from the elements and isolate the transducers from vibrations of the mounting bar. The most recent design has proved to have excellent coupling and high-frequency response. The shell of the holder is constructed of PVC pipe, which shows very little resonance and prevents steel-aluminum contact that could cause corrosion. The rubber vibration isolators connecting the transducers to the raise/lower mechanism have given reliable coupling on even the rougher chip-seal surfaces.

Two air cylinders lower the high-frequency and low-frequency pneumatic sources (see figure 6.2) on their mounting assembly to rest on the pavement surface. The pneumatic hammers give good high-frequency and low-frequency signals of adequate strength that are very repeatable. The accumulator with a computer-controlled solenoid valve has an adequate cycle time of less than 0.5 second. The source feedback control circuit adjusts the fire time based on the signal shape.

Electronic Components

The signal-conditioning circuits include thermocouple conditioning, accelerometer power supplies and amplifiers, and geophone amplifiers. Thermocouple conditioning is done with a single specialized integrated circuit with better than one degree centigrade accuracy. The accelerometer and load cell signal conditioning consists of line-condition warnings, two operational amplifiers with an input buffer, independent gain, zero offset, and 50 KHz anti-alias filters. The geophone signal conditioning consists of two operational amplifiers with independent gain, zero offset, and 5 KHz anti-alias filters.

The user-interface software will run on an IBM PC-AT (or equivalent) computer with Hercules, CGA, or EGA/VGA graphics, 640 Kb ram, two floppy drives or one hard drive, and one serial port. The data-acquisition software and hardware run in an IBM PC-AT equivalent machine with 4 Mb ram, two serial ports, and four expansion slots. A 33 MHz, 80486 CPU was used to speed up the Fast Fourier Transforms in data acquisition and to permit more extensive diagnostics to be made in real time.

The data acquisition hardware is a Metrabyte DAS-50 A/D board, which samples four channels at 250 KHz at 12-bit resolution. The Metrabyte PIO-12 has three parallel I/O channels that

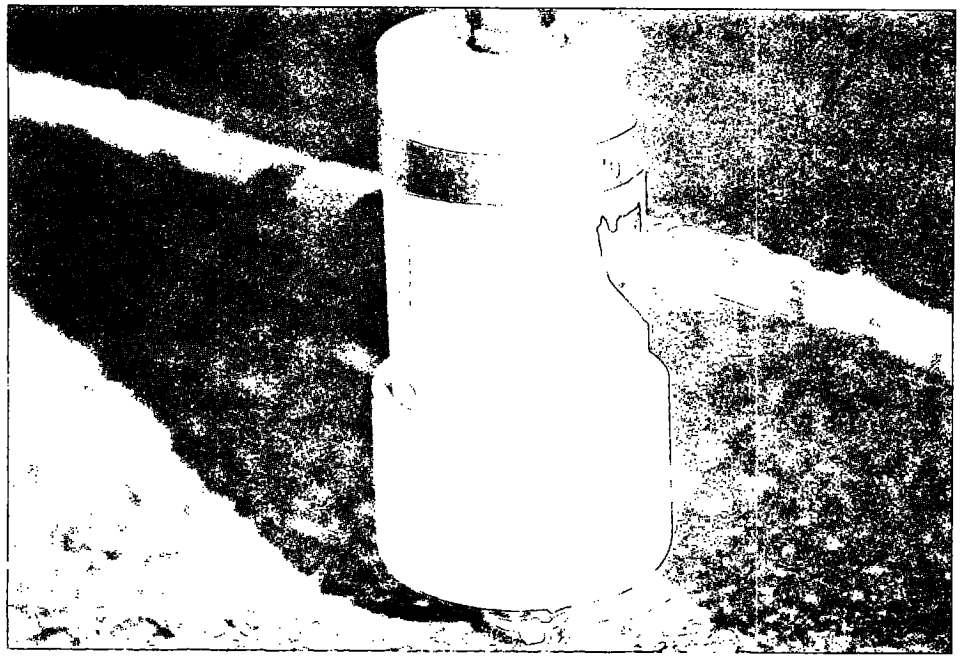

Figure 6.1 - Transducer holder

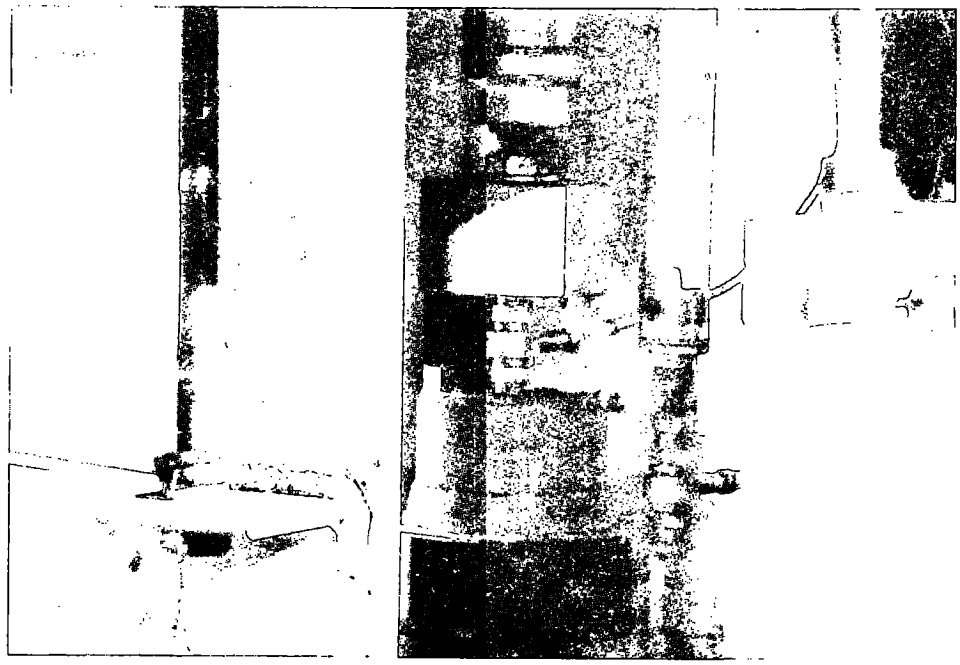

Figure 6.2 - Pneumatic sources

control and sense the electro-mechanical state of the Analyzer. These components are housed inside the computer.

Software Subsystems

Data-Acquisition Software

Data acquisition is based on the concept of exchanging information through the user interface. The user interface provides all parameters for data acquisition—including transducer multiplexer assignments, gains, sample rates, transducer spacings, and measurements—every time data collection is initiated.

Interpretation Software

Interpretation software is based on an inductive hypothesis-testing approach, using set theory. All distress-precursor hypotheses are tested by comparing moduli and thickness values with table-defined polygons. If a point falls within a polygon, the hypothesis is confirmed. If a point falls outside a polygon, the distance to the polygon is saved for comparison with distances for other hypotheses. If measurements are exterior to all polygons, relative distances are normalized to probabilities on each hypothesis.

SPA also includes "quick-look" technique for qualitatively comparing moduli and thickness values from different measurements. This simulates a pavement cross-section in appearance and serves as a visual indicator of measurement quality during routine analysis or as quick screening for pavement sections requiring more in-depth analysis. An example of such a graph is shown in figure 6.3. A key is also provided for convenience.

Database-Management Software

The current prototype formats parameters collected by the data-acquisition hardware for entry into Borland's Paradox relational database manager, under control of the user-interface software.

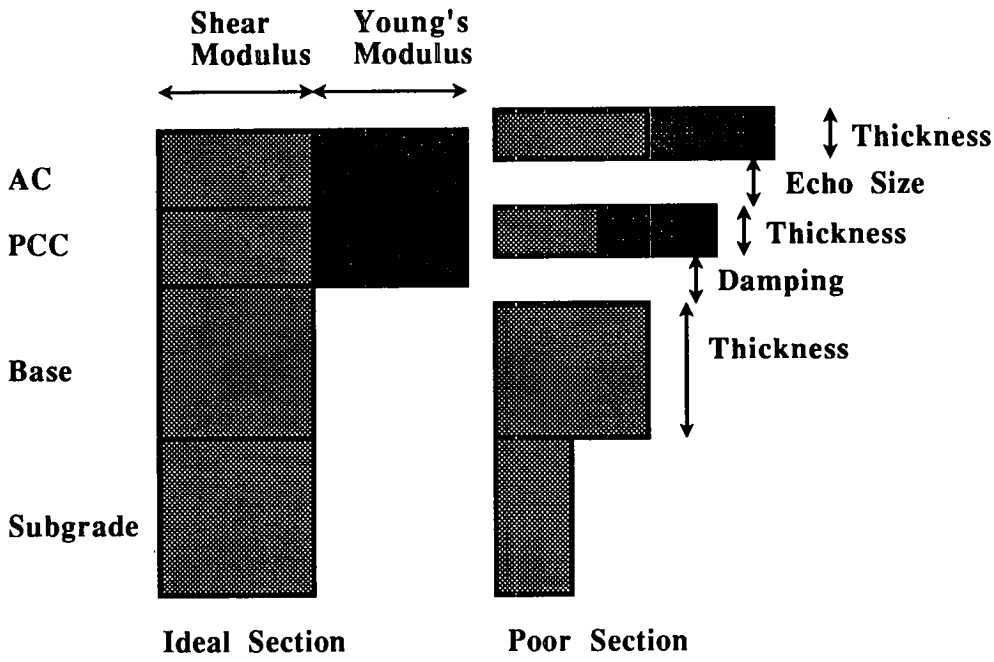

a) Legend

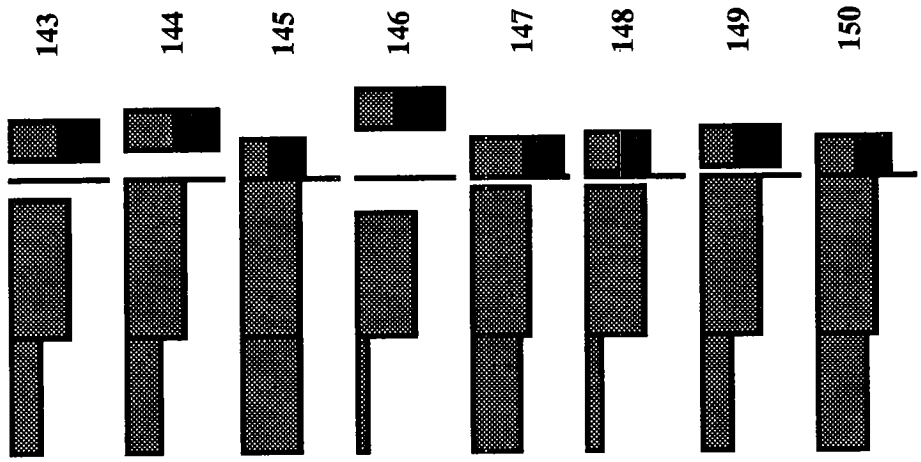

b) Actual Data

Figure 6.3 - Example of graphical viewing of collected data

The five database tables saved by the data-acquisition software are

1. Moduli Values
   - Measurement ID
   - Young's Modulus, Shear Modulus, Thickness of Asphalt
   - Young's Modulus, Shear Modulus, Thickness of Concrete
   - Young's Modulus, Shear Modulus, Thickness of Base
   - Shear Modulus of Subgrade
   - Air Temperature, Ground Temperature
   - Densities

2. Time-Location
   - Measurement ID
   - Date
   - Time
   - Location
   - Equipment Serial Number

3. Error Messages
   - Measurement ID
   - Error
   - Error Source

4. Surface Wave Dispersion Data
   - Measurement ID
   - Curve fits and ranges on three segments

5. Compressional Velocities
   - Measurement ID
   - Four compressional velocity estimates

The database load and retrieve formats are identical and are read by the interpretation software and quick-look graphical display.

With the Paradox relational database, data can be retrieved into Borland's Quattro Pro spreadsheet. The spreadsheet can perform summary computations and statistical calculations, and create graphs or reports. Data-retrieval-and-analysis scripts can be written in both the database and the spreadsheet to generate reports automatically that a particular highway

department might desire. This eliminates the need for general purpose analysis, display, and reporting software.

7

Data Collection and Reduction

The previous chapter discussed the conceptual and theoretical aspects of data reduction. This chapter describes the processes of data collection and data reduction at a typical site. It also discusses a step-by-step procedure for each testing methodology.

Data Collection

Upon initiating the testing sequence through the computer, the technician lowers the sensors and impact unit onto the pavement surface. The high-frequency source is then activated.

The outputs of the three accelerometers closest to the high-frequency source, as well as the load cell connected to this source, are used first. The source is fired four to seven times. For the last three impacts of the source, the output voltages of the load cell and the receivers are saved and averaged (stacked) in the frequency domain. The other (prerecording) impacts are used to adjust the gains of the pre-amplifiers. The gains are set in a manner that optimizes the dynamic range.

The same procedure is followed again, but the first three accelerometers are replaced by the last three accelerometers. A multiplexer switches the accelerometers. The middle accelerometer (third closest accelerometer to the source) is active in both sets of experiments.

Typical voltage outputs of the load cell and the three near accelerometers are shown in figure 7.1. Naturally, as the distance from the source increases, the amplitude of the signal decreases.

To ensure that an adequate signal-to-noise ratio is achieved in all channels, signals similar to those shown in figure 7.1 are normalized to a maximum amplitude of one, as shown in figure 7.2. In this manner, the main features of the signals can be easily inspected. The signal-to-noise ratios are quite adequate and the signals follow the classic pattern of wave propagation in pavement layers.

In the next phase of data collection, the low-frequency load cell and the three geophones are recorded. The procedure described above for each of the accelerometer banks is utilized. A typical output of the three geophones is shown in figure 7.2c in the normalized fashion. Once again, the quality of the data is adequate.

The data collected in this fashion have to be processed using signal processing and spectral analysis. These processes are described in the next section.

Data Reduction

The data collected in the manner described above are manipulated in several ways to determine the parameters enumerated in Chapter 5. The rest of this chapter discusses the procedures for each testing technique.

Impulse-Response Method

This method uses the voltage output from the first geophone (the geophone closest to the source) and the load cell. (See figure 7.2c.)

The load cell record consists of a half-sine wave approximately 2-msec long. The small reverberation past the actual impact corresponds to the reflection of the wave inside the source assembly. The amplitude of this reverberation is muted so it does not affect the results. The response of the geophone is a steady-state damped response. The slight time delay between the geophone and load cell records is the result of the separation between the source and the receiver.

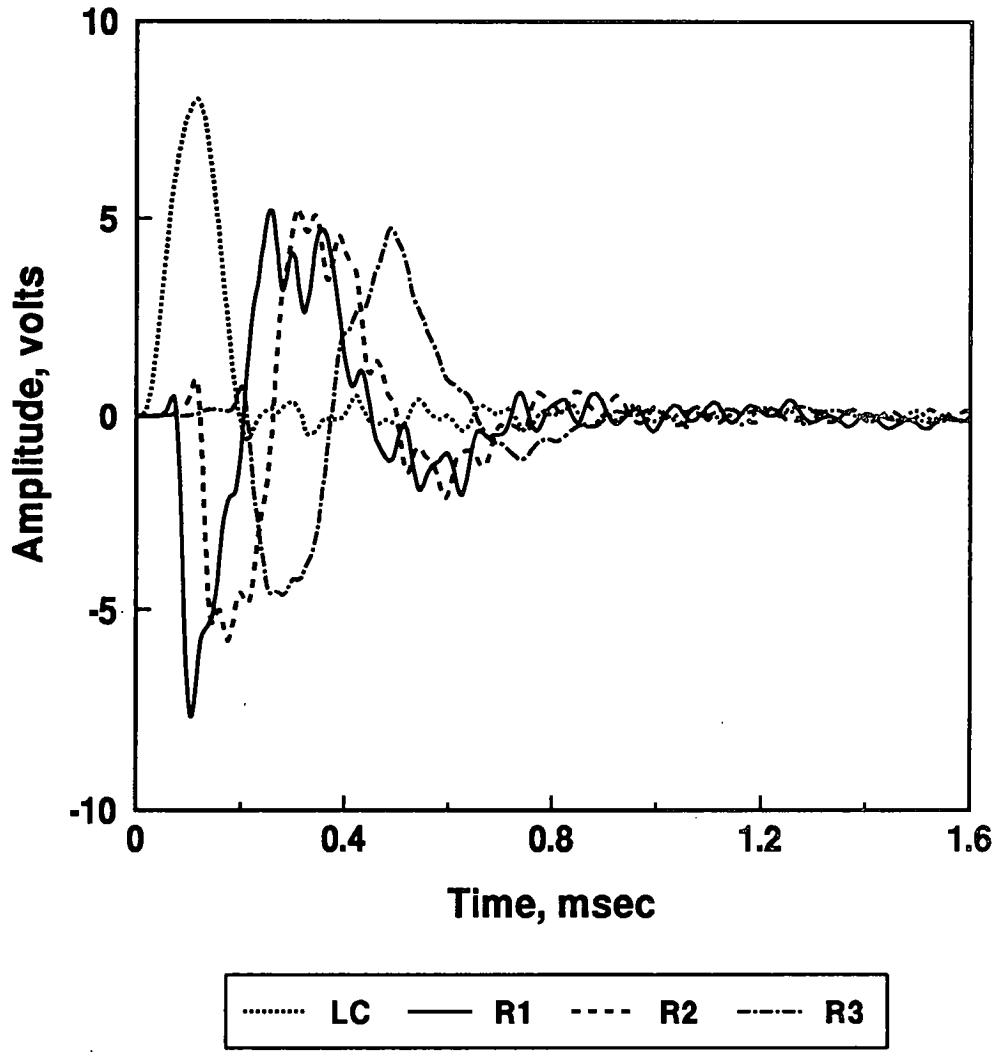

Figure 7.1 - Typical time records from accelerometers

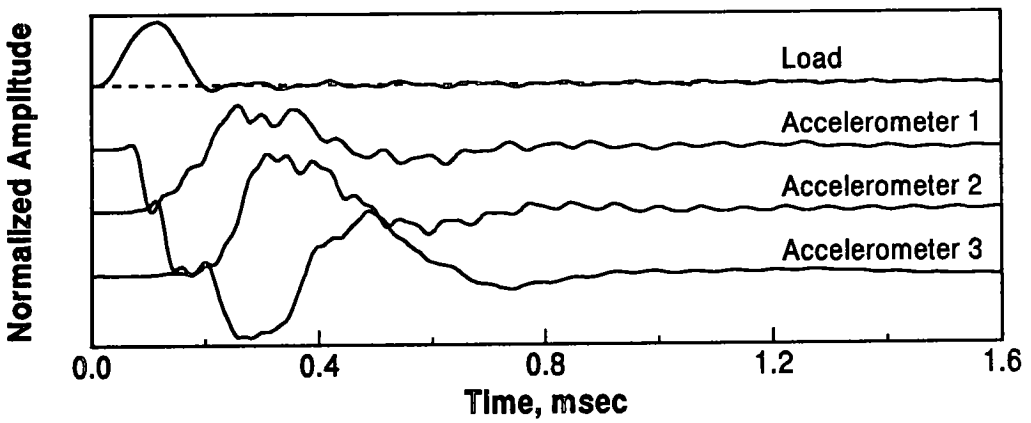

a) Near Accelerometers

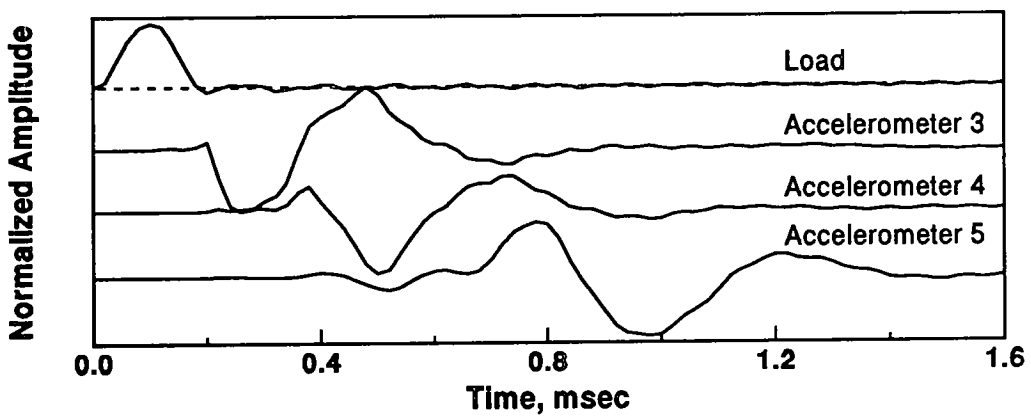

b) Far Accelerometers

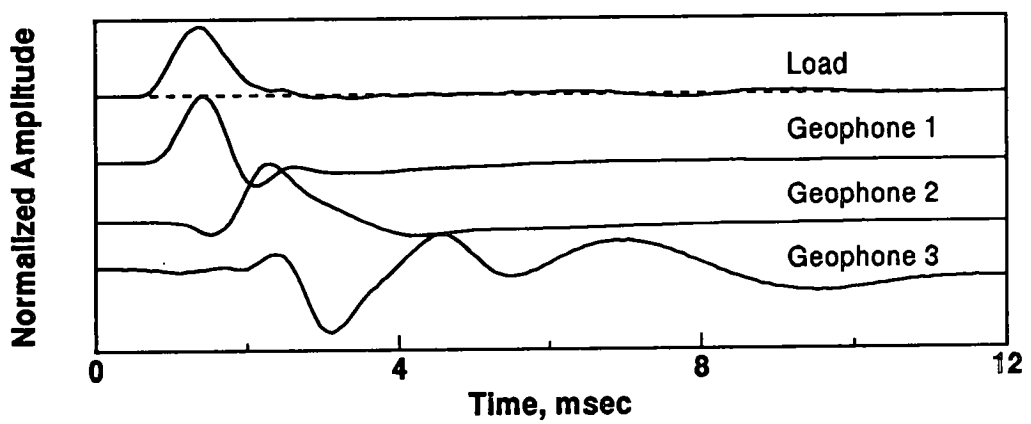

c) Geophones

Figure 7.2 - Typical normalized time records obtained with SPA

A detailed description of steps necessary to complete the data reduction can be found in Nazarian et al. (1993). Briefly, the output of the load cell and geophone are transformed into the frequency domain using a Fast-Fourier Transform (FFT) algorithm, obtaining the ratio of the particle velocity and the load at each frequency. This function, the mobility spectrum, is then integrated to obtain the flexibility spectrum. The flexibility spectrum is used to determine the parameters for detecting voids or loss of support.

A typical flexibility spectrum is shown in figure 7.3a. The response is as expected, except for frequencies below approximately 50 Hz. The erratic nature of the signal at low frequencies is probably because of the movement of the trailer. This problem is discussed elsewhere in this report.

The coherence function associated with this record is shown in figure 7.3b. The coherence values are close to unity except at low frequencies. A coherence value of unity corresponds to a highly coherent signal between the load cell and receiver. In other words, there was no incoherent background noise in the signals.

In the next step, a complex-valued curve representing a single-degree-of-freedom (SDOF) dynamic system is fitted to the flexibility spectrum. A typical fitted curve is shown in figure 7.3a. The agreement between the measured and the fitted data is good. However, once again, because of a lack of quality data at low frequencies, the fit is not adequate in this region.

Impact-Echo Method

The impact-echo method is similar to the impulse-response method. However, the impact-echo method uses the records from the small load cell and the accelerometer closest to the high-frequency source. Typical outputs from the accelerometer and the load cell are shown in figure 7.2a.

In the next step, the two signals are transformed into the frequency domain following the procedure outlined above for impulse-response testing. A typical frequency-response spectrum for a site is shown in figure 7.4a.

The major peak seen in figure 7.4a (at about 10 kHz) corresponds to the thickness of the layer and is called the return (resonant) frequency.

The coherence function is shown in figure 7.4b. In general, the data collected with the device have no incoherent noise, except at several isolated frequencies.

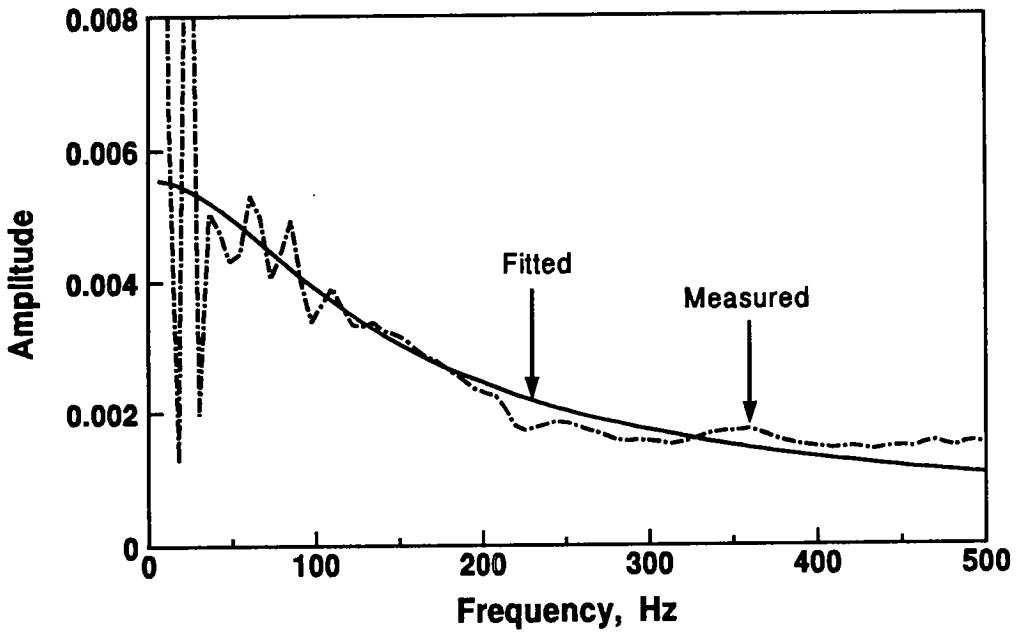

a) Transfer Function

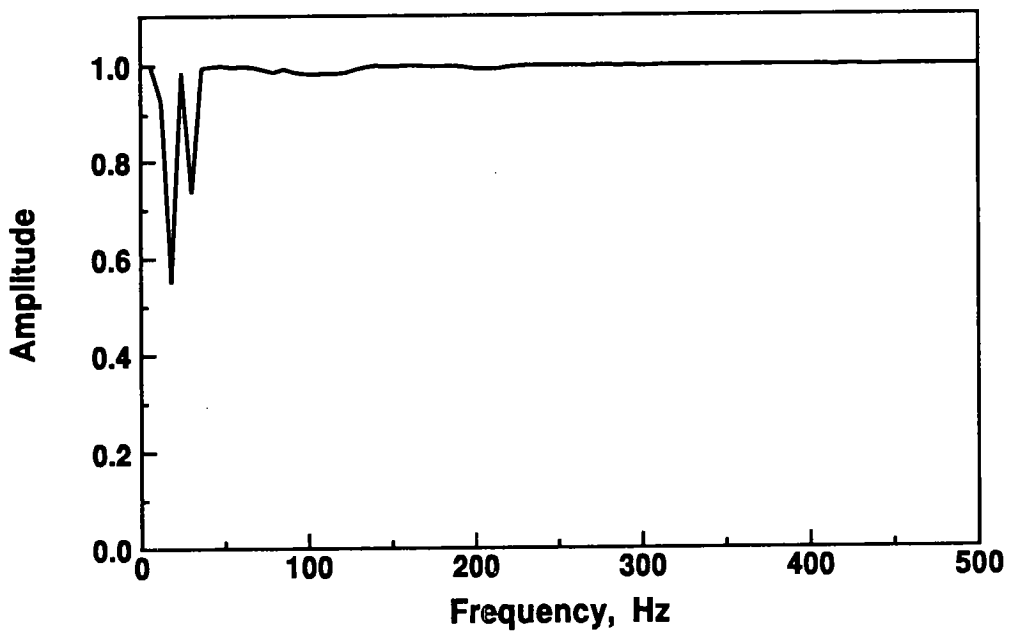

b) Coherence Function

Figure 7.3 - Typical spectral functions used in impulse-response test

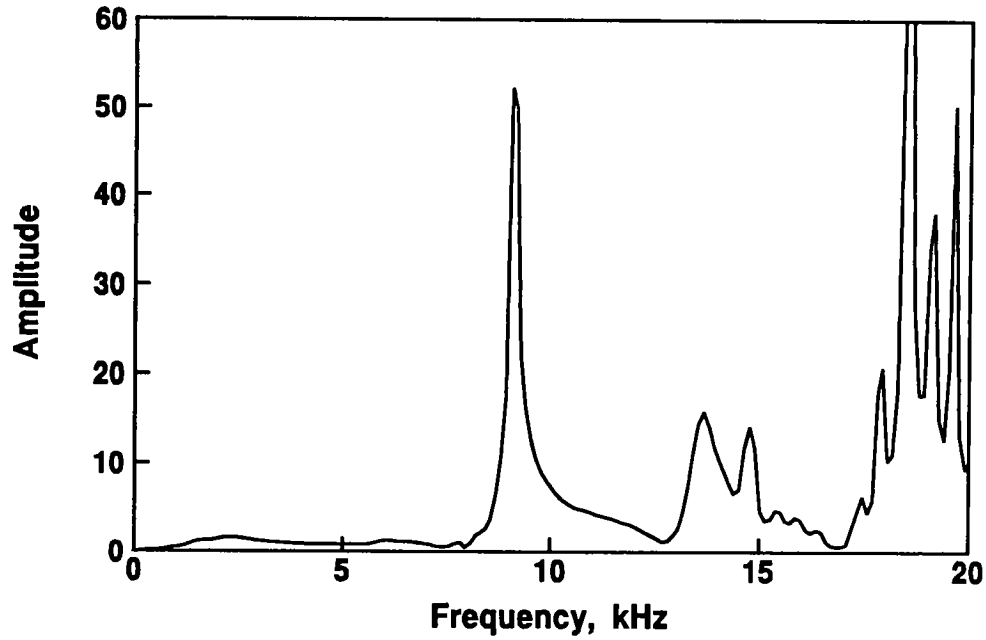

a) Transfer Function

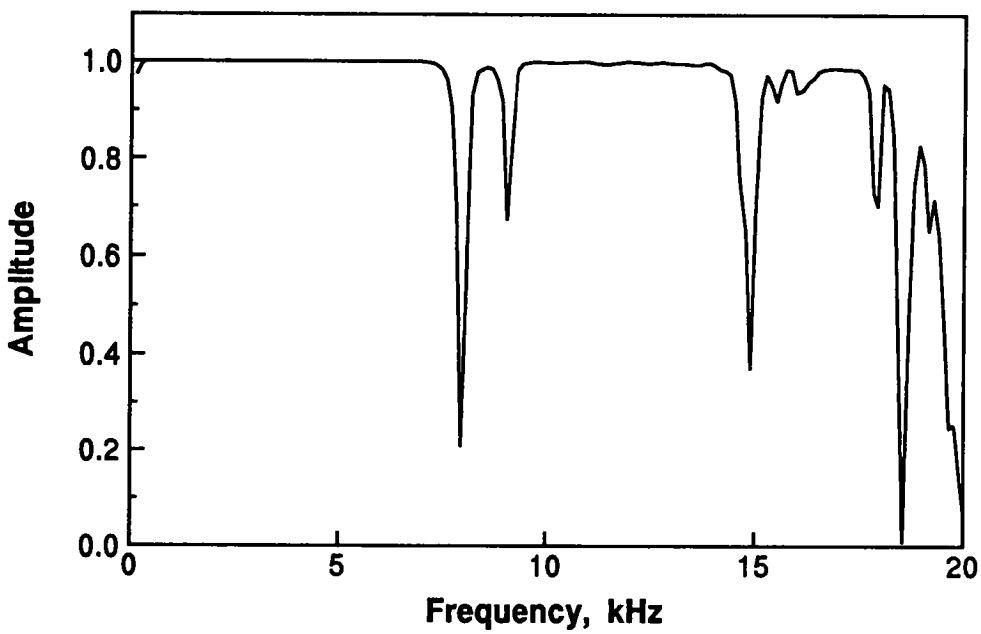

b) Coherence Function

Figure 7.4 - Typical spectral functions used in impact-echo test

To calculate the thickness of the layer, the compression wave velocity of the material is determined using the ultrasonic-body-wave method. The thickness is equal to one-half of the ratio between the compression wave velocity and the return resonant frequency.

Ultrasonic-Surface-Wave Method

This method determines the shear modulus of the top layer, using the time records of two accelerometers, accelerometer 2 (150 mm away from the source) and accelerometer 3 (300 mm away from the source) (see figure 7.2a). These two signals are Fourier-transformed and the ratio of the two signals is calculated in the form of the transform function. However, unlike the previous two methods, the ultrasonic-surface-wave method uses only the phase of the transfer function.

A phase spectrum for time records similar to those shown in figure 7.2a is shown in figure 7.5a. The phase oscillates on a radius between π and $-\pi$ radians (180 and -180 degrees). This is the standard method of presenting phase data, because the detailed variation in the data can be observed in a small space.

The data shown in figure 7.5a are smooth and do not exhibit much scatter in phase with the frequency, up to a frequency of 35 or 40 kHz. However, the data are rather noisy above a frequency of 35 or 40 kHz.

The coherence function associated with this record is shown in figure 7.5b. The coherence is almost equal to one, up to a frequency of 35 or 40 kHz. Above the frequency of 35 kHz, the data are of low quality and are not usable.

The frequency of 35 kHz for this experiment corresponds to a wavelength of less than 38 mm. Shorter wavelengths can be investigated using accelerometer 1 and accelerometer 2 (which are spaced 75 mm apart). One physical limitation is the aggregate size. Wavelengths shorter than the maximum aggregate size probably do not follow the laws of wave propagation in solid medium.

The shear modulus of the top layer was obtained using a complex-valued curve-fitting process with the coherence as the weighing function (Nazarian and Desai, 1993). The results are shown in figure 7.5a. The actual and fitted curves compare quite favorably up to a frequency of 30 kHz.

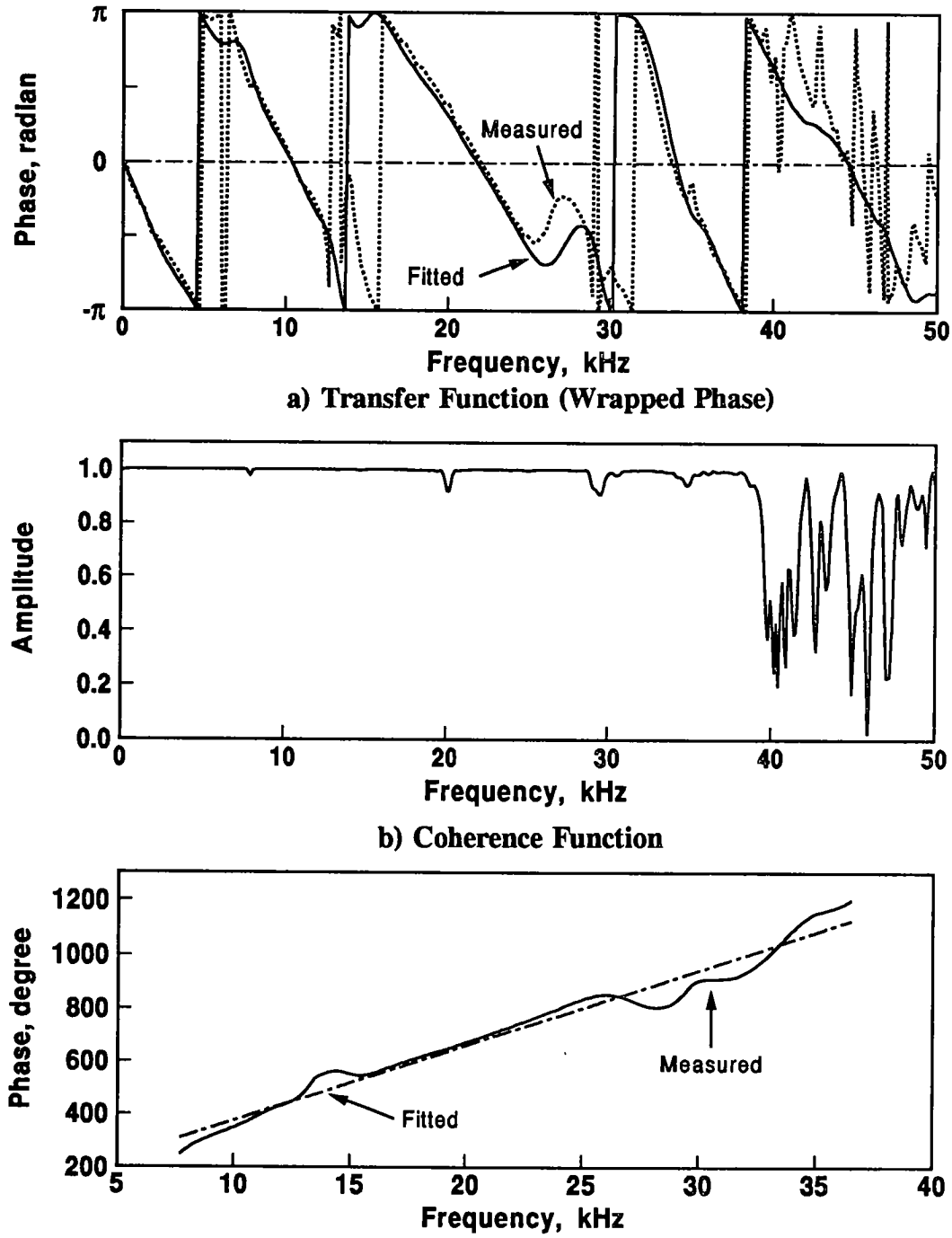

Figure 7.5 - Typical spectral functions used in ultrasonic-surface wave test

In the next step, the phase is "unwrapped"; that is, the appropriate number of cycles is added to each phase. The unwrapped phase for the "wrapped" phase shown in figure 7.5a is shown in figure 7.5c. The slope of the line is basically constant with frequency.

Finally, a line is fitted to the curve in the range of frequencies corresponding to wavelengths shorter than the thickness of the top layer. The slope of the line can be used to determine the shear modulus (see Chapter 6).

Ultrasonic-Body-Wave Method

The ultrasonic-body-wave method uses the same records as in the ultrasonic-surface-wave method. In figure 7.2, the arrival of the compression waves (P-waves) cannot be identified in part because the surface wave energy dominates all signals. To determine the arrival of the P-waves, the gain of all amplifiers is set at the maximum possible range to collect data for determining compression wave velocities. Such a record is shown in figure 7.6. Accelerometers 1 and 2 cannot identify the energy associated with the compression waves, because the seismic energy has not traveled over enough distance to separate into different types of waves (see Appendix A). However, the other accelerometers, can identify the arrival of the P-waves. In figure 7.6, the arrows in each record correspond to the arrival of these waves; typically, accelerometers 3 and 4 record the arrival of energy most consistently.

To obtain the Young's modulus, the difference in the arrival time between the two receivers is calculated. The compression wave velocity is calculated from the distance between the receivers and the difference in the travel time. The compression wave velocity can then be converted to Young's modulus.

Spectral-Analysis-of-Surface-Wave (SASW) Method

The two main goals of SASW testing are to obtain a dispersion curve and to invert the dispersion curve to obtain the shear modulus profile. Each step is briefly described below.

The initial steps involved in obtaining a dispersion curve are similar to those described for the ultrasonic-surface-wave method. Time records from each two consecutive sensors are Fourier-transformed; spectral analysis is applied to obtain the phase information of the transfer function and the coherence function. The curve-fitting procedure described for the ultrasonic surface waves is implemented; from the fitted phase spectrum, the dispersion curve

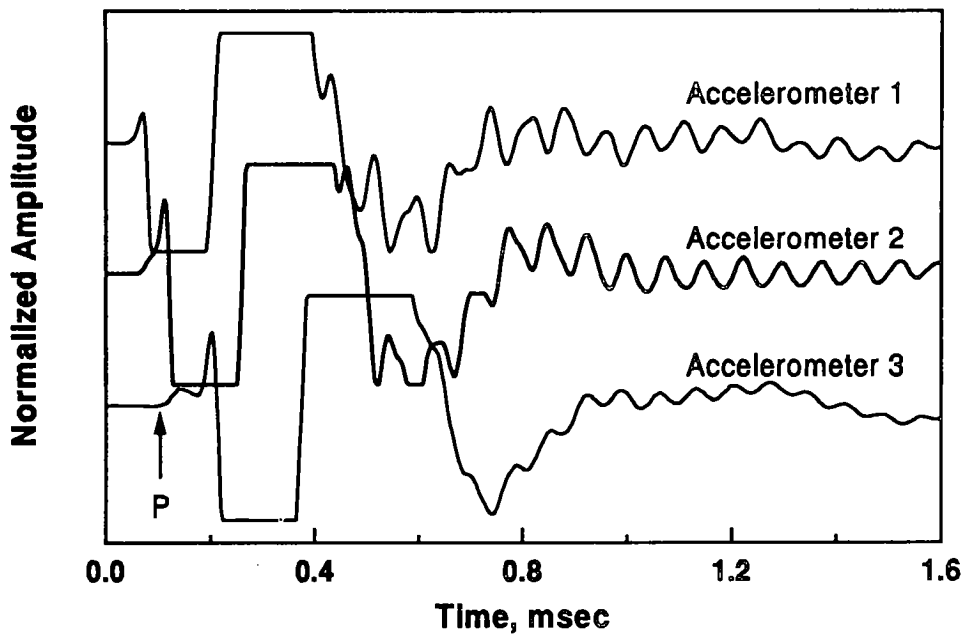

a) Near Accelerometers

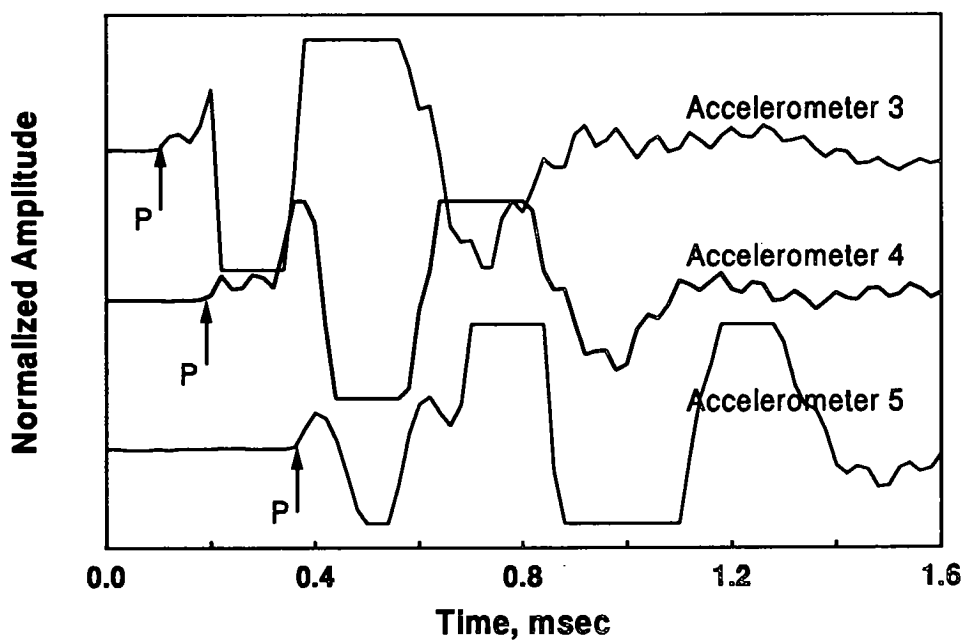

b) Far Accelerometers

Figure 7.6 - Typical amplified signals used in ultrasonic-body-wave test

(phase velocity versus wavelength) associated with that record is determined. This process is repeated for all receiver spacings. Finally, the representative dispersion curve is obtained by combining the dispersion curves from different spacings using an L1-norm curve-fitting process. The details of this process can be found in Nazarian and Desai (1993).

The accelerometer records are used for near spacings. Four sets of phase spectra are utilized. These are phase spectra between accelerometers 1 and 2 (spacing of 75 mm); accelerometers 2 and 3 (spacing of 150 mm); accelerometers 3 and 4 (spacing of 300 mm); and accelerometers 4 and 5 (spacing of 600 mm). An example of the phase spectra and the coherence functions for one test is shown in figure 7.7.

In addition to the accelerometer records, two geophone records are used to obtain a dispersion curve associated with longer wavelengths. The example in figure 7.7 used geophone 2 (approximately 1200 mm away from the source) and geophone 3 (approximately 2400 mm away from the source).

Also shown in figure 7.7 are curves fitted to the phase spectrum. Once again, the fitted and measured curves compare favorably.

The next step is to determine the final dispersion curve. The dispersion curves obtained from all receiver spacings are combined as shown in figure 7.8. A curve is fitted to this data to obtain the "fitted-measured dispersion curve." This fitted curve is used in the inversion process. Shown in figure 7.8 is the fitted-measured dispersion curve obtained by the automated algorithm (termed "fitted" in the figure). The idealized curve is representative of the raw data.

Finally, an automated inversion process developed by Yuan and Nazarian (1993) determines the final Young's modulus profile for a site. The modulus profile at the example site is shown in figure 7.9.

To ensure that the inversion process is successful, the fitted-measured dispersion curve is compared with the theoretical dispersion curve (obtained from the Young's modulus profile shown in figure 7.9). This comparison is depicted in figure 7.8. It can be seen that the theoretical (labeled "from inverted model" in the figure) and experimental data (labeled "L1-norm fitted" in the figure) compare favorably.

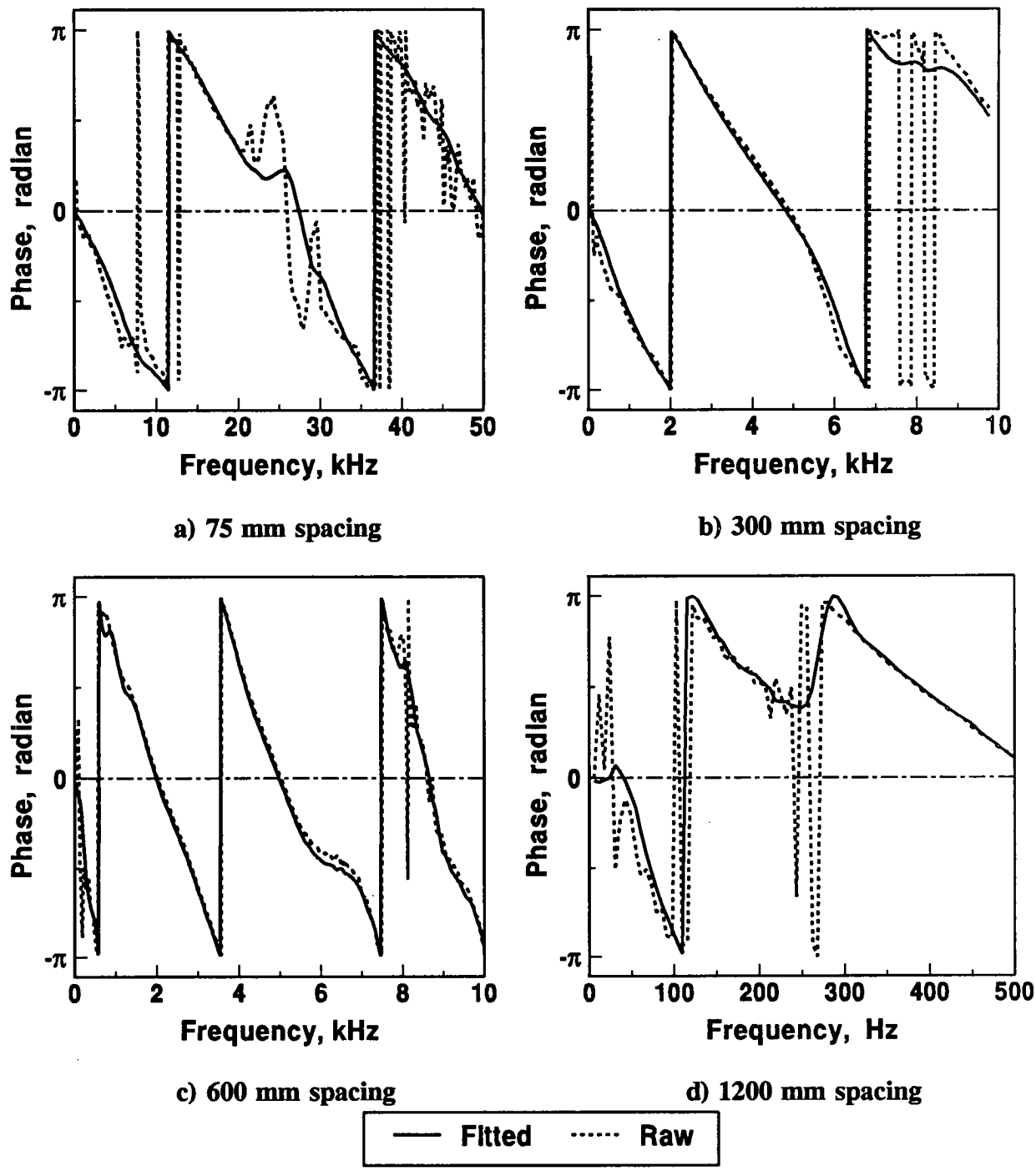

Figure 7.7 - Typical spectral functions used in SASW test

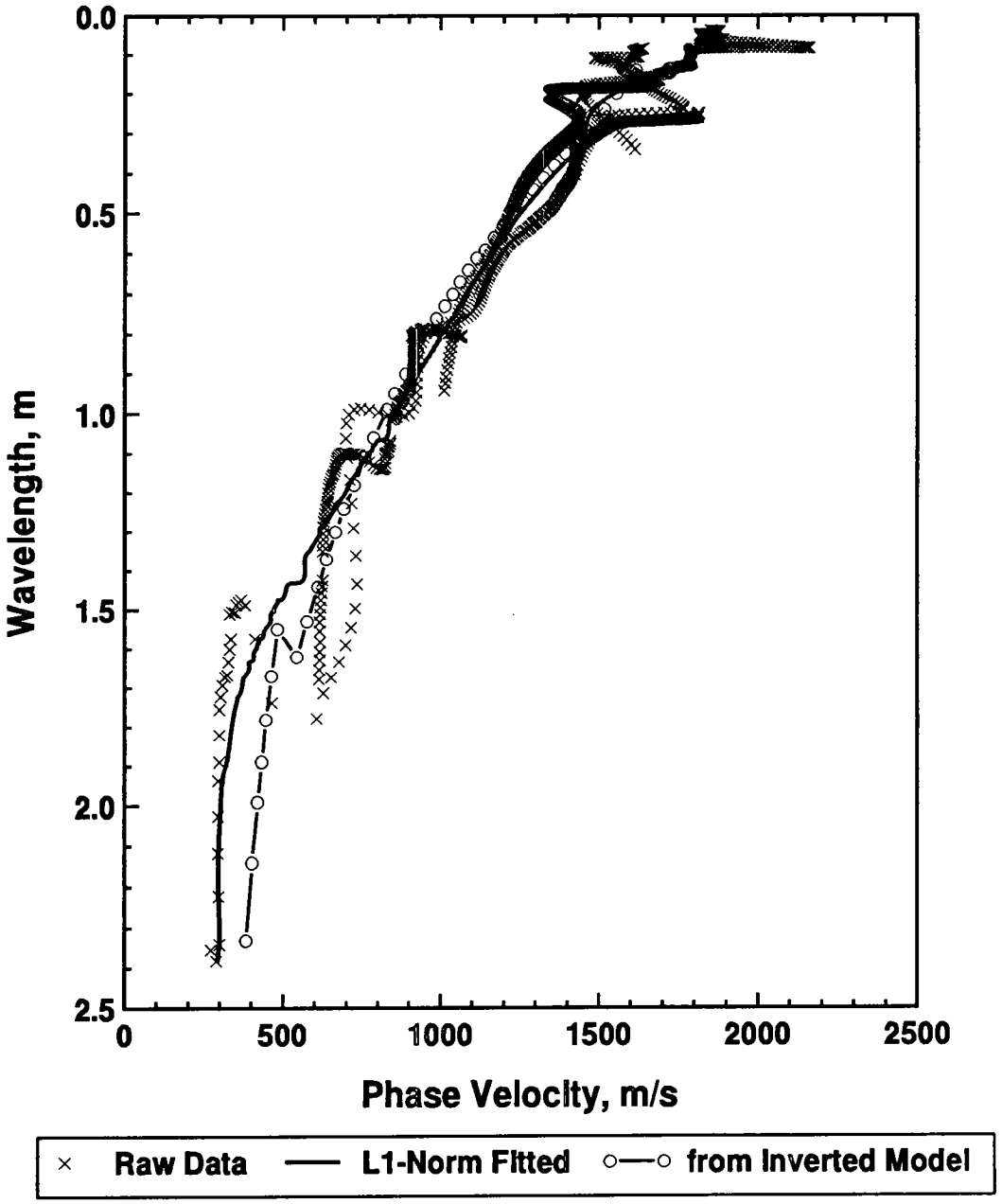

Figure 7.8 - Typical dispersion curves from SASW test

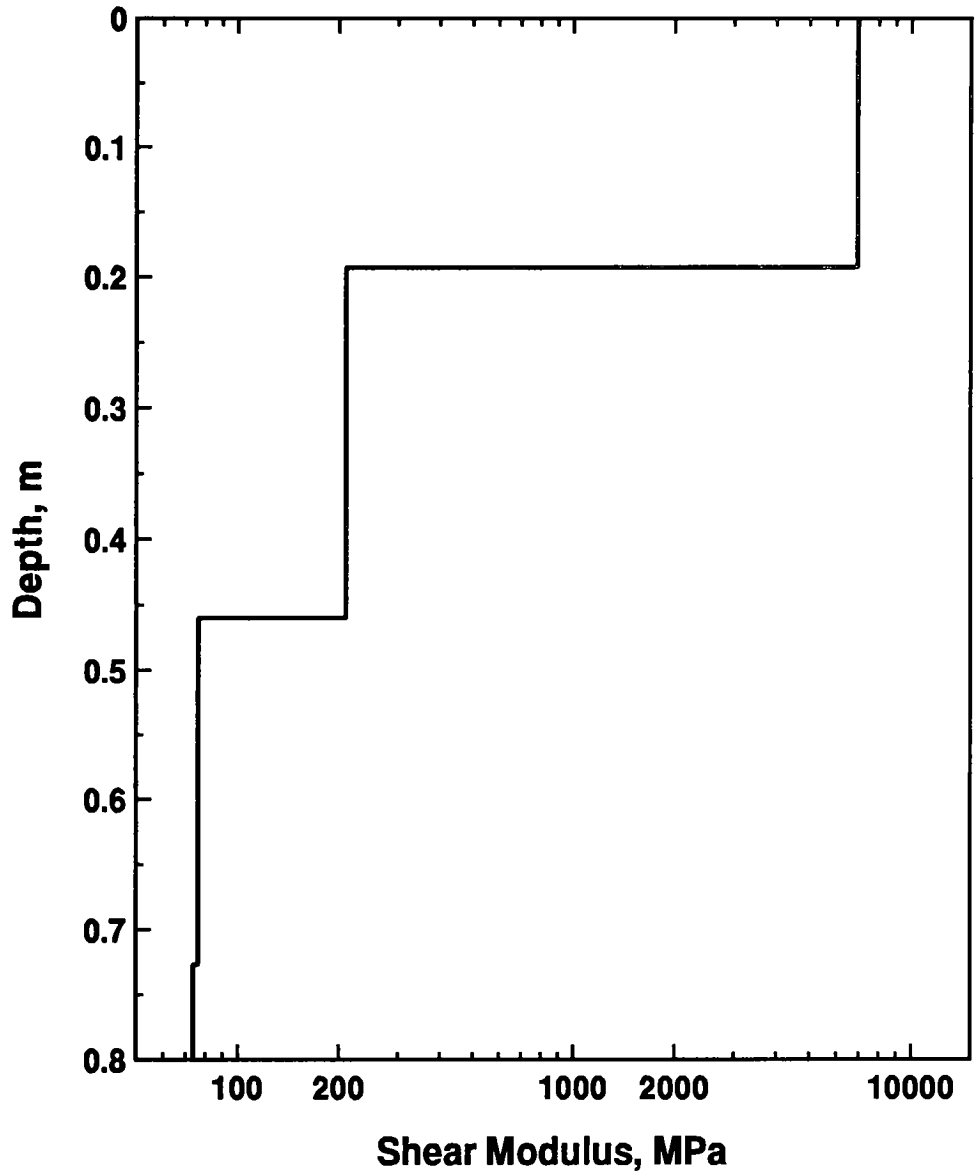

Figure 7.9 - Typical shear modulus profile from SASW test

8

Case Studies: General Comments

The remainder of this report summarizes the results from case studies carried out as a part of this project. The main goals of these tests were to determine the overall effectiveness of the Seismic Pavement Analyzer (SPA) and to confirm that the SPA produced results that were comparable with the conditions being measured. Several intermediate objectives were included in the testing:

1. To ensure that all hardware components of the SPA were working properly;
2. To ensure that the software components were functioning accurately;
3. To ensure that the SPA was easy and fast enough for practical use;
4. To ensure the field-worthiness and ruggedness of the device; and
5. To document ways that the system could be improved and used for maximum efficiency.

The prototype was tested to ensure that the five targets stated above were met; recommendations for improving the design of the device are based upon these tests. The device was evaluated in two phases, local evaluation and field evaluation.

Local Evaluation

Local evaluation focused on confirming that all hardware and software were functioning properly. Testing took place on a facility built at the University of Texas at El Paso (UTEP)

and also at a local Strategic Highway Research Program (SHRP) site. Most of the validation and comprehensive testing was carried out at the UTEP facility. Because of difficulties associated with establishing ground truth, tests at the SHRP site evaluated factors that were not considered at the UTEP facility.

The results from these tests are reported in the next chapter. They prove that the device is adequately replicable and accurate. All parameters can be measured with levels far below the threshold measurement levels for effective maintenance requirements as defined in Chapter 3. Occasional inconsistencies in the results were found. In most cases, the inconsistencies are related to the construction of the facility.

Field Evaluation

In addition to evaluating the software and hardware, the field evaluation also considered the practicality and field-worthiness of the SPA, documenting ways to improve the system. Field testing occurred at seven sites in two states, Texas and Georgia.

Three sites were tested in Texas, one rigid and two flexible. The rigid pavement site had voids and loss of support under the slab. One flexible-pavement site contained areas with wet base. The final site, which was susceptible to stripping, was tested to determine if it would be feasible to predict stripping with the device. The results from these sites are summarized in Chapter 10.

Even though the SPA functioned satisfactorily at the Texas sites, the layering and structure of most pavement sections were ill-defined and more complex than the cases where the prototype was supposed to be functional. This complication promoted changes in the software to make it more robust and more adaptable to the significant and gross variations between the actual and perceived pavement structures.

The improved software was tested in Georgia and found to be more stable and robust. Even though further software modification would be desirable, the testing in Georgia clearly showed that the objectives of the project have been met and all the specified levels of accuracy and precision (see Chapter 11) were within the tolerances defined in Chapter 3.

Four sites were tested in Georgia:

1. A flexible pavement in the early stages of stripping;
2. A rigid pavement with two layers of debonded concret;

3. A flexible pavement with moisture in the foundation; and
4. A rigid pavement containing voids under the slab.

The results from these tests are reported in Chapter 11. Also included in that chapter is the comparison of the ground truth with the actual results. The results from tests in Georgia demonstrate that the device can be appropriately utilized in many maintenance projects.

Determining "Ground Truth"

Two of the most important criteria of the usefulness of any device are accuracy (i.e., the closeness between the existing conditions and the results reported by the device) and precision (i.e., how consistently the device can predict the same condition, if tested several times).

Tests to determine the accuracy should be conducted under controlled conditions: all the relevant parameters should be accurately known or measured. Laboratory testing is ideal. Unfortunately, because of the size of the SPA (about 5 m), actual laboratory tests are not feasible.

As a more realistic approach, the SPA was tested on a prototype facility, that is, on small-scale pavement sections built with typical construction practices and equipment. Better quality control was implemented in the middle of each section than would be on actual roads. However, because of the size of the facility, too many geometrical boundaries had to be included. Typically, it is difficult to obtain the same level of consistency in quality at the boundaries.

In these prototype facilities the interaction between related parameters cannot be considered. For example, the variation in modulus with moisture can be obtained; but the effects of traffic load cannot. Field testing is necessary to study such interactions.

Testing actual pavement sections provides insight to the behavior of pavements when considering the interaction among parameters. However, determining the ground truth is more complex and challenging. First, a base line for comparing the results has to be developed. This base line can be one of several parameters: for example, the laboratory results on the cores obtained at the site, or the results of other accurate field testing devices can be effective.

The current laboratory practice in modulus testing (such as resilient modulus tests) does not provide accurate enough results for this study. Many researchers have shown the problems

with laboratory tests, including specimen disturbance, variation in the state of stress, and the limitations of laboratory equipment.

No existing field testing technique can provide accurate stiffness parameters comparable to those measured with the SPA. The falling weight deflectometer device is used extensively in this study because of a lack of a better alternative. Unfortunately, in most cases the backcalculation process was not successful. Therefore, the variation in the deflection basins was used to determine the variation in stiffness.

Traditionally, pavement engineers have dealt with static (destructive) in situ or laboratory methods to determine the moduli of different layers. These tests yield relatively small modulus values. The deflection-based nondestructive testing devices have traditionally yielded higher moduli than those obtained from the static laboratory or field tests. This result is expected because of the levels of strains and stresses involved and because of different boundary conditions.

The SPA obtains moduli that are even greater than those obtained from the deflection-based equipment. The SPA is strictly measuring linear elastic material properties, whereas the deflection-based devices provide an "effective" linear modulus. However, this matter should not be considered a limitation because of the comparative nature of our testing program. However, the FWD moduli cannot be quantitatively compared with the SPA results.

Field testing of the SPA sometimes resulted in inconsistent data. In many instances, the reasons for the anomaly could be easily identified. Most abnormalities were related to visible distresses on the pavement. Occasionally, a software misinterpretation caused the anomalous results. However, not all ambiguities could be attributed to visible distress or obvious malfunction in the software. We believe that these abnormalities were related to the pavement behavior; however, in-depth investigation was not possible, because of lack of time and funds. In the future it may be appropriate to collect the data at each site first. Based upon the data analysis, several obviously good and bad sections should be cored. A thorough data analysis should determine the abnormal and anomalous points. A second series of coring and field testing could then determine the reasons for the abnormal behaviors. Only in this manner can the strengths and the weaknesses of the device be thoroughly described.

One other limitation of the field tests is that the series of tests was executed only once. Therefore, comparative results are not available to track the weakening effects of the distress precursors with time and traffic. As discussed in Chapter 3, this makes it difficult to develop effective distress models. Future work must address this matter. One simple compromise may be to utilize accelerated testing facilities, such as Accelerated Loading

Facility (ALF) owned and operated by the Federal Highway Administration (FHWA) or the Mobil Load Simulator (MLS) operated by the Texas Department of Transportation.

The field testing program carried out in the present study is not complete: better and more comprehensive field evaluation is needed. Nonetheless, the results demonstrate that

1. An extremely versatile and user-friendly device has been developed
2. All the main objectives of the project have been met
3. The state-of-the art in nondestructive testing devices has been vastly improved
4. A commercially viable device has been manufactured.

More field and laboratory studies are required to fine-tune the device and to strengthen its interpretive power; however, the device can be effectively used on many projects in its present configuration.

Ease of Use

The SPA was exhibited at the 1993 Transportation Research Board Annual Meeting in Washington, D.C. The device was demonstrated to engineers specializing in diverse aspects of pavement engineering. Their reactions to different features of the device, including its ease of use, were carefully documented. The general consensus was that the device is easy to operate. In addition, as the mechanical system is quite simple, they recognized that maintaining the device should also be routine and simple. The ease of maintaining the SPA has been proven during the field testing. Users who operate or manage other NDT devices offered several valuable suggestions, some of which have been implemented. The other suggestions will be implemented in the next modification of the device.

The graphical algorithm feature for demonstrating the results of the data was designed to make the SPA easier to use. The group inspecting the device found that feature quite helpful.

To quantify the operation of the device, the actual speed of the operation was also evaluated. Based on our field documentation, the average testing time—including placing the device, performing tests, reducing field data, and moving to the next point—was about 35 minutes per km when tests are completed at 30-m intervals. Rigid pavements could be tested at about 5.5 minutes per slab for comprehensive analysis (5 points per slab, two edges, two quarter points and the middle), and at about 3.5 minutes per slab for tests carried out at the two joints and the middle of each slab.

The setup time in the morning was about 20 minutes; this time could have been shorter with a dedicated vehicle. Routing the wiring through a junction box on the trailer would also reduce setup time. This will be implemented in the next prototype.

Precision of Measurements

The precision of the measurements was determined by conducting tests at the same locations between five and ten times. These tests were conducted at almost all sites tested. To determine the precision, it was assumed that the operator would not use any judgement at all; that is, the data were collected but never inspected during the tests. The coefficients of variation of the reduced data are reported as the indication of precision in table 8.1. Each value we obtained by averaging the results from tests carried out at all sites.

In general, the precision reported for tests in Georgia is better than that obtained from tests in Texas. This improvement is the direct result of software changes made after tests in Texas. A detailed description of these modifications is included in Chapter 10.

The precision levels with which the measurements have to be carried out were introduced in Chapter 3. These precision levels are a function of acceptable levels of distress and the number of years before maintenance. In all cases, the precision levels reported in table 8.1 are much less than those necessary for small amounts of acceptable distress (less than 5 percent) with a three-year lead time for scheduling maintenance. Therefore, the precision reported in table 8.1 is quite adequate for maintenance purposes.

A specific example may be helpful. From table 8.1, the Georgia tests showed a precision of about 13 percent when using the inversion process to determine the modulus of base. From table 3.2, a level of precision of 13 percent will translate to a condition where the maintenance engineer can examine a site before any cracking is evident and predict whether 15 percent or more of the section will crack within the next three years.

In another example, the impulse-response test is used to determine the existence of voids under rigid pavements. From table 8.1, a 6 percent precision was obtained in Georgia for the impulse-response tests. Based upon table 3.3, this will allow testing a slab and determining if 5 percent of the slab will crack within the next three years. Therefore, it can be seen that the levels of precision reported for the SPA are more than adequate for maintenance measurements.

Table 8.1 - Precision associated with each measurement technique

Measurement Technique		Precision, percent	
		Texas	Georgia
Ultrasonic Surface Wave		5	5
Ultrasonic Body Wave		17	9
Impulse Response		8	6
Impact Echo		21	9
SASW	Dispersion Curve	-*	7
	Inversion Process	-*	13

*SASW Tests were not used at these sites.

Field-Worthiness of the SPA

The SPA was towed for more than 8,000 km. It was driven from El Paso, Texas to Houston, Texas; College Station, Texas; Washington, D.C.; Atlanta, Georgia; Augusta, Georgia; and Las Vegas, Nevada. Including the tests at UTEP and around El Paso, more than 1500 individual tests have been carried out so far. The following mechanical problems have occurred:

1. Loss of an air compressor ($60) as a result of running the computer on the same power line as the compressor. This was remedied by isolating the electric line to the compressor.

2. Loss of one load cell wire ($12) because of fatigue stress on the connector.

3. Breaking of one wire on the hammer mounting assembly ($12) from the wire tie.

4. Malfunction of one source piston in subfreezing temperature because of freezing water introduced in the lines by condensation. The problem can be remedied by adding a moisture trap and filter between the compressor and the pistons at a cost of about $50.

5. Scraping of the sensor feet and loss of the protective material at the end of the feet ($1 per sensor). This problem occurred under two circumstances: driving off of or onto very steep ramps, and driving while the sensors are still placed on the pavement. The former can be addressed by raising the entire sensor assembly system. The latter can be prevented by adding a parking brake switch to the system to cut off the electric power to the SPA, which immediately removes all sensors and the source assembly from the pavement.

6. Failure of several electronic components occurred during the early stages of operating the SPA. Most of these failures were eliminated by slight redesign of the faulty components.

In general, even though some redesign and mainstreaming of the SPA may be desirable, in its present stage the prototype seems rugged and field-worthy.

Format of Presentation of Case Studies

At each site tested, the primary goal was to detect a specific pavement condition. The SPA measures a large number of parameters, some of which are critical for detecting the condition. Many secondary parameters, not necessary to detect a particular condition, are collected anyway to gain experience with the device. The extra time required for collecting and reducing a complete set of data is minimal.

Each case study states the primary goal, the primary pavement parameters, and the test methods. The numerical results are presented and interpreted. Conclusions are drawn regarding the applicability and success of the SPA. The secondary parameters are presented, interpreted, and discussed in the appendices.

9

Case Studies: Local Sites

Tests were carried out at the University of Texas at El Paso (UTEP) facility to determine the accuracy and precision of the Seismic Pavement Analyzer under controlled conditions. One rigid- and two flexible-pavement sites were tested. In addition a Strategic Highway Research Program (SHRP) test site near El Paso, Texas was tested. The results are summarized below.

UTEP Rigid-Pavement Facility

The rigid-pavement facility at UTEP is about 9 m wide 13.5 m long, and 200 mm thick. The facility is designed to simulate a two-lane highway with a concrete shoulder on one side and a free edge on the other. A schematic of the slabs is shown in figure 9.1. As seen in the figure, the facility consists of four full slabs, each 3.6 m $\times$ 4.5 m and eight smaller slabs. These eight slabs consist of four 3.6 m $\times$ 2.3 m, two 4.5 m $\times$ 1.8 m, and two 2.3 m $\times$ 1.8 m. Half of the facility is control section with no defects introduced. Numerous defects have been introduced into the other half of the facility:

1. Voids under the slab (corner, edge, and middle voids);
2. Moisture under the slab; and
3. Delamination of concrete.

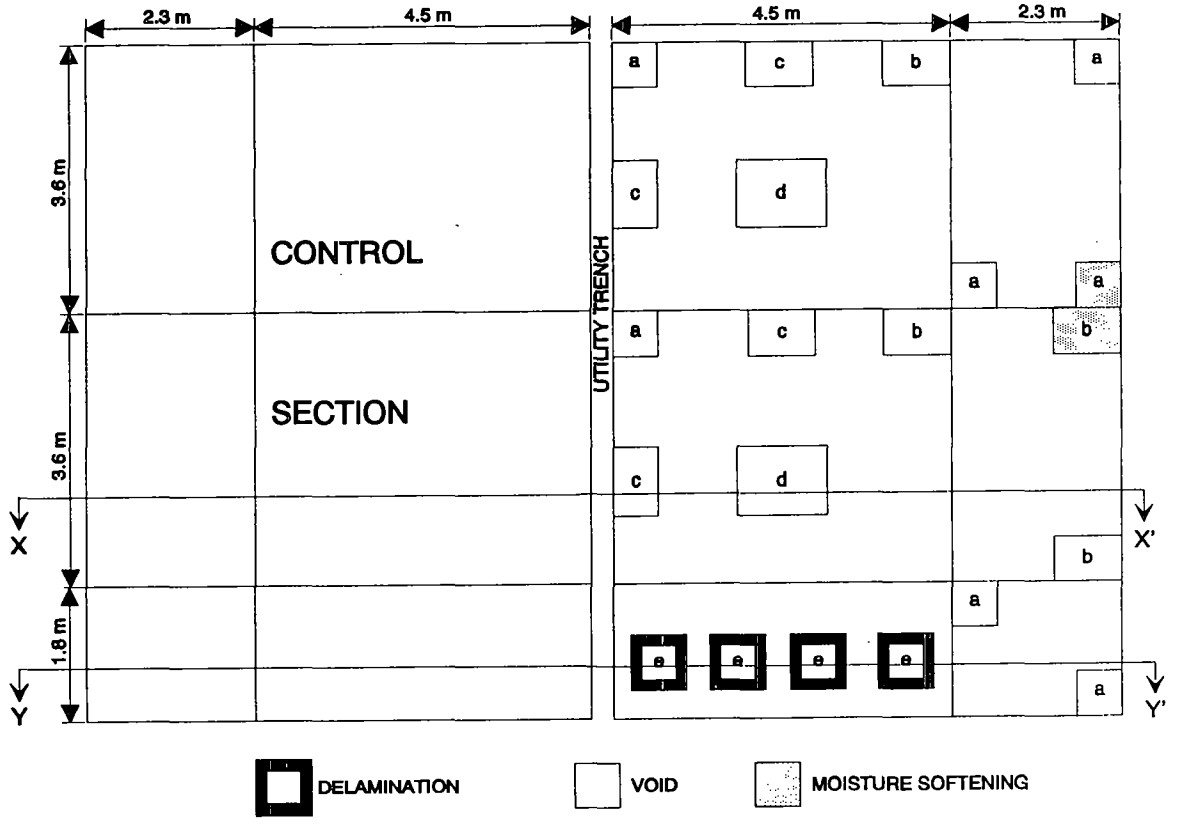

a) Plan View

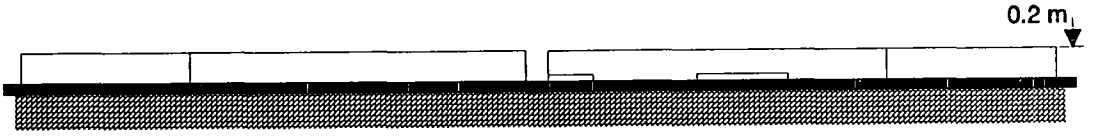

b) Section X-X'

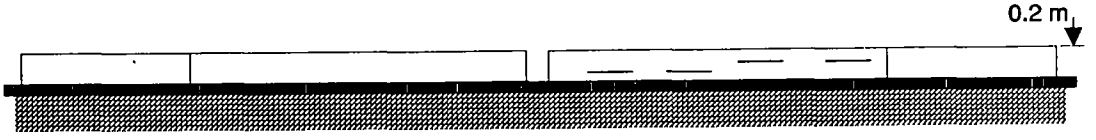

c) Section Y-Y'

Figure 9.1 - UTEP-rigid pavement facility

The corner and edge voids were constructed by placing plastic bags filled with sugar under the wet concrete. Once the concrete dried, the sugar was removed using air pressure. The middle voids were constructed using styrofoam materials. The thickness of the voids varied from 3 mm to 12 mm. All voids, except those in the middle, were equipped with a 6-mm hose so that water could be introduced into them.

Many tests were conducted at this facility. However, the results from the wet condition are not included. Phase II of this study demonstrated that as long as a void is not completely saturated, the water would not substantially affect the major parameters for detecting voids (i.e., the modulus of subgrade and the damping ratio). Given the nature of the subgrade at the UTEP facility, full saturation is not possible without substantial and unrecoverable damage to the facility.

Repeatability of Various Tests

Some tests evaluated the SPA's ability to repeat results. In this report, precision is used to indicate such repeatability. Furthermore, the coefficient of variation (standard deviation divided by the mean) is used to represent precision.

One point was tested ten times to determine the repeatability of the results. To minimize the bias in the data collection, the results were not inspected in the field. Therefore, occasional outliers that would typically be removed from the data set were included. Statistical analyses determined the coefficient of variation. These results are obtained from the latest version of software, modified after the preliminary tests at the local sites and the three Texas sites. Therefore, the results represent the state of the equipment at the completion of the project. These levels of precision also correspond to the case studies executed in Georgia.

The values of Young's modulus from the ten ultrasonic-body-wave tests are shown in figure 9.2. The modulus is about 33 GPa, which indicates average concrete. Some surface honeycombing has occurred at the site. The results were consistent except for the first two repeats, possibly because of the SPA's placement. At any rate, the maximum difference between the largest and smallest value is less than 7 percent. The coefficient of variation for determining Young's modulus with the ultrasonic-body-wave method is about 2 percent. Such a level of repeatability is excellent, and no further modification is necessary to improve this algorithm.

The results from repeatability tests of other parameters are included in table 9.1 but are not shown graphically.

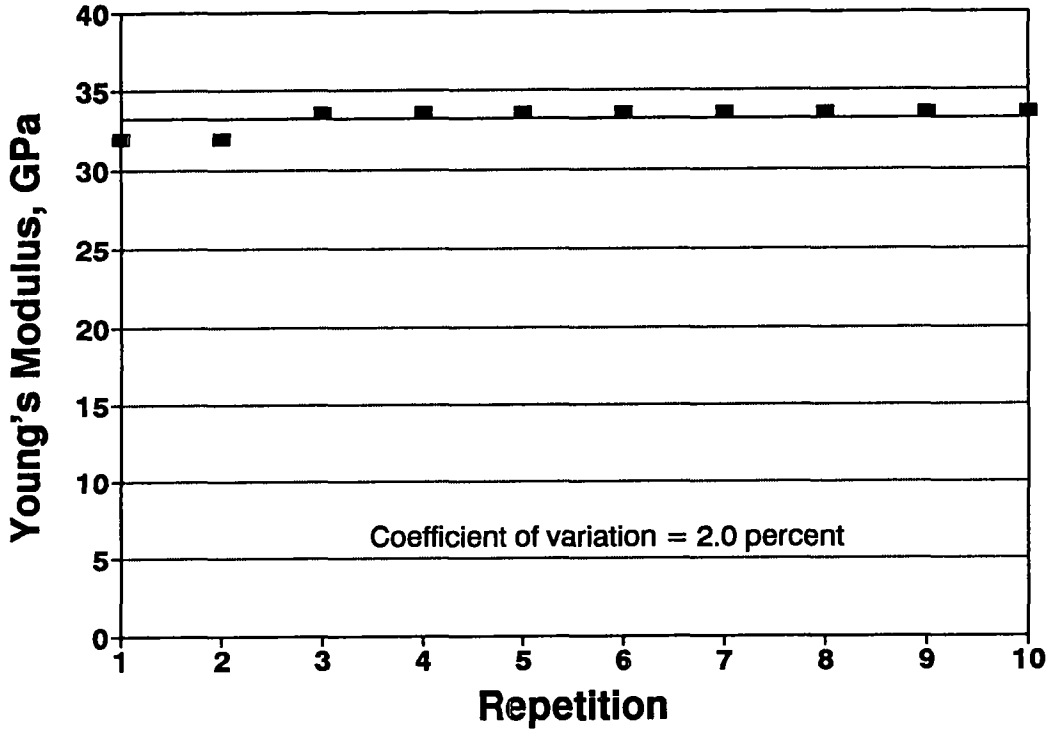

Figure 9.2 - Repeatability of SPA in measuring Young's modulus with ultrasonic body wave method

Table 9.1 - Levels of repeatability of different tests on rigid pavements

Test Method	Specified Precision,* percent	Measured Precision, percent
Ultrasonic Body Waves (Young's Modulus)	10	2.0
Ultrasonic Surface Waves (Shear Modulus)	10	2.1
Impact Echo (Thickness)	10	3.8
Impulse Response (Modulus)	15	5.5
Impulse Response (Damping Ratio)	15	15.1 (with one outlier) 7.0 (without outlier)

*Developed based on experience with method and approved during conceptual design.

Shear moduli from the ultrasonic-surface-wave method are determined with even higher precision. Basically, all the modulus values were close to 14 GPa, from the shear and Young's modulus, with a coefficient of variation of about 2 percent. Poisson's ratio can be calculated (see Appendix A). Poisson's ratio for this material was calculated as about 0.16, which is quite reasonable. Based on these tests, it can be concluded that the ultrasonic-surface-wave method has excellent repeatability and can be used reliably.

The impact-echo (IE) technique was used to determine the thickness of the portland cement concrete. The average thickness of the slab was measured as 190 mm, with a coefficient of variation of about 5 percent. The actual thickness of the concrete at the facility is about 200 mm $\pm$ 10 mm. The coefficient of variation of the IE test is directly influenced by the coefficient of variation associated with the ultrasonic-body-wave (UBW) tests, because the compression wave velocity obtained from the UBW method is used in determining the thickness. As such, the precision of the IE method is typically less than that of the UBW method. A five percent coefficient of variation is quite acceptable and, therefore, the method can be used with confidence.

The variation in subgrade modulus from the impulse-response technique is slightly higher than that of the other techniques discussed so far. The subgrade modulus varied from a low of about 17 MPa to a high of about 20 MPa, with an average value of about 18.5 MPa. This represents a soft subgrade, which is characteristic of the subgrade at the facility. The precision of the method is less than 6 percent, far below the 15 percent level originally expected from the method and the analysis.

The damping ratio exhibited an oscillation between 60 and 70 percent, with an average of about 65 percent with one outlier. The coefficient of variation of the damping ratio when the outlier was included is about 15 percent. Without the outlier, the precision is about 7 percent. A level of 15 percent was originally thought to be achievable. For damping ratios around and above 70 percent, where the maximum stiffness occurs at 0.0 Hz (static) frequency, more scatter in data would be expected. For lower damping ratios, the precision should be better because the dominant peak is much sharper.

From this exercise it can be concluded that the SPA meets or exceeds all precision levels specified for rigid pavements.

Accuracy in Detecting Voids

A series of tests was carried out to determine the ability of the SPA to detect known voids. Tests were carried out along a longitudinal line on both the intact and the defective slabs as as shown in figure 9.3. The slab was tested at 30-cm intervals. The primary test for detecting voids is the impulse-response test.

The measurements of the modulus from impulse-response testing at the site are also shown in figure 9.3. Three defects existed in the defective slabs. The first defect was located between the edge of the slab and test point 2 (void 1 in figure 9.3); the second defect was located between test points 5 and 9 (void 2 in figure 9.3); and the third one between test point 12 and the edge of the slab (void 3 in figure 9.3). The existence of void 1 is difficult to interpret from the data because it is rather small. The two peaks at test points 2 and 13 occur because of the geometry of this specific test slab. It was difficult to situate the device precisely on these points. The other two voids are quite nicely exhibited in the figure. For void 2, the modulus decreases to two-thirds of the modulus measured at the intact slab. For void 3, the decrease is about 25 percent. The reason for such a small change in the modulus is that the intact slab had eroded at the corner as a result of the unexpectedly wet seasons El Paso had been experiencing. The damping ratio very nicely supports the fact that tests carried out on the defective points exhibit much lower damping ratios (see figure 9.3).

This example demonstrates that the SPA can accurately measure voids in actual pavements.

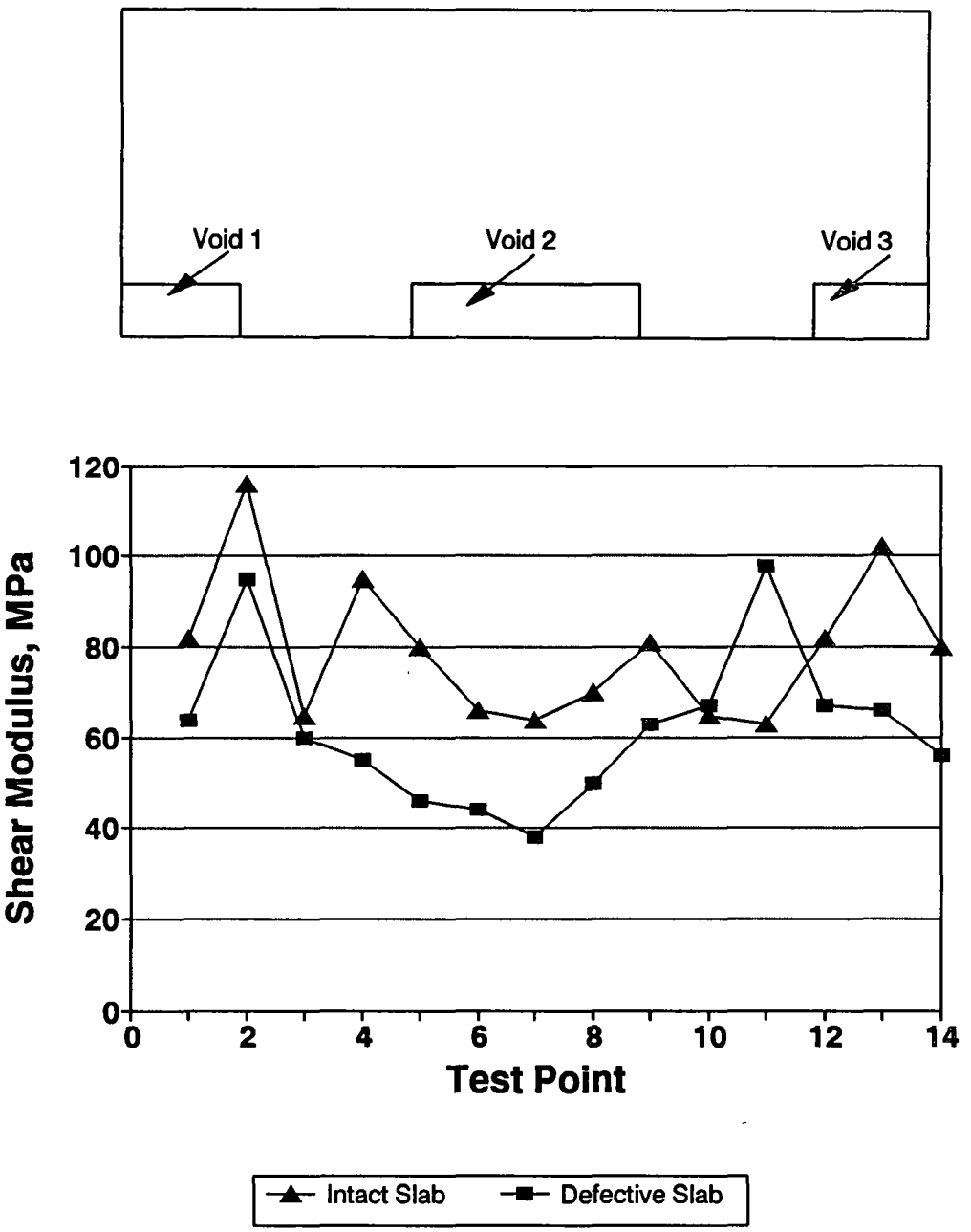

Figure 9.3 - Variation in subgrade modulus from impulse-response test

UTEP Flexible-Pavement Facility

The flexible-testing facility consists of two 6-m by 6-m test pads. One section consists of 75 mm of asphalt concrete with 150 mm of base over subgrade. The other section consists of 150 mm of AC with 300 mm of base over subgrade. Each test pad is divided into two longitudinal sections (see figure 9.4). One half (3 m by 6 m) is used as the control section. Defects are introduced into the other half. The half containing defects is divided into three sections. One of the following defects is introduced into each section:

1. Stripping of the asphalt layer;
2. Moisture in the base; and
3. Moisture in the base and subgrade.

All paving materials were acquired from vendors approved by the Texas Department of Transportation (TxDOT). All mix designs met the requirements of the TxDOT.

Moisture can be introduced to the base and subgrade or to the stripped section using soaker hoses spaced 30 cm apart. The amount and pressure of water introduced to the area are carefully controlled with an accurate flow-meter and a pressure regulator.

Repeatability of Various Tests

On the rigid slab, a series of tests evaluated the SPA's ability to produce repeatable results. Both the thick and the thin pavement structures were tested.

The measurements of Young's modulus from the ultrasonic-body-wave tests, the shear modulus from the ultrasonic-surface-wave tests, and modulus of the subgrade from the impulse-response tests for the thin and thick sections are all shown in Table 9.2. For all tests, the coefficients of variation for this section are between five and six percent. Considering that the data reduction is completely carried out in the field, such a variation is quite acceptable and these levels are well within the anticipated levels of precision specified in Chapter 3.

The coefficients of variation for the thick section are even less than those obtained for the thin section. The variation is on the order of 1.5 percent to 4 percent, except for the ultrasonic-surface-wave method where an outlier exists. In this case the precision is about 13.8 percent. If the outlier is ignored, the coefficient of variation is less than 5 percent.

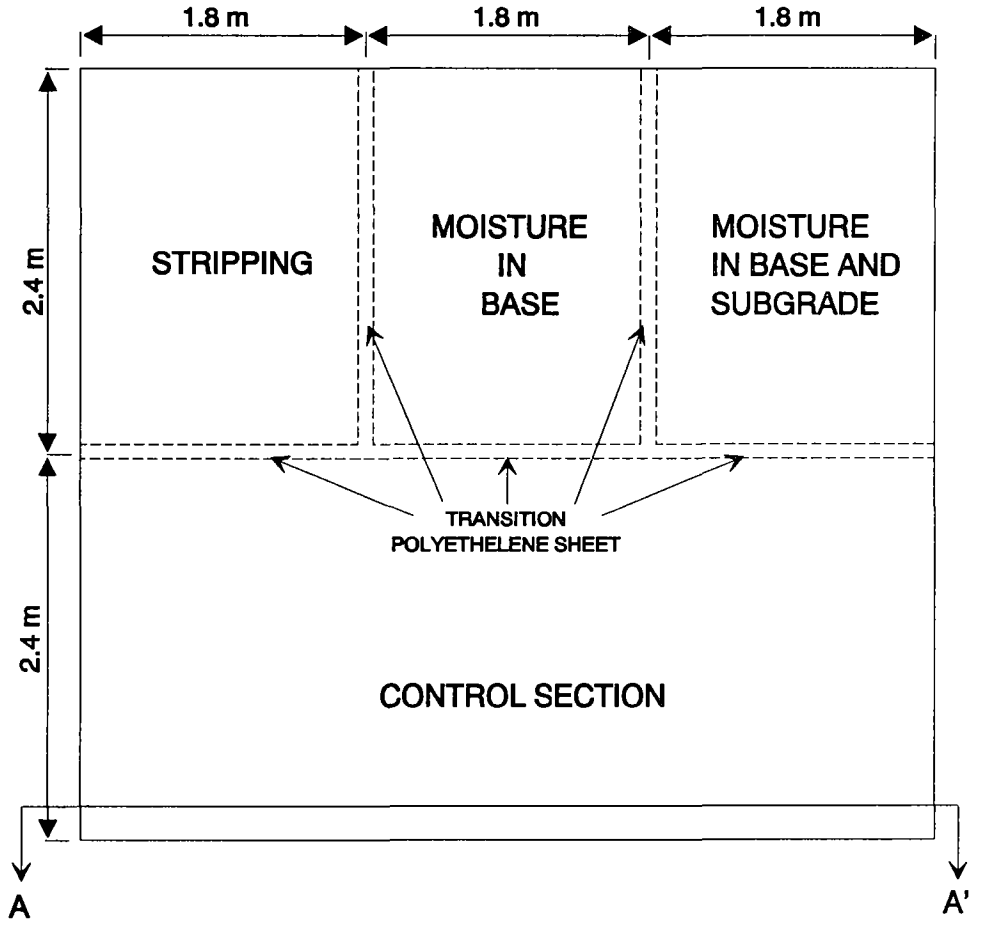

a) Plan View

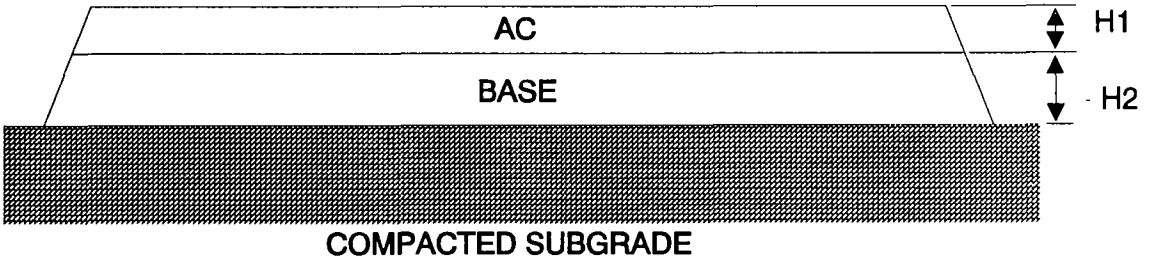

b) Section A-A'

Figure 9.4 - Schematic of flexible-pavement sites

Table 9.2 - Levels of repeatability of different tests on flexible-pavement sections

Test Method	Precision, percent		
	Specified*	Thin Section	Thick Section
Ultrasonic Body Waves (Young's Modulus)	10	5.8	1.5
Ultrasonic Surface Waves (Shear Modulus)	10	4.9	13.8 (with one outlier) 4.8 (without outlier)
Impulse Response (Modulus)	15	5.7	2.8

*Developed based on experience with method and approved during conceptual design.

This indicates that the thicker pavements are tested with a better repeatability. Since the same size aggregates were used in the base and AC of the thick and thin sections, it is normal to obtain a more uniform material property for the thicker section. However, for all results shown, the level of repeatability is quite acceptable, and the levels of precision specified were achieved.

The repeatability of the SASW method was also established at this site but those results are not included in table 9.2. Five dispersion curves from five repeat tests were within 5 percent of each other, and in no case were the differences more than 9 percent. Shear modulus profiles were obtained from individual dispersion curves. The greatest difference in the moduli was for the base layer, at about 13 percent (specified as 20 percent). The modulus of the AC and subgrade were within 5 to 9 percent (specified as 10 and 15 percent, respectively) of each other. Once again, all specified precision levels are met.

Effects of Moisture in the Base and Subgrade

A series of tests was carried out to evaluate the effects of change in moisture on the modulus of the base and subgrade. To achieve this goal, the two sections marked as "Moisture in Base" and "Moisture in Base and Subgrade" were continuously tested for about 6 hours. For the first section ("Moisture in Base"), water was introduced only to the base layer. For the other section, water was introduced simultaneously to the base and the subgrade.

The water was slowly introduced to the base and subgrade so that the average water content of the material changed at a rate of about 2 percent per hour. The amount of water introduced to the base was carefully monitored. To obtain the average change in water content, the amount of water added to the base was divided by the mass of the material being tested. This allows some approximation of the value of the moisture. Tests were

executed every 30 minutes. Tests were stopped when the water started seeping from the sides of the section.

The two test methods appropriate for determining the softening of base and subgrade are Impulse Response and SASW. The impulse-response tests determine the variation in the overall stiffness of the section with moisture (see Chapter 4). The SASW method is employed to obtain a more comprehensive picture of the section.

Moisture in the Base

The measurements of the effective subgrade modulus as the water content changed are shown in figure 9.5. Each test was repeated five times. The mean and the range within one standard deviation is shown in the figure. The standard deviation is larger than anticipated because of difficulties in situating the device on the slab. The latest version of the SPA is about 5 m long, and the distance between the source and the last sensor is about 2.1 m; the effective width of the section tested is about 1.5 m. To place as many sensors as possible on the section, the SPA had to be located almost at the edge of the AC (about 15 cm from the edge). As indicated in Chapter 8, the edge may not be as uniform as the center at facilities such as UTEP. In general, however, the coefficient of variation is less than 12 percent, which is quite acceptable.

The variation with moisture in the subgrade modulus exhibits a gradual increase in the modulus from the "dry" state to a peak, followed by a gradual decrease until the saturated condition is reached. This is a valid variation, as demonstrated by Wu et al. (1984) and Qian (1990). They have shown that for each material an "optimum" water content (or degree of saturation) exists at which the modulus is maximum. If the moisture content is less or more than the optimum value, the modulus will be lower. They have also shown that the modulus in the dry state is approximately equal to the modulus in the saturated state. Given the amount of solar heat and radiation that the pavement sections are exposed to in El Paso, it is not unreasonable to have a relatively dry material. Some specimens were taken from the base and subgrade to determine the water content. It was found that the in situ water content of both materials before adding water was about 3 to 5 percent. The optimum water content of the base was about 11 percent. Therefore, the material has dried substantially in the 1.5 years from the completion of the facility to the testing period.

As reflected in figure 9.5, the effective subgrade modulus before adding water was about 35 MPa. Upon adding water the modulus became as high as 50 MPa, a 40 percent increase. The modulus in the saturated condition was about 35 MPa. Once again, this behavior is representative of the behavior described above.

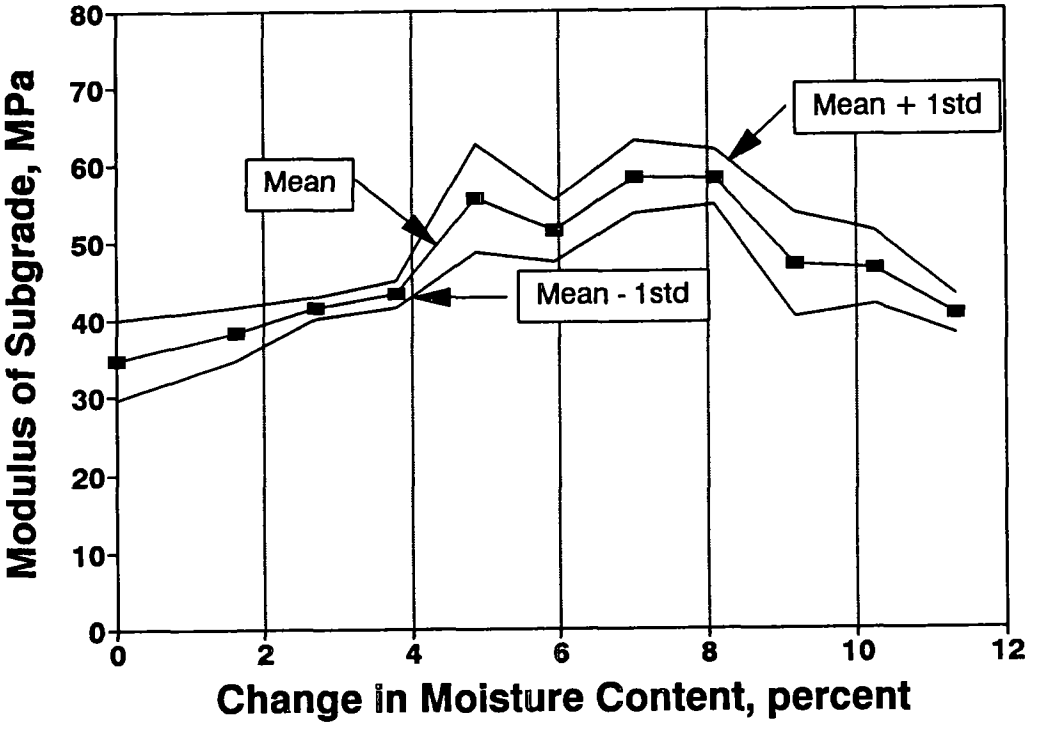

Figure 9.5 - Variation in modulus with moisture content when water introduced to base

The results from the SASW tests for the wet, dry, and moist conditions are summarized in table 9.3. The moist condition refers to the case when the change in water content was about 7 percent. The modulus of the AC layer was generally constant at about 4200 MPa. This is indicative of a normal AC layer. Not much variation in the modulus was observed because of the small variation in the temperature (from about 18° to 23°C).

Table 9.3 - Variation in moduli of different layers with moisture when water added to base

Moisture Condition	Shear Modulus, MPa		
	AC layer	Base	Subgrade
Dry	4594	149	145
Moist*	4281	172	141
Saturated	4033	160	138

*Refers to the case when the change of moisture content was about 7 percent.

The modulus of base varies between 150 MPa for the dry condition, to about 170 MPa for the moist condition, to about 160 MPa for the saturated condition. The variation is smaller than from the impulse-response test because the last sensor used in the SASW tests was located on the opposite side of the section from where the water was introduced. This resulted in a dispersion curve that covers a region partially affected by the water and partially not. However, the variation in the modulus of the base clearly shows the increase and decrease in the modulus.

Finally, the modulus of the subgrade is quite constant during the test. This is expected because the water was introduced to the base from the interface of the base and AC layer; therefore, most of the water was contained in the base layer.

Several conclusions can be drawn from this study. First, the moisture content of one layer alone is not a good indication of softening of the base or subgrade. As shown above and as reported in the literature, the increase in water content in some cases may have a stiffening effect.

The impulse-response method can determine the overall softening of the pavement section. The SASW method can determine which layer has been affected by the moisture.

Moisture in the Base and Subgrade

Similar tests were repeated at the section labeled as "Moisture in Base and Subgrade" in figure 9.4. In this case, the water was simultaneously introduced to the base and subgrade. The measurements of the effective modulus as the moisture changed are presented in figure 9.6. The trend observed here is similar to the results of the previous case. As moisture was added to the base and subgrade, the modulus first increased and then decreased. Therefore, an optimum water content exists for the material: the modulus varied between a minimum of about 12 MPa for the dry and saturated conditions to a maximum of about 20 MPa for the moist condition.

The modulus of subgrade measured in the dry state at this section is significantly lower than that of the section where water was introduced only to the base. This occurred because the SPA had to be situated close to the free edge of the facility, where the materials are typically softer.

As shown in figure 9.6, the modulus increased until the water content had increased by up to approximately 7 percent. This is comparable with the results when water was added to the base only as illustrated in figure 9.5. A change in water content of up to 12 percent (saturation condition) did not result in a lower modulus than the initial condition.

The SASW results for the dry, saturated, and moist conditions are included in table 9.4. The modulus of the AC layer varied between 3500 MPa and 4100 MPa. Therefore, the AC modulus was not significantly affected by the change in water content. This behavior was expected, because the temperature did not vary much during these tests.

The shear modulus of the base layer varied—from 134 MPa in the dry condition, to a maximum of 174 MPa in the moist condition, to 125 MPa in the saturated condition. A

Table 9.4 - Variation in moduli of different layers with moisture when water added to base and subgrade

Moisture Condition	Shear Modulus, MPa		
	AC layer	Base	Subgrade
Dry	3700	134	107
Moist*	4117	174	117
Saturated	3509	125	92

*Refers to the case when the change of moisture content was about 7 percent.

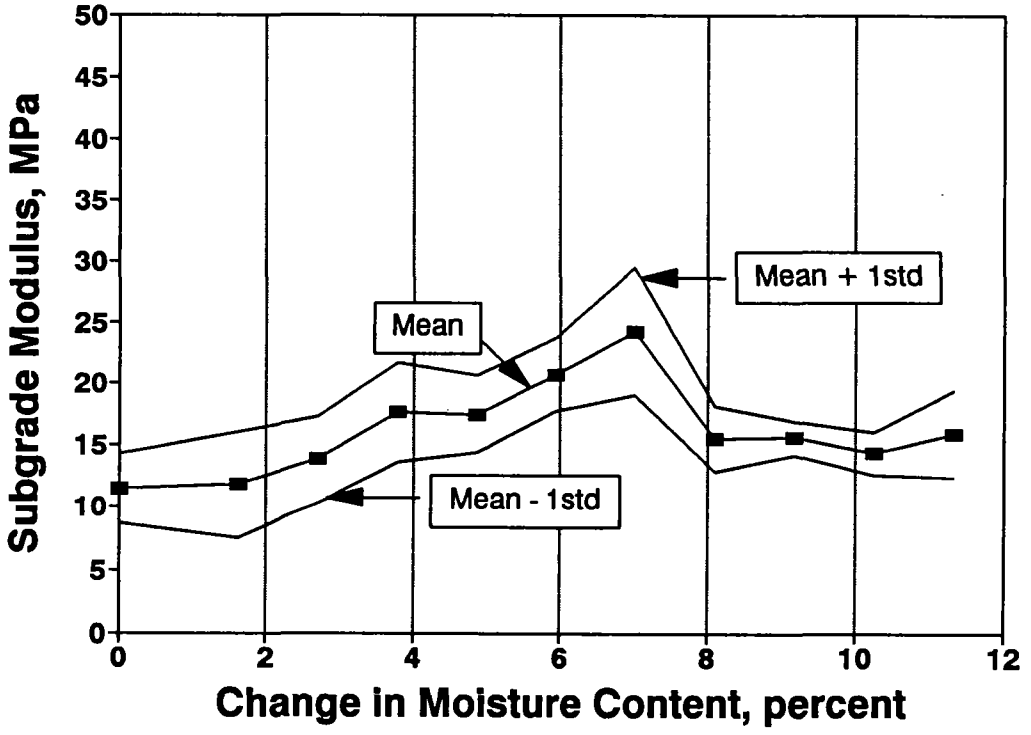

Figure 9.6 - Variation in modulus with moisture content when water introduced to base and subgrade

comparison of tables 9.3 and 9.4 reveals that the modulus of base for the dry and moist conditions are quite comparable between this experiment (where water was added to the base and subgrade) and the previous case study (where only the base was wetted). However, the modulus for the saturated case is lower when water was introduced to the base and subgrade. This may be because water was introduced at both the top and the bottom of the layer: the base layer might have been much wetter than when the water was introduced only to the base. The modulus of the subgrade is also lower when water was introduced to the base and subgrade than when the moisture was added only to the base, for the same reasons.

The subgrade modulus varied from 107 MPa to 117 MPa to 92 MPa for the dry, wet, and saturated cases, respectively. Once again, the modulus increased with the moisture to a maximum, and then decreased with further moisture.

This case study demonstrates that the methodology proposed is effective and can successfully determine which layer or layers are most affected by a change in moisture. In addition, it has been shown that the moisture content alone is not a significant factor affecting the stiffness of a section. Other factors such as the type of soil and optimum water content should also be considered.

SHRP Site

A section of a SHRP site near El Paso, Texas, was tested with the SPA. SHRP has been studying the effects of a number of preventive maintenance treatments on the performance of rigid and flexible pavements. Flexible sites—Special Purpose Sites 3 (SPS3)—are located throughout the United States. Four different treatments are applied at SPS3 sites: thin AC overlay, crack seal, chip seal, and slurry seal. An untreated control section also exists at each site.

The original pavement at the SHRP SPS3 site near El Paso consisted of 61 mm of asphalt concrete, over 213 mm of crushed-stone base, over a silty subgrade. Four treatments were applied to the site: a 25-mm overlay, a 13-mm slurry seal, crack seal, and finally, a chip seal with a thickness of about 13 mm.

The section numbers and corresponding treatments are summarized in table 9.5. Tests were carried out at 30-m intervals between the start and end of the first three sections. The last two sections could not be tested because of lack of time and bad climatic conditions.

Table 9.5 - Characteristics of points tested at SPS3 site

Section	Treatment	Remarks
48L310	Thin Overlay	25 mm thick
48L320	Slurry	13 mm thick
48L330	Crack Seal	---
48L340	Control	---
48L350	Chip Seal	13 mm thick

FWD tests were carried out at the sites one week after the SPA tests were performed. The deflection basins at each section are represented in figure 9.7. The deflection basins vary significantly within each section; however, on the average, the overlaid section seems stiffest because of the lowest deflections. In contrast, the crack-sealed section yielded the highest deflections and should be the least stiff of the three sections.

Attempts to back-calculate the moduli using the BISDEF program failed because of the large differences between the measured and calculated deflections. The absolute percent sums of mismatch in deflection-basin fitting were typically about 8 percent and therefore the moduli are not presented here.

The moduli of the AC layer tended toward the upper limit of the acceptable modulus values input to the BISDEF program. The modulus values of the base layer varied significantly. The modulus values of subgrade varied between 100 MPa and 180 MPa. In general, given the large mismatch in the basin-fitting, the values of back-calculated moduli are questionable, and they are not considered further.

This case study also exhibits the comprehensiveness of data collected with SPA. The moduli and other information for each point are collected and reduced in about 57 seconds.

Ultrasonic-Body-Wave Method

The values of Young's modulus for the three sections tested are shown in figure 9.8. The variation in the modulus is rather small. The pavement temperature at the time of the field test varied between 13.5° and 16.5°C. For such a temperature range, the Young's moduli correspond to an average-quality AC material.

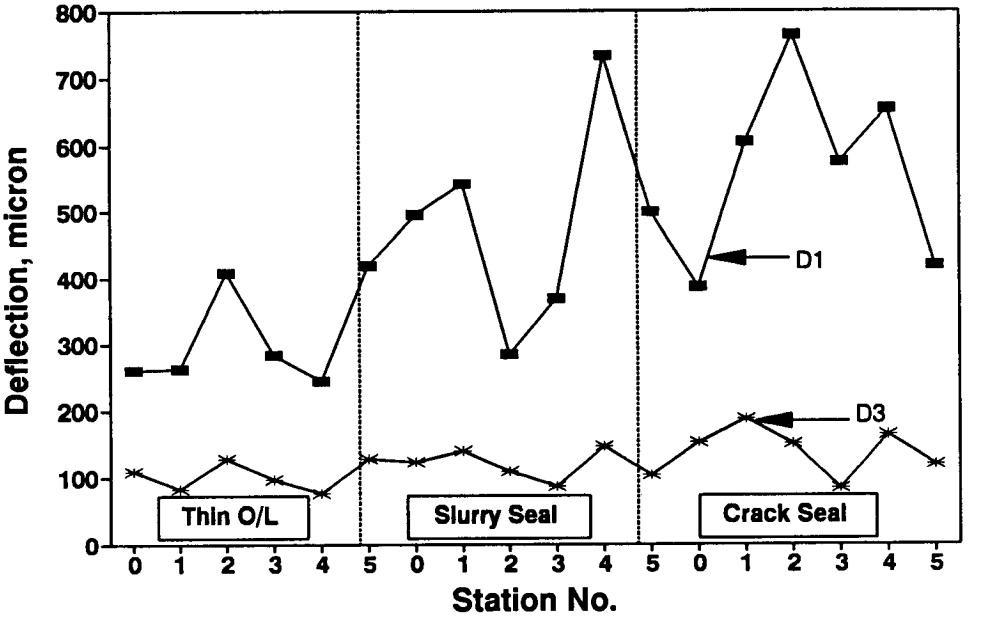

a) Sensors Close to Load

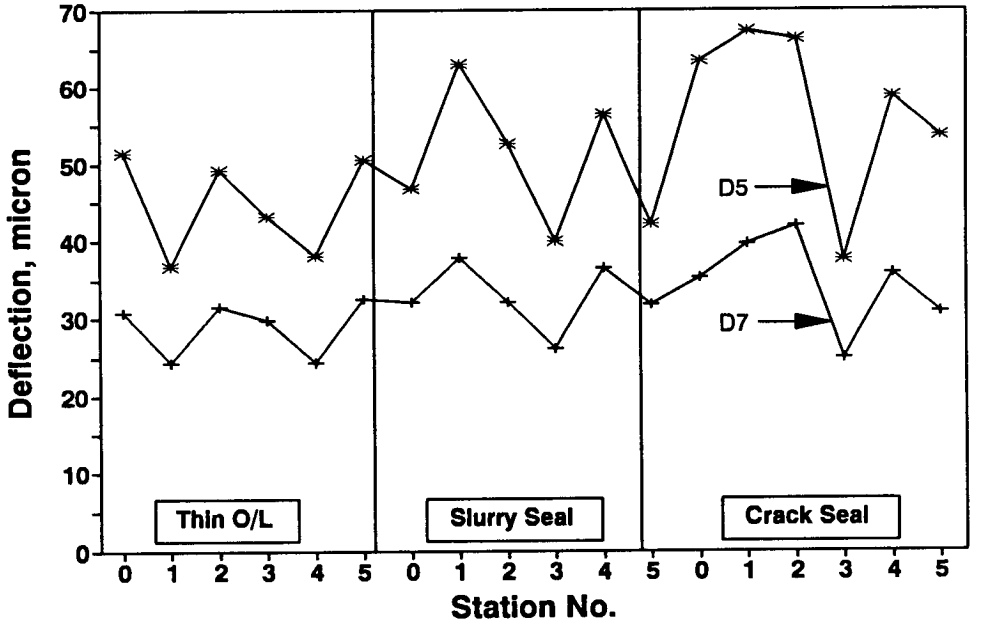

b) Sensors Far from Load

Figure 9.7 - Deflection basins measured at SPS3 using an FWD device

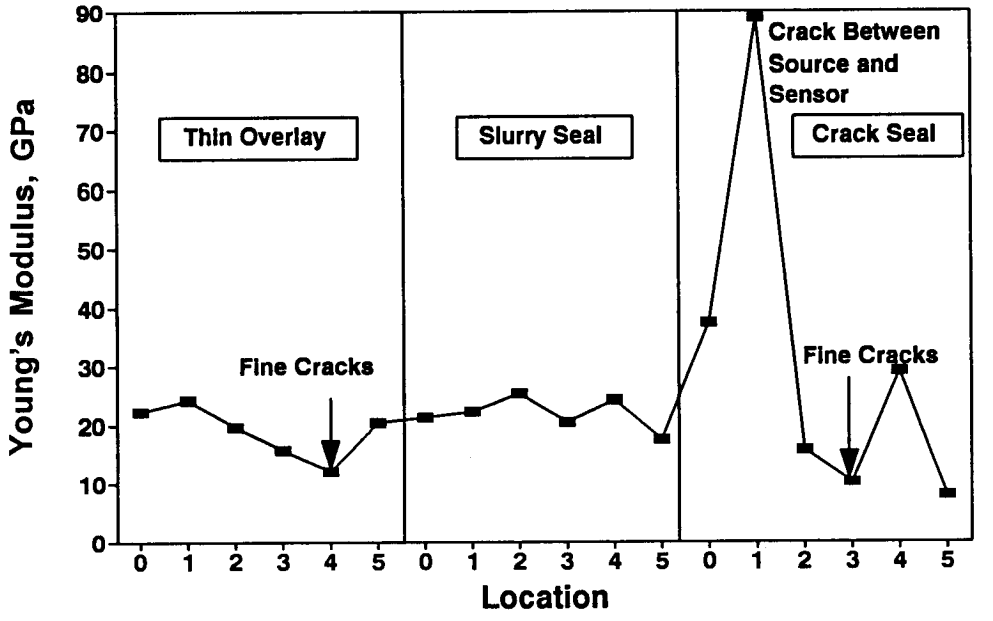

Figure 9.8 - Young's moduli determined at SPS3 site

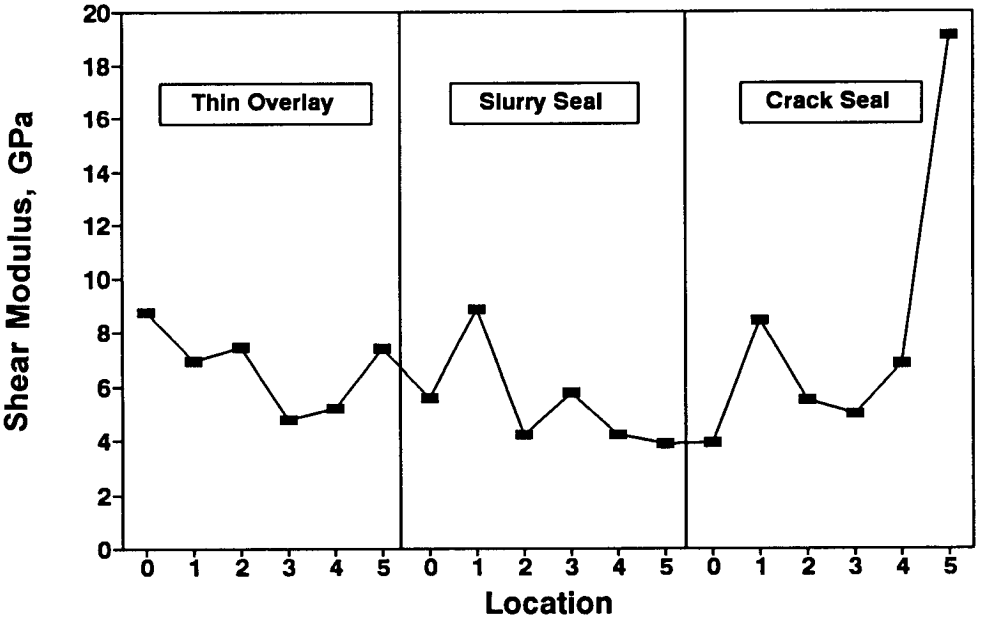

Figure 9.9 - Shear moduli determined at SPS3 site

Three anomalies can be seen in the data. Two points (point 4 on the thin-overlaid section and point 3 on the crack-seal section) were tested on sections with fine cracks not propagating through the pavement. The third point (point 1 at the crack-seal section) was tested where a crack existed between the source and receiver; the result is therefore of questionable value.

Ultrasonic-Surface-Wave Method

The AC shear moduli from the ultrasonic-surface-wave tests are reported in figure 9.9. Again, the scatter in data is rather small. The quality of data was high; therefore, reducing data was simple. Based on the Young's and shear moduli reported, the Poisson's ratio of the AC is appropriately 1/3, which is reasonable for this material. An anomalous data point can be seen at point 5 of the crack-seal section. The reason for this anomaly is unknown.

Based upon the moduli measured, the AC layer exhibits similar behavior in each of the three sections. Unfortunately, the results from these tests could not be compared with those of the FWD tests because of problems with the deflection-basin fitting. In addition, these data could not be confirmed with tests on core data, since coring is not allowed on SHRP test sites.

Impulse-Response Method

The results from the impulse-response tests are summarized in figure 9.10. The damping ratios are not reported because they are above critical damping throughout the sections. This pattern is expected at all flexible sites because of the close contact between adjacent layers.

The subgrade modulus of the underlying layers varies significantly among the three sections. The stiffest section is the overlaid section. The slurry section is relatively stiff initially, but turns soft toward the end of the section. The section treated with the crack seal is quite soft. The condition survey of the deterioration of the sections corroborated these results. The most deteriorated section was the crack-seal section; the overlaid section contained the fewest cracks. The deflection basins from the far sensors of the FWD confirm this trend. Once again, comparison of moduli is not possible because of the problems with deflection-basin fitting.

Point 3 on the thin-overlay section was at a transverse crack. That section was so soft during testing that the data were outside the specifications even at the lowest gain of the

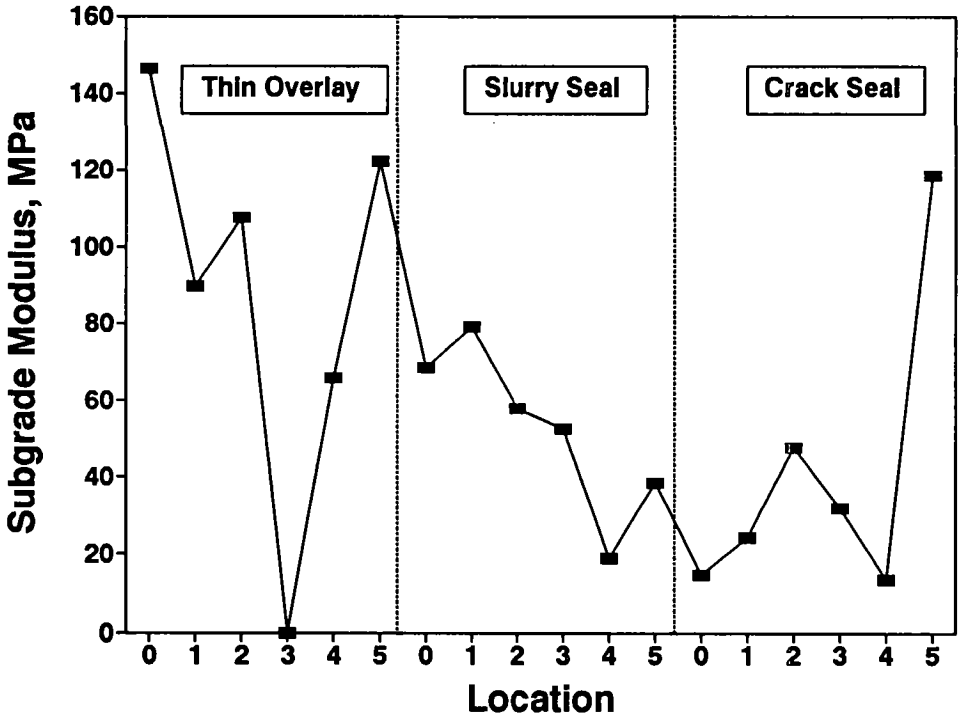

Figure 9.10 - Subgrade moduli measured at SPS3 site using impulse-response test

amplifier. Therefore, data reduction could not be carried out. This implies that the SPA may be too sensitive to test severely deteriorated pavements.

SASW Method

SASW tests were also performed at the three sections. Each section was tested at corresponding point 2, approximately halfway in the section. The results are summarized in table 9.6. The moduli of the base and the subgrade are quite close to each other. This is in character with the geology of the section, as the natural soil in that part of El Paso is quite stiff.

Again these moduli cannot be compared with the FWD moduli because of the problems with the basin-fitting program. However, the measured deflections can be compared, at least qualitatively. The trend of the deflections, shown in figure 9.7, indicates that the stiffness of the paving layers at the thin overlay should be higher than the other two sections. The data in table 9.6 seem to verify this interpretation. Furthermore, the modulus of the subgrade follows the logical pattern for the FWD data collected at the same site.

Table 9.6 - Shear modulus profiles obtained at SPS3 site

Section	Treatment	Modulus, MPa			Thickness, mm	
		AC	Base	Subgrade	AC	Base
48L310	Thin Overlay	6471	258	213	67	217
48L320	Slurry	4923	220	197	76	197
48L330	Crack Seal	5144	203	215	59	217

The layer thicknesses as measured by the SPA are also recorded in table 9.6. The thickness of the base is more or less constant at about 210 mm. This is quite close to the thickness reported by SHRP. The thickness of the AC layer, however, varies between 60 mm and 76 mm. The thin overlay section contains a 67-mm thick AC layer, thinner than the expected value of 86 mm. The AC layer thickness of the slurry-seal and crack-seal sections is quite close to the reported thickness.

This testing program demonstrates that the SPA provides comprehensive information on different types of pavement surfaces. The outcome from all tests is quite reasonable, even though it was not possible to verify the accuracy because of lack of ground truth at the site. However, the results are consistent with both the condition of the site and the trend of deflection from FWD deflections.

Finally, in about the same length of time required for deflection measurements, the SPA executed a full survey of each site. The SPA could be of great value in determining the effectiveness of different treatments at other SHRP sites.

10

Case Studies: Texas Sites

One rigid and two flexible pavement sites were tested in Texas. The site in Tomball was tested to determine the effects of moisture on softening of the base. The second site, on US 59 near Houston, was tested to detect voids and loss of support. The site located on I-45 in Madison County was tested to evaluate the Seismic Pavement Analyzer's ability to detect stripping.

Tomball, Texas

The site was located on FM 2920 near Tomball, Texas. The pavement section at the site reportedly consisted of 100 mm of asphalt concrete over a 300-mm cement-treated base over subgrade. However, based upon layer thicknesses obtained from cores, the thickness of the base was always less than 190 mm. A 300-m section of the highway was selected and tested at 15-m intervals. In addition, several points corresponding to cored locations were tested. The FWD device was also used. The goal of these tests was to determine the softening of the base as a result of the penetration of moisture. The site was selected because it contained a flexible base; because of the high cement content of the base, the section was treated as a composite rigid pavement.

The layer thicknesses and moisture contents from the six points cored are presented in table 10.1. The thickness of the AC layer varied from 80 to 120 mm, and the base thickness ranged from 140 to 190 mm. The moisture content of the base from all cores (except core

0) was rather constant at around 5.5 percent. The moisture content of the subgrade (except core 1) varied between 8.4 and 11.3 percent.

Table 10.1 - Variation in thickness and moisture contents of cores at Tomball site

Core No.	Distance, m	Thickness, mm		Moisture Content, percent		
		AC	Base	Base (top)	Base (bottom)	Subgrade
0	72	90	180	--	--	Submerged
1	126	110	140	4.8	6.3	11.3
2	157	100	140	6.4	5.6	9.9
3	213	80	190	5.6	5.0	8.4
4	256	120	150	5.6	--	8.6
5	282	80	150	4.7	4.2	9.2

The condition survey indicated that the site was in reasonably good condition except for transverse cracks at 5-to 10-meter intervals and occasional minor cracking of the AC layer.

FWD Tests

The deflection measurements for a nominal load of 40 KN are charted in figure 10.1. Based on the measured deflections, the first 50 to 75 meters and the last 25 meters of the section are softer than the rest of the section.

The modulus values obtained from these sections are not shown in this report. The back-calculation process could not be carried out with small basin-fitting errors; therefore, the modulus values may not be as reliable. For almost all data points, the moduli of AC and base layers were equal to the upper limit assigned to the moduli, i.e., 35 MPa.

Diagnostic Approach

The base was heavily stabilized with portland cement; therefore, the distress precursor investigated at this site was the softening of support in the subgrade layer. The impulse-response (IR) tests were the primary technique for predicting the loss of support.

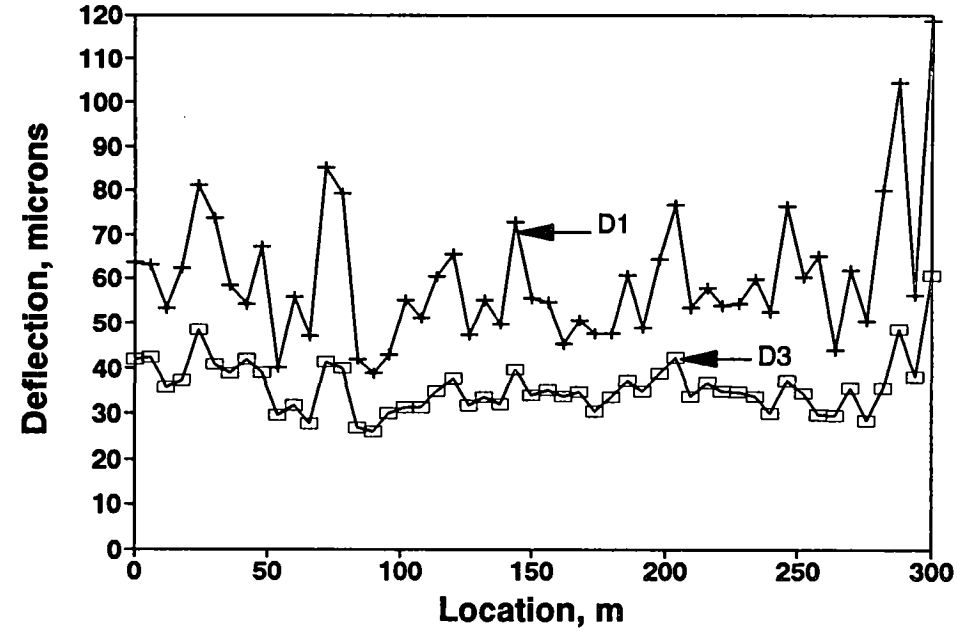

a) Near Geophones

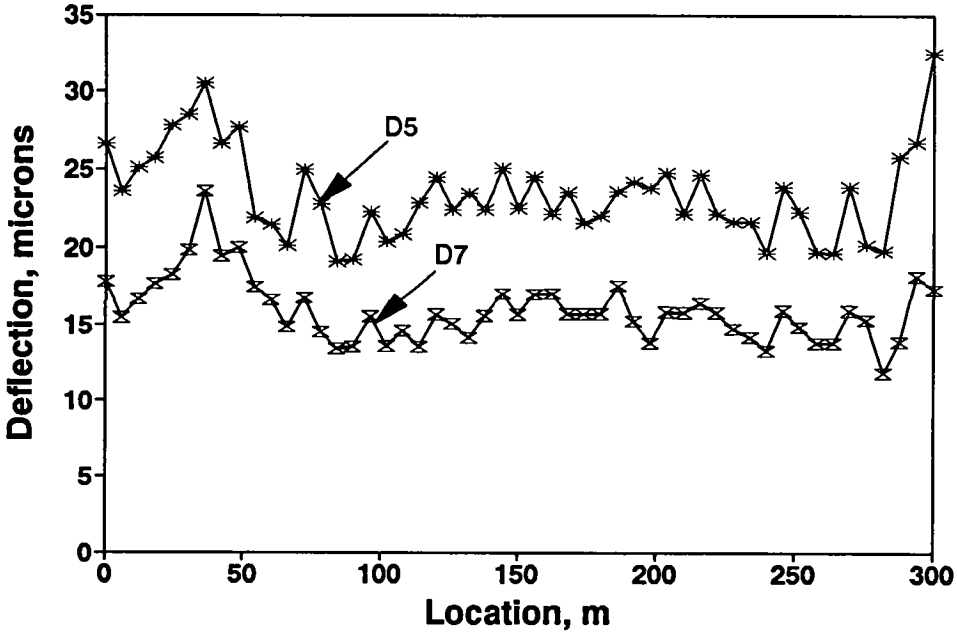

b) Far Geophones

Figure 10.1 - Variation in FWD deflections at Tomball site

The measurements of subgrade moduli across the test location are presented in figure 10.2a. Large variation in the data can possibly be because of a lack of precision in data collection, or because of variability in the material parameters. To isolate the latter cause from the former, each site was tested with the SPA several times (typically 10 times) at one point. The standard deviation associated with each parameter was then calculated. The coefficient of variation was also calculated and used to indicate the repeatability of the test results.

Figure 10.2a has three horizontal lines. The middle line (around 490 MPa) corresponds to the mean of all the measurements carried out at this site. The upper and lower horizontal lines correspond to the mean plus and minus one standard deviation, respectively, where the standard deviation was calculated from the repeat tests. The large observed variations are well beyond the repeatability variations. This suggests that the variability is due to variation in material properties, and not due to imprecise data.

The mean value can help to determine if the site is worth maintaining. If the mean subgrade modulus is less than desirable for a given pavement structure, maintenance may not be of any use; it may be better to rehabilitate or strengthen the section. In this case, the subgrade modulus of 490 MPa corresponds to a strong subgrade indicating that the problem may be in the paving layers.

The lower line is used to determine if maintenance is required. Any point between or above the three lines can be considered average or above average. Points below the lower line correspond to problem areas that may need some attention. At the Tomball site, the first 100 meters of the section, and the last 50, may be candidates for some maintenance. In all cases the moduli are quite acceptable.

The damping ratios shown in figure 10.2b can confirm whether or not the subgrade is saturated. At a damping ratio above 70 percent, depending upon the subgrade modulus, the test point is either intact or is a water-saturated defect. A damping ratio less than 30 percent typically indicates unsaturated voids. Finally, a damping ratio on the order of 50 to 70 percent, with a small subgrade modulus, corresponds to a large water-saturated softened subgrade. From the figure, it seems that the sections in the problem zones (first 100 meters and last 50) are quite wet.

The six data points corresponding to the six core holes are also shown in figure 10.2. The least stiff point corresponds to core 0, where the subgrade was submerged—the water table was practically at the ground surface. The saturation of the defect at this point is confirmed with a damping ratio close to 70 percent. The stiffest points (cores 2 and 3) do not correspond to points with particularly different moisture contents of base or subgrade layers

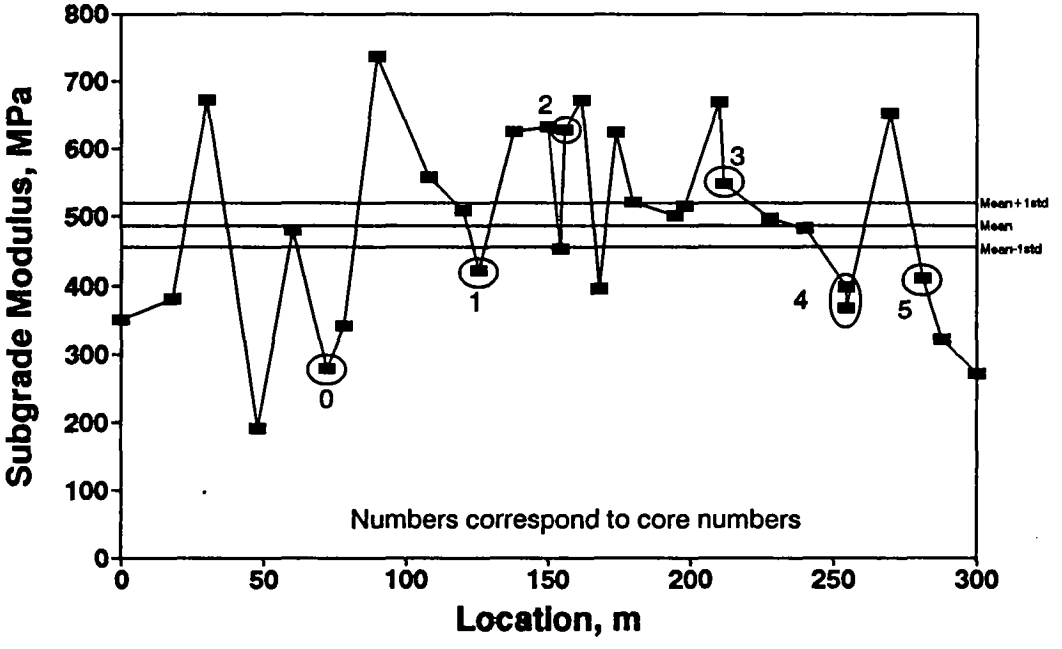

a) Subgrade Modulus

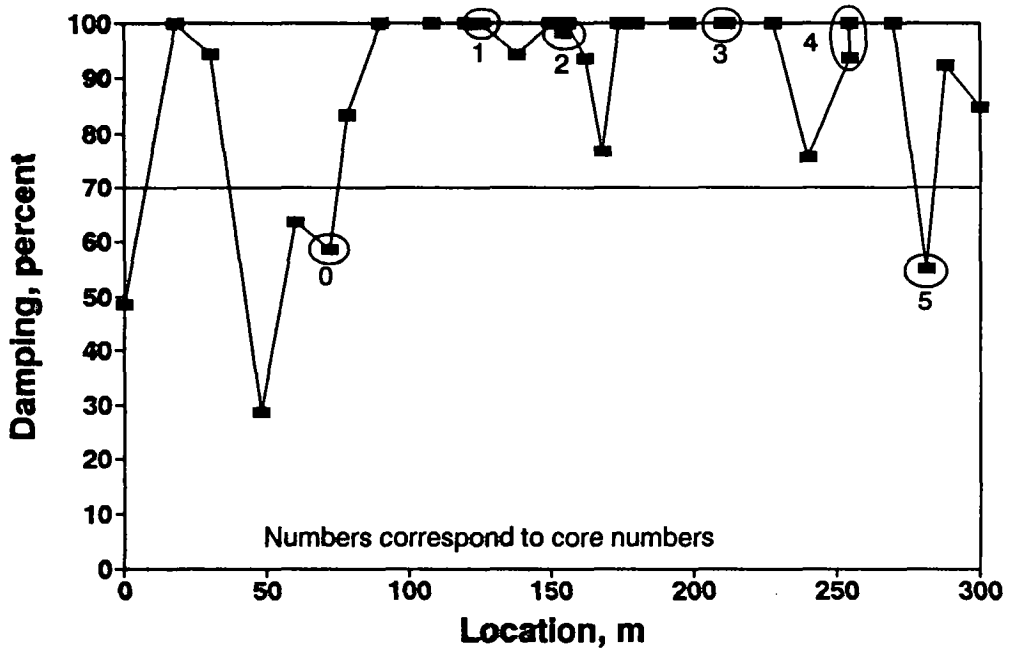

b) Damping Ratio

Figure 10.2 - Variation in parameters obtained with impulse-response tests at Tomball site

or layer thicknesses. This suggests that the moisture level in the subgrade at the base interface may not be a good indication of the softness of the base. The deflection data support the fact that these points are stiffer.

The three remaining data points exhibit roughly the same degree of stiffness. The two data points corresponding to core 4 are about 0.3 m apart. The repeatability of the test can be recognized from these two data points.

Unfortunately, only a limited ground truth operation was performed. It would have been helpful to determine the optimum moisture content of the subgrade, as well as the ideal moisture level in the cement-treated base.

As indicated in Chapter 3, the water content has little value in itself and it should be considered in the context of its softening effects. If the actual water content is significantly different from the optimum water content, a change of only a few percentage points would not significantly affect the stiffness.

The deflection basins shown in Figure 10.1 indicate that the first 75 meters of the section are quite soft. The SPA yields similar information, in addition to information about quality and thickness of other layers in the system (see Appendix B). One advantage of the SPA is that it measures the modulus of the subgrade, and many other parameters, in about the period of time that the FWD measures the deflection basin, without any need for back-calculation.

In general, the SPA accurately determined the softening of the subgrade. The device functions well in areas where the FWD back-calculation is difficult. All layers in the system are analyzed to determine the layers that contribute to the distress. As shown in Appendix B, some aspects of the software, especially those dealing with ultrasonic body waves, required modifications to become more robust. These modifications were implemented.

Houston, Texas

A section of US 59 near Houston, Texas, was tested to detect the existence of voids and loss of support. The highway was a four-lane divided highway. The pavement section at the site consisted of 250-mm (nominal) jointed concrete pavement over a 150-mm cement-treated base. The pavement was contained by an AC shoulder.

The portland cement concrete slabs were 6.1 m long and 3.6 m wide. Thirteen slabs in the southbound inside lane were tested; the joints are numbered 0 through 13. Five points at each slab were tested. The five points were located at 15 cm south and north of each joint, two quarter points, and the center point of each slab.

FWD Tests

FWD tests were carried out within 30 minutes of the SPA tests. The FWD tested both sides of each joint and the midpoint of each slab. The deflection results of the first sensor are shown in figure 10.3. The deflections vary between 45 and 60 microns between joints 1 and 8. Between joints 9 and 13, the deflections vary more significantly. Joints 0 and 12 seem more flexible than the other joints.

Another way to inspect the data for voids is to determine the load transfer at each joint, as shown in figure 10.4. The load transfer is the ratio of the deflection measured with a sensor at the opposite side of a joint with respect to load pad to the deflection obtained from the sensor on the same side of the joint as the load pad. Intuitively, the load transfer should be less than unity. As shown in figure 10.4, the load transfer is often larger than 100 percent. This indicates that in response to the impact at the edge of one slab, the edge of the adjacent slab located on the opposite side of the joint moved more than the slab receiving the impact. The only plausible explanation for this phenomenon is that the slabs that moved were located on a bed of an incompressible medium (perhaps water).

Several points show the load transfers on only one side of the joints; FWD tests were not performed for the opposing side.

Diagnostic Approach

The primary test to detect void or loss of support under PCC slabs is the impulse-response (IR) test (see Chapter 4).

The modulus of subgrade and the damping ratio from IR tests are shown in figure 10.5. As reflected in figure 10.5a, the mean subgrade modulus is about 55 MPa. This indicates that the condition of the subgrade material for this pavement structure is far below average. According to our results, the whole section should be rehabilitated.

The coefficient of variation of these measurements as reflected in the figure was about 11 percent. Even though the entire section is weak, there are some areas that are weaker. For

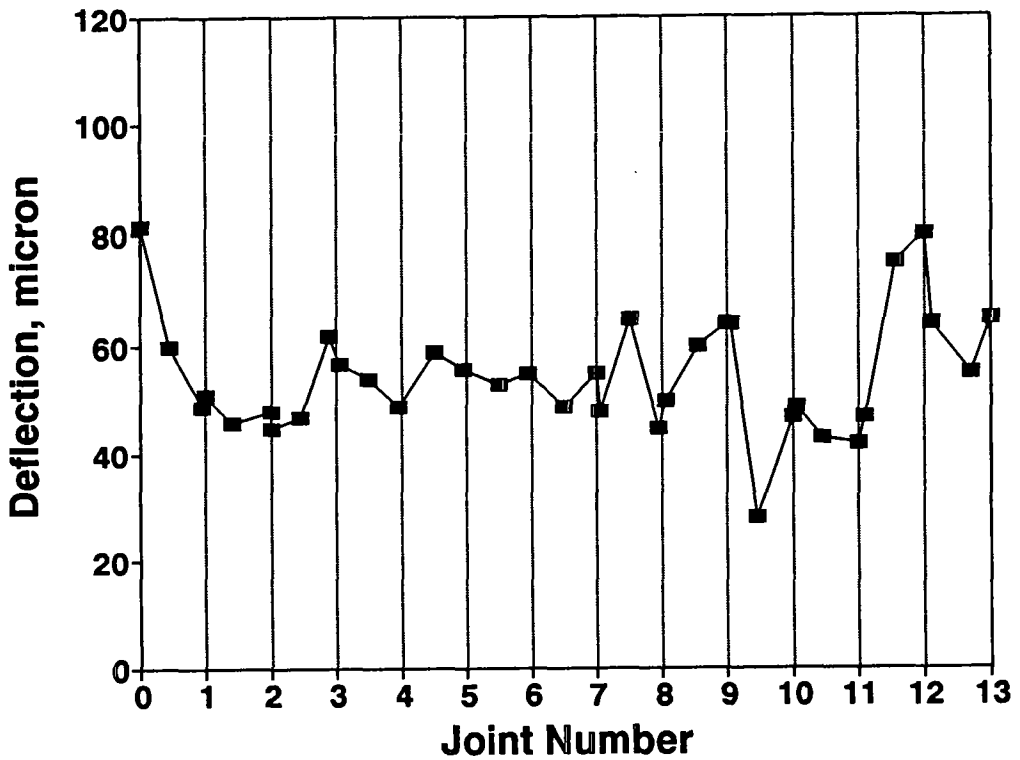

Figure 10.3 - Variation in deflection of sensor 1 from FWD tests at Houston site

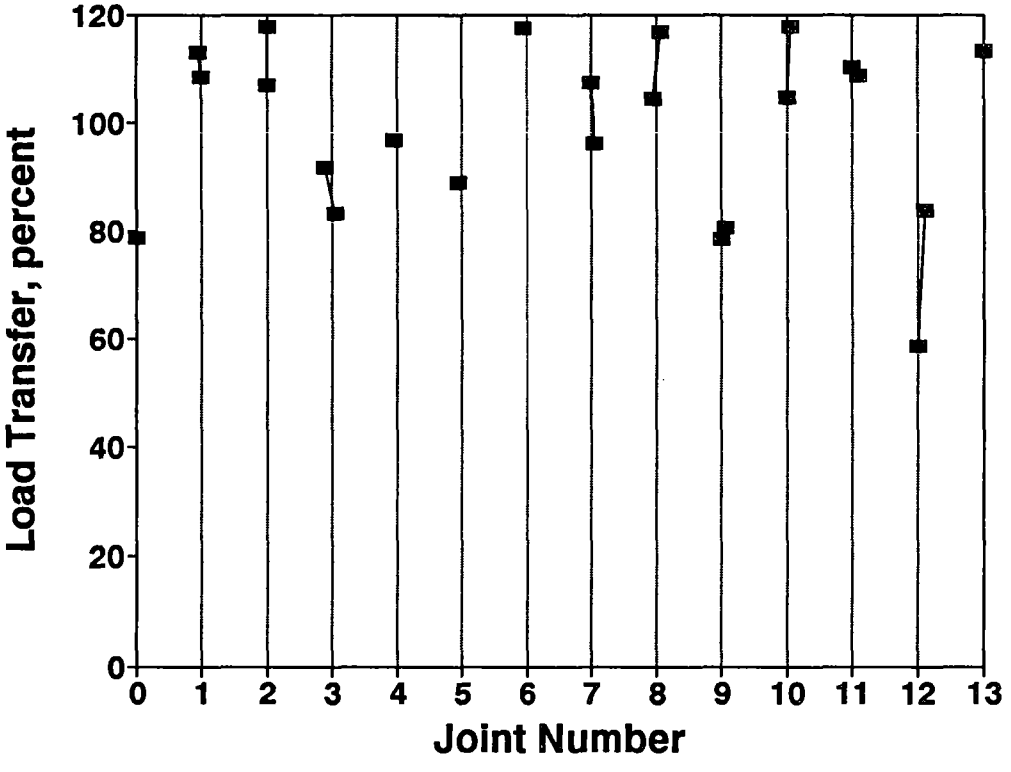

Figure 10.4 - Variation in load transfer from FWD tests at Houston site

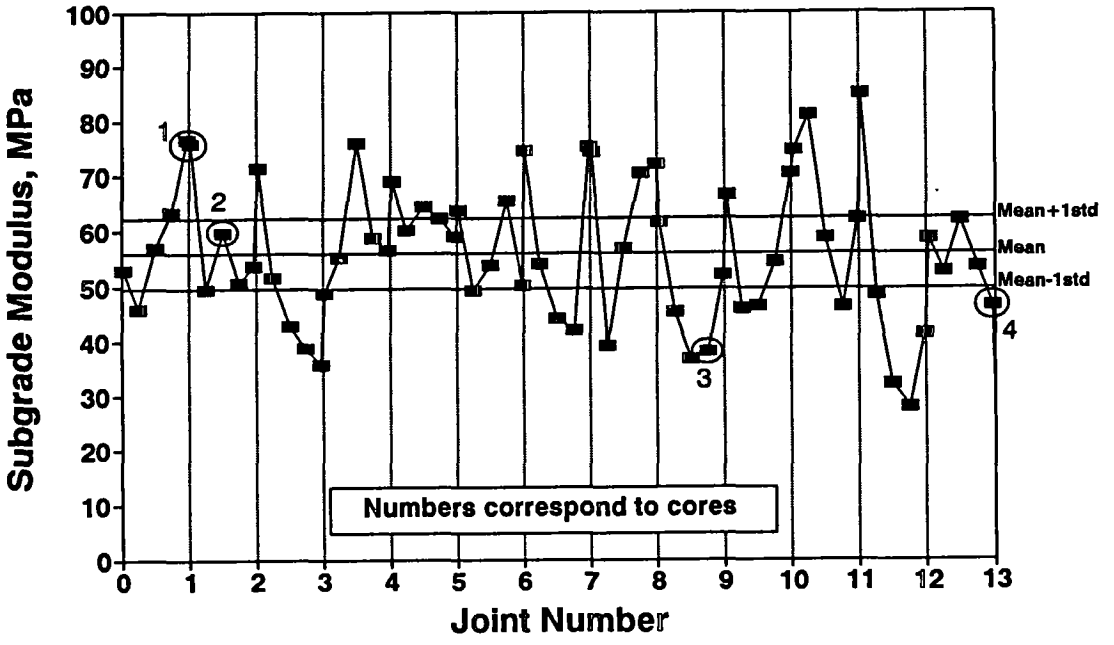

a) Subgrade Modulus

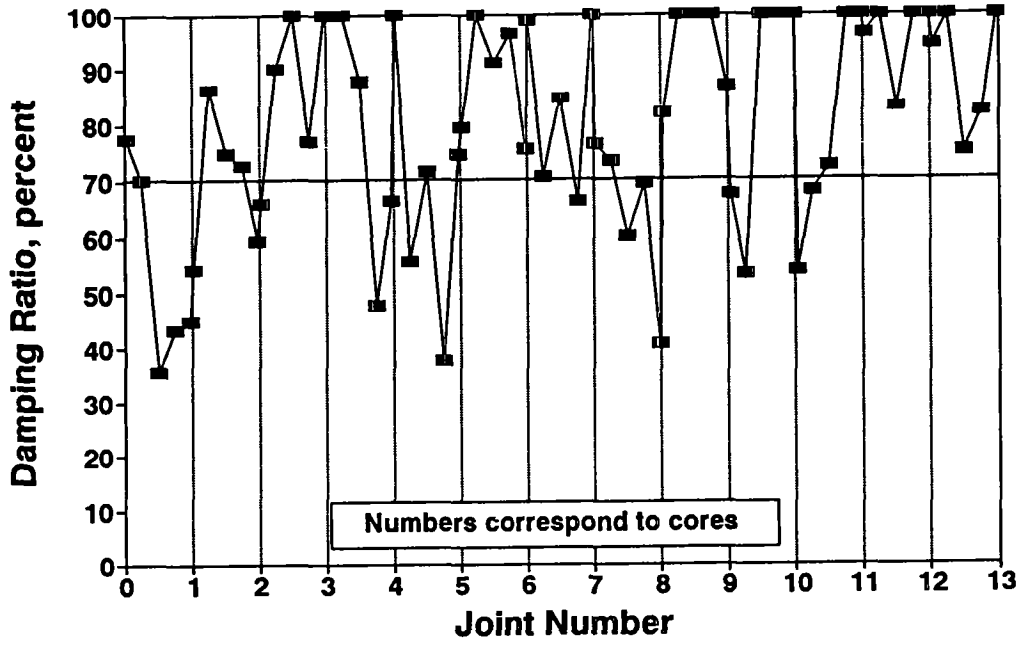

b) Damping Ratio

Figure 10.5 - Variation in parameters measured with impulse-response tests at Houston site

example, the subgrade moduli under slab 3 (between joints 2 and 3), slab 7 (between joints 6 and 7), slab 9 (between joints 8 and 9), and slab 12 (between joints 11 and 12) are extremely weak. Once again, because even the best point shows a very soft subgrade, there is not much difference in the moduli between the stronger and weaker points.

The damping ratios follow a logical pattern. An undersealing contractor was working on the section at the same time these tests were being performed. The contractor had installed one or two holes in each slab shortly before our tests. The holes were inspected prior to tests with the SPA and any presence of moisture in the holes was noted. Slabs 1, 2, and 5 were dry; the rest of the holes were wet. The damping for the dry slabs is typically less than 70 percent, indicating the existence of voids; however the other slabs exhibit damped characteristics, confirming the presence of moisture.

The results from the epoxy core tests conducted at this site were not conclusive, because shortly after the cores were filled with epoxy, the undersealing contractor applied grout in the adjacent grouting holes. Nevertheless, the void sizes in cores 1 through 4 were measured at 9 mm, 25 mm, 9 mm, and 6 mm, respectively.

Both the FWD and SPA tests measure the load and deflection of the slab. However, the methods of performing the tests and analyzing the data are different. The load plate of the FWD is about 300 mm; the SPA source's is only 50 mm in diameter. In addition, the FWD impacts heavy loads which may close the gap of a thinner void. The SPA impacts the slab with much smaller loads, and the primary parameters measured are the stiffness and the amount of energy trapped in the slab. Therefore, the SPA can detect smaller voids. Based on the deflections from FWD and the moduli and damping ratios from SPA, larger voids can be detected with either the FWD or the SPA. However, smaller voids can be better determined with the SPA , because the loads are applied more locally and a more rigorous data reduction scheme is used.

The site tested was not a good candidate for maintenance; because of the variable modulus of subgrade, the entire section is extremely weak and should be reconstructed. The loss of support throughout the section is validated by an average subgrade modulus measured at 5.5 MPa (slightly better than water).

The other information collected at the site is presented in Appendix B.

Madisonville, Texas

The site in Madisonville, Texas was tested for stripping of the AC layer. Because the SPA was not designed to detect this pavement condition, the site was tested on an experimental basis to understand the potential of the device to identify stripped sections. Approximately 1000 meters of the section was tested at 60-m interval.

The site consisted of 180 mm to 200 mm of AC over 230 mm of concrete. The AC layer consisted of several layers. From the top, the first layer consisted of about 70 mm of newly placed asphalt overlay. The second layer consisted of about 10 mm of iron-ore gravel remaining from earlier milling of a layer. The third layer, approximately 45 mm thick, was a pea-gravel AC layer with a highly variable condition. The modulus of this layer varied from fair to very poor. Finally, the original layer (65 mm thick) was in good-to-fair condition.

The major problem encountered at the site was a lack of robustness of SPA software. In most cases, the ultrasonic-body-wave method yielded a compression wave velocity that corresponded to the refracted wave path from the top of the concrete layer. With modifications to the software, the detection of stripping may be possible.

11

Case Studies: Georgia Sites

Two rigid-pavement sites were tested in Georgia. The first site was located on I-85 north of Atlanta; this site was tested to determine the accuracy with which SPA can detect debonding of two layers of concrete. The second site, on I-20 west of Augusta, was tested to detect voids and loss of support under slabs.

Two flexible-pavement sites were also tested in Georgia. One site was located in Jonesboro (near Atlanta) on US 19/US 41. Testing at that site evaluated the Seismic Pavement Analyzer's ability to determine stripping. The cores from the site exhibited the early signs of stripping. When they were cut in half, moisture could be felt on the specimen. Because the data did not indicate any sign of stripping, the results from this site are not reported. The second flexible-pavement site was located near Augusta on River Watch Parkway. That site was tested to determine the effects of moisture on softening of the base and subgrade.

Gwinnett County, Georgia—I-85

The site was located on I-85 in Gwinnett County near Atlanta, and was tested to determine the accuracy of the SPA in detecting the depth to a delaminated or debonded layer.

The pavement section reportedly consisted of 230 mm of jointed concrete, overlaid with three different portland cement concrete layers. The first section of the site was overlaid with about 115 mm of continuously reinforced PCC. The second section was similar to the

first, except the overlay was about 150-mm thick. The final section tested had an overlay 150-mm thick, with joints at 5-m intervals. The sections were tested between 11:00 AM and 3:00 PM, the least favorable time for testing for delamination and voids because of the temperature regime within the concrete.

Diagnostic Approach

Impact-echo (IE) tests were used to evaluate these sites to determine the thickness of the upper layer. If debonding exists, the measured thickness corresponds with the thickness of the overlay. In a bonded section, the thickness corresponds to the composite thickness of the overlay and the original concrete.

The debonding was developed by applying an antibond agent to the concrete. When coring to verify thicknesses, practically no gap was detected between the overlay and the base concrete layers. Therefore, it would have been impossible to detect debonding using other common nondestructive testing devices. However, the IE method can be effective because the slightest air gap at the interface causes a strong reflection of energy; the thickness found will correspond to the thickness of the top layer. This method produces reasonable results, even though there may be partial contact between the aggregates of the overlay and the base concrete.

The overlay at the thin continuously reinforced section, which was about 115-mm thick, was extensively damaged and patched. Therefore, only about 45 meters of the section was tested. Reflective joints from the lower concrete were evident at 5-m intervals. Therefore, tests were carried out at 2.5-m intervals.

The results of the impact-echo tests are shown in figure 11.1. Some variation in thickness can be seen. The points tested at joint 2 and in the middle of slab 2 exhibited thicknesses in excess of 150 mm and were located on a repaired patch. Therefore, the condition of the concrete at those points was unknown.

The expected thickness of the overlay and the expected precision in measuring this parameter are shown as three horizontal lines in figure 11.1. The thicknesses from the remainder of test points are within 15 percent of the expected value. Given the difficulty in measuring the compression wave velocities because of the patchiness of the section, such a variation is expected.

To verify the results, one data point was cored. The thickness of that point (joint 5) is marked on the figure as well. The measured thickness was about 130 mm, whereas the

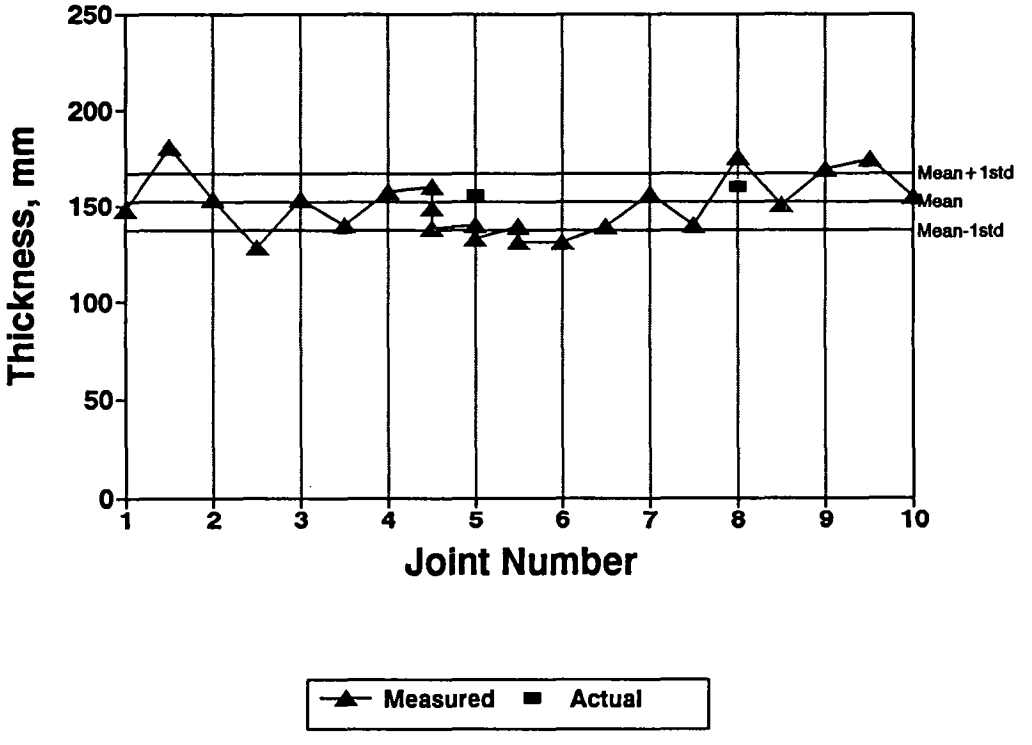

Figure 11.1 - Variation in thickness of overlay at thin CRCP section tested on I-85

actual thickness was about 120 mm. As the thickness measured corresponds to the thickness of the overlay, the sample verifies that the two concrete layers are debonded.

Similar tests were carried out at another section where the thickness of the overlay concrete was 150 mm. In this section, 10 joints were tested, and the results are detailed in Appendix C. Two points were cored to verify the thicknesses determined by the SPA; the actual and predicted thicknesses were within 15 percent of each other. Again, the dominant impact-echo response was from the interface of the two concrete layers, indicating debonding.

Finally, thicknesses from two cores located on the jointed overlay section were compared with the measurements of the SPA (see Appendix C for details). In one case, the thickness was reasonably predicted. At the second point, located in a highly cracked region, the thickness was greatly underpredicted. A peak corresponding to reflections from other sources (most probably from the cracks) was slightly more dominant than the peak corresponding to the thickness of the debonded layer.

The tests at this site indicate that the SPA can effectively detect the debonding or delamination of two concrete layers. However, the accuracy with which it measures the thickness is related to the degree of cracking and patching at the site. It is difficult to determine the "true" compression wave velocity of a layer when it is cracked. The SPA was mandated as a maintenance tool and was therefore designed for use on sites that contain little or no distress. Finally, based on the additional information included in Appendix C, the new ultrasonic body wave subroutine is much more robust than the older version used in Texas.

Augusta, Georgia—I-20

A section of I-20 near Augusta was tested to detect the existence of voids and loss of support in the pavement. The highway was a four-lane divided highway. The pavement section at the site consisted of 225 mm jointed-concrete pavement over a cement-treated base. The pavement was contained by an AC shoulder.

The PCC slabs were 9 m long and 3.6 m wide. Twelve slabs—thirteen joints numbered 1 through 13—were tested in the eastbound outside land. Three points were tested at each slab. The three points were located at 15 cm east and west of each joint and in the middle of each slab.

Diagnostic Approach

The impulse-response (IR) test was used to detect voids and loss of support. The resulting moduli of subgrade and damping ratios are shown in figure 11.2. As reflected in figure 11.2a, the mean subgrade modulus is about 175 MPa. This indicate an above-average subgrade material. This section is in good condition, which is to be expected because the section was recently rehabilitated.

The data presented here indicate the need to inspect and maintain the approach side of each joint for possible voids, especially for joints 2, 3, 5, 6, and 9. The two slabs between joints 11 and 13 are in very bad condition and should be repaired. These recommendations are consistent with the condition of the pavement.

Most of the damping ratios shown in figure 11.2b are above the critical damping ratio, indicating either water saturation of voids or good contact at the interface of the concrete and base layer. As indicated in Chapter 4, the water-saturated voids and intact locations are both highly damped; however, the intact points exhibit substantially higher moduli of subgrade.

To verify these results, five epoxy core holes were installed at the section, as marked in figure 11.2. Points 2, 4 and 5 were selected as areas where voids were suspected. These three core points validated the SPA prediction that they were water-saturated voids (low modulus of subgrade, high damping ratio). Upon coring, the holes filled with water almost instantaneously. The other two cores were selected as intact concrete. Points 1 and 3 proved to be on relatively dry and intact subgrade.

This case study demonstrates that the SPA is capable of evaluating rigid pavements for the existence of voids and loss of support in both dry and saturated conditions. At the five points where ground truth is available, the predictions were accurate.

Augusta, Georgia—River Watch Parkway

A series of tests was performed at the River Watch Parkway in Augusta, Georgia. The typical pavement cross section consisted of 210 mm of AC over 250 mm of granular base over a corrodible sandy subgrade. A 1300-m section of the highway was selected and tested at 30-m intervals. The FWD device was used three weeks after the SPA tests were completed. These tests determine the softening of the subgrade as a result of the penetration of moisture.

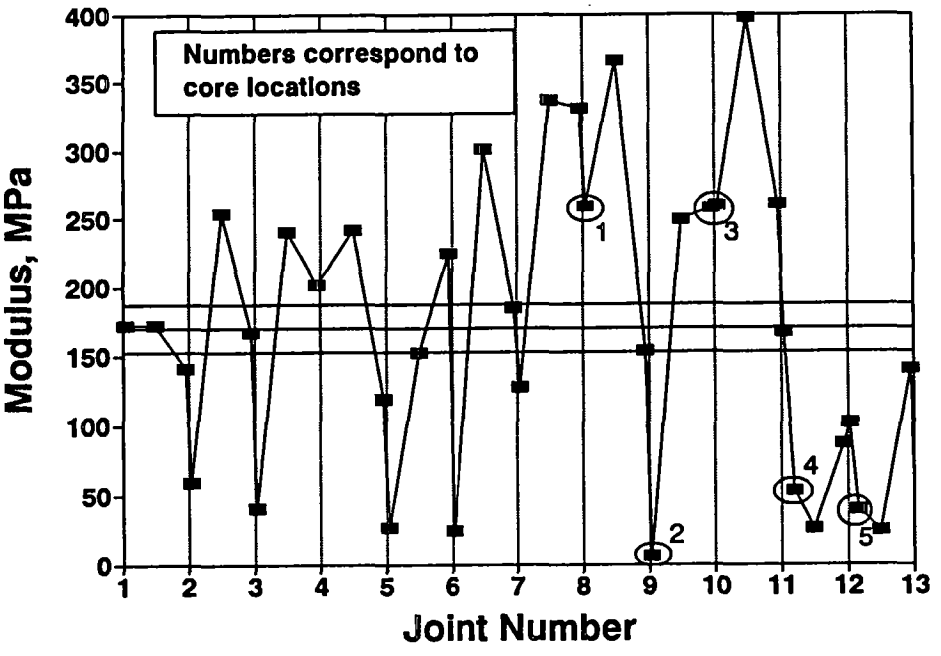

a) Subgrade Modulus

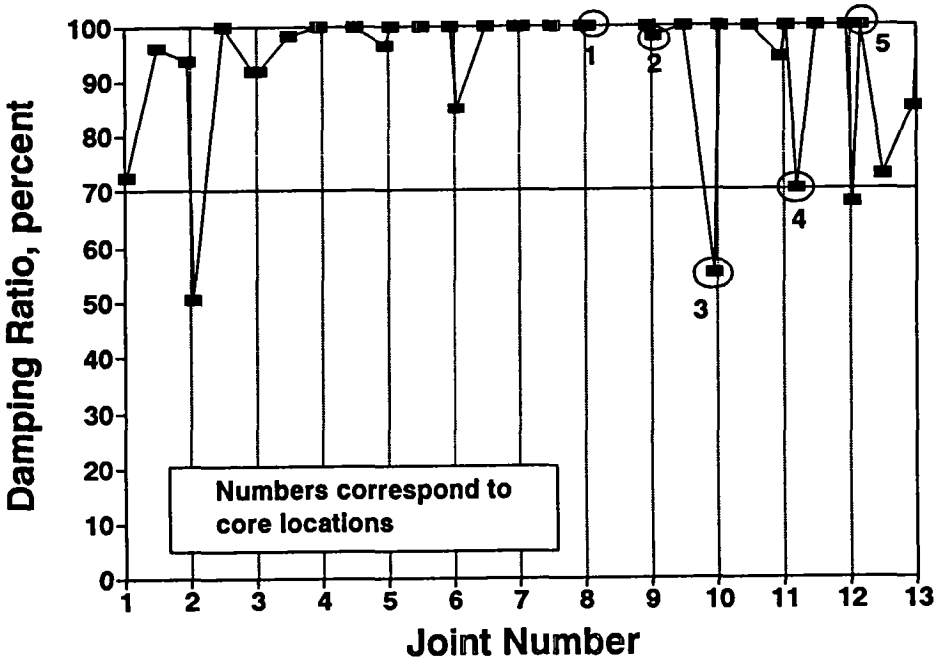

b) Damping Ratio

Figure 11.2 - Variation in parameters measured with impulse-response method at I-20

FWD Tests

The deflections for a nominal load of 40 KN are shown in figure 11.3. A large variation in the deflection basins can be observed, possibly indicating the variability in the overall stiffness of the section. The variations in the deflections also may result from variations in the thickness or stiffness of the layers.

The modulus values obtained at the site from BISDEF are not included because back-calculation was not successful. At all points, the modulus of the AC was back-calculated as the upper prescribed range of 17.5 GPa, and the base modulus was always equal to 35 MPa (the lower range assigned to the material for the back-calculation). This may be partly the result of the dynamic interaction between the bedrock and the FWD. A large portion of the site was in a cut section.

Diagnostic Approach

The impulse-response test were used to determine the effects of moisture variation in the base and subgrade. The impulse-response test was utilized to determine the overall variation in stiffness, and the SASW method was employed for more thorough analysis.

The measurements of the modulus of the subgrade soil are shown in figure 11.4. The pavement in the range of -50 m to -80 m corresponded to a saturated base and subgrade. The rest of the section seemed to be in reasonably good condition. However, the data indicate some potential problems in the 200-m to 350-m section. The level of water in a ditch on the side of the road was rather high in this area.

The results from the SASW tests are summarized in table 11.1. These tests were carried out at some of the core locations; therefore, they do not correspond to test results described above.

The moduli of the AC layer are relatively constant. The base moduli are similar, except for the two points tested at -84 m and -54 m. The base material at the -84 m location was saturated, and water was seeping to the pavement surface. The point tested at -54 m was also wet. The subgrade moduli are rather high for points 360 m and 900 m, and are representative of most of the pavement section. The test point at 270 m corresponds to the area that the IR tests diagnosed as soft. At this point, the subgrade is quite soft, whereas the AC and base layers are in good condition.

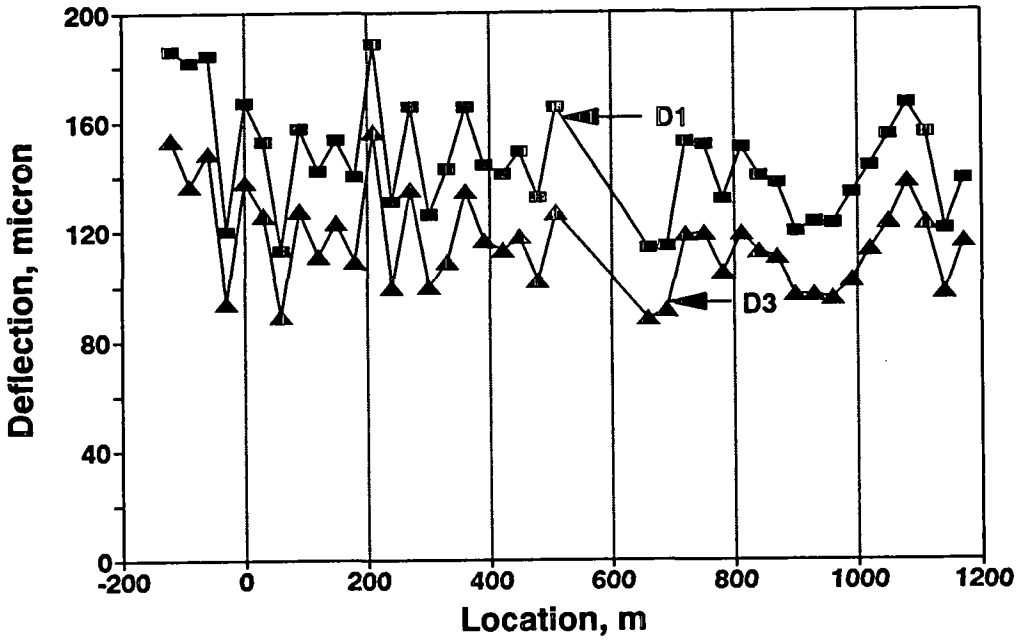

a) Close Geophones

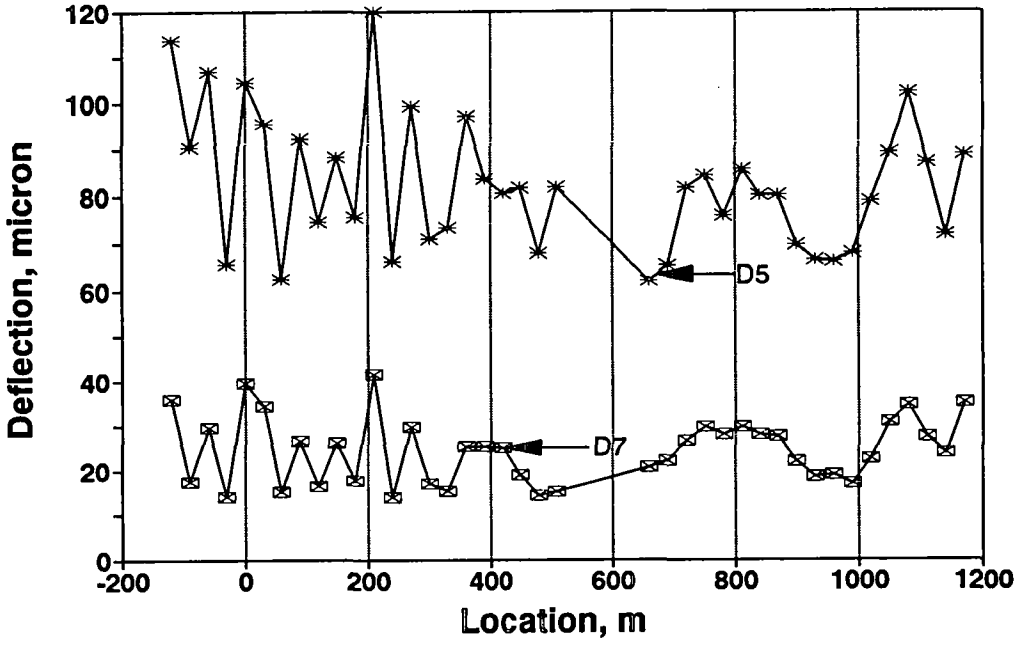

b) Far Geophones

Figure 11.3 - Variation deflection basins at River Watch Parkway

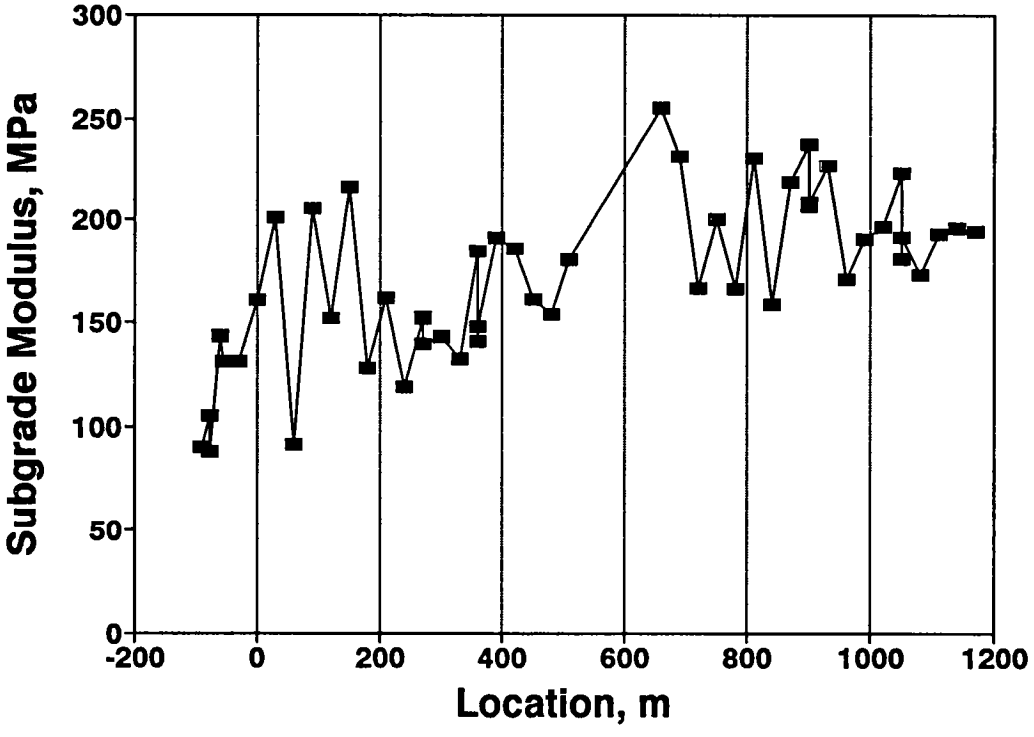

Figure 11.4 - Variation in modulus of subgrade soil from IR tests at River Watch Parkway

Table 11.1 - Shear modulus profiles obtained at River Watch Parkway

Location, m	Shear Modulus, MPa			Water Content, percent		FWD Deflection*, micron	
	AC	Base	Subgrade	Base	Subgrade	D1	D7
-84	7530	78	45	6.2	14.4	179**	17
-54	6433	127	89	5.7	--	182**	29
270	6944	210	77	4.0	11.8	160	29
360	8486	214	150	6.0	14.1	160	25
900	7960	205	136	4.1	15.7	112	21

* Deflections, which are reported for a nominal load of 40 KN, should be considered with caution, as a stiff layer existed under the pavement at variable depths.

** FWD tests were not carried out at this location; the closest point tested is reported.

The water contents (also recorded in table 11.1) were obtained in the field with a pan-dry oven. As indicated, the base at -84 m has the highest water content and also the lowest modulus. The two points located at 360 m and -54 m exhibit similar water content; however, the moduli of these two points are significantly higher than that of point -84 m. Point 360 m, with base moisture similar to point -84 m, is significantly stiffer than point -84 m. Both independent tests (IR and SASW) concur that point -84 m is not as stiff as point -54 m or point 360 m. Based on engineering intuition, the pavement structure at point -84 m should therefore be softer than the other points. Points -84 m and -54 m are located in a rock cut, whereas point 360 m was almost in a fill section. Therefore, the dynamic interaction would affect the deflections from FWD and the SPA results could not be verified.

Establishing a relationship between the modulus and water content—without considering other factors such as the type of the base and subgrade materials, optimum water content for the base and subgrade, and the period of time that the material is exposed to the moisture—should be considered.

A comprehensive set of data was collected at this site and is discussed in Appendix C. Based on the results shown here and in Appendix C, the site is extremely well-characterized and diagnosed, even though the results could not be compared directly with other parameters. The stiffness, Poisson's ratio, and the thickness of the AC layer were determined and it was shown that the material was quite uniform and of good quality.

The IR test also showed that the pavement in the regions of -50 m to -80 m and 200 m to 350 m was rather soft and required more investigation. The SASW demonstrated that in the region between -50 m and -80 m, both the base and subgrade were soft and should be considered for remediation. The other region (between 200 m and 350 m) contained a competent base material, but the subgrade was of concern.

In general, this case study clearly shows the potential, accuracy, and the robustness of the SPA. At this site, the FWD deflections could not be used for comparison, and back-calculation could not be carried out successfully because of the variable depth to a rigid layer in the vicinity of the pavement surface. Furthermore, this site again demonstrates that water content per se may not be a good distress precursor.

12

Summary, Conclusions, and Recommendations

This report highlights three years of effort focused on developing a new nondestructive device that maintenance and pavement engineers can use to evaluate pavement. In general, the project was a great success and all objectives were achieved.

The goal of the project was to develop a device that was more accurate and versatile than the state-of-the-art in pavement evaluation, that had more interpretive power than the state-of-the art device, and yet was easy to use. These goals were achieved in the Seismic Pavement Analyzer (SPA).

Summary

The SPA was designed to evaluate specific pavement conditions: moisture in the foundation under flexible pavements, voids or loss of support under rigid pavements, overlay delamination, and fine cracking. The project also developed a framework for measuring the parameters needed to describe pavement aging.

In order to measure the usefulness and appropriateness of the SPA for pavement maintenance, acceptable levels of accuracy of measurements for each distress were defined. This exercise resulted in a new methodology for organizing maintenance priorities, based on a mechanistic approach.

The principles of measurement and the diagnostic approach that SPA uses to determine each distress precursor were clearly defined, and the theoretical background behind each testing technique was briefly discussed. This document also presented an overview of the conceptual design of the SPA, as well as a description for the implementation of that design. Typical data collection and data reduction procedures were discussed using comprehensive examples.

Several case studies determined the accuracy, applicability, and limitations of SPA. A facility was designed, constructed, and tested at University of Texas at El Paso specifically for this project. Four different sites were tested in Texas; based upon these tests, the software was modified. Another four sites were tested in Georgia.

The field tests demonstrated the use of the various measurement methods embodied in the SPA on a variety of pavement conditions. At each site the SPA results were correlated with ground truth measurements and (for all but two) with FWD measurements. The specific SPA methods and associated conditions are summarized in table 12.1, along with the outcome of verification tests.

Four of the six SPA tests methods were successfully utilized in the field program. The remaining tests—the ultrasonic-surface-wave and ultrasonic-body-wave—were used to support the results from the other methods, and did not clearly relate to the site conditions of interest. Five of the seven distress precursor pavement conditions of interest were evaluated. The two which were not evaluated (aging and fine cracking) were not specifically found at the test sites.

The selected sites did not present the optimal conditions for the desired evaluations. For example, the RiverWatch Parkway site, selected for variation in base moisture, revealed a very uniform base moisture content. The overlay delamination site (Georgia I-85) was totally delaminated by design, so that no comparison of delaminated versus solid areas could be made. Nevertheless, valuable data were collected and a number of important results have been achieved, as summarized below

1. Moisture content cannot be counted on as an indicator of softening of base and subgrade. This was found in both granular and cement-treated bases.

2. The SASW test produces results consistent with the FWD deflections. However, the SASW test can compute layer moduli in situations where backcalculation cannot be carried out with the FWD data.

Table 12.1 - Summary of field test results

Pavement Condition	Site	Diagnostic Method	Results of Verifications
Voids under PCC slabs	US 59, TX	IR	No clear relationship between IR results and measures voids, suggesting that voids are everywhere. Dry areas=low damping; wet areas=high damping, supporting this hypothesis.
	I-20, GA	IR	Low modulus correlates with voids; damping ratio correlates with moisture.
Softening due to moisture in base and subgrade	Tomball, TX	IR	General correlation between IR moduli and FWD deflections, but as expected no correlation between moduli and moisture content.
	Riverwatch Parkway, GA	IR SASW	IR moduli consistent with FWD deflections. No correlation between moduli and moisture content (as expected). SASW moduli consistent with IR moduli. SASW moduli used to determine the layer contributing to pavement condition.
Overlay Delamination	I85- GA	IE	IE data clearly revealed the overlay to be structurally separate from the layer below.

3. The results support the use of the impulse-response data to reveal voids under portland cement concrete slabs, and to distinguish water-filled from dry voids. More data are needed to confirm the algorithm used for making these distinctions.

4. The results support the use of the impact-echo method for detecting debonding and delamination of concrete overlays. However, no comparison could be made between the debonded versus intact concrete. A future test would have to validate the ability to make this distinction.

5. The SASW test has shown to be useful in locating the layer contributing to pavement distress when a weak point was identified by the impulse-response tests.

The ultrasonic-surface-wave and the ultrasonic-body-wave tests were not directly used to identified pavement conditions, but may prove to be useful in the future in dealing aging and fine cracking.

Conclusions

At the end of this project, it can be concluded that

1. The new SPA nondestructive testing device is useful for maintenance activities.

2. The SPA can easily, accurately, and repeatably collect and reduce information about the condition of pavements.

3. The SPA meets or exceeds the specifications for accuracy and precision developed to determine its usefulness for maintenance.

4. The SPA is field-worthy and rugged, and can handle different climatic conditions.

5. The final versions of the software and hardware function well and accurately determine a wide range of pavement conditions.

6. The SPA is ready for commercialization.

Recommendation for Future Developments

A fully functional prototype SPA system meeting the Strategic Highway Research Program performance specifications has been developed and tested. As with any prototype, further testing and development are required to establish confidence in the operation, durability, and usefulness of the SPA. The following aspects of the SPA would benefit from additional testing

1. The long-term reliability of the electrical and mechanical components in this application is unknown because the last prototype has been used for only six months. So far the device has performed with minimum problems; however, continued and extensive testing is required to establish the level of reliability.

The SPA hardware and software should be tested under a wide variety of pavement conditions to induce software and hardware failures, with consequent improvement in the robustness of those components.

2. The SPA has been tested on a limited set of pavement conditions. The system was specified and designed to estimate moduli in a three-layer pavement-base-subgrade system. The robustness of moduli estimation algorithms under other pavement conditions should be investigated.

3. Methods and software for converting the mechanical properties computed by the SPA to pavement conditions have been developed, but evaluation has been limited. More tests should be performed to develop a large database on this matter. Good candidates for these tests are SHRP General Purpose Sites (GPS) and Special Purpose Sites (SPS), as well as any site being tested with accelerated-testing facilities (Accelerated Loading Facility (ALF), Mobile Load Simulator (MLS), etc.).

Lessons Learned

The selection and testing of sites and determination of ground-truth for case studies are quite involved; extreme care and significant effort must be focused on these tasks. The proper site selection should involve many steps. Several sites should be selected ahead of time. A preliminary coring and visual inspection should be carried out to ensure that actual pavement sections are close to the original specifications. After the candidate site is selected, extensive site characterization should be undertaken; if applicable, "undisturbed" specimens of the subgrade and bag specimens of the base should be obtained for laboratory testing. The testing program should be implemented along with any other supporting tests. Based upon the results, several points should be cored for verification. The collected data should be carefully reexamined in the office. A second series of site tests should carefully investigate anomalous results. This process is time consuming and expensive; however, it is the best way to understand the limitations of the device.

Commercialization

The Seismic Pavement Analyzer has great potential for commercialization. The device has been designed and built to meet the needs of pavement and maintenance engineers. The

equipment can assist highway agencies in several ways. Its most obvious use is in network-level surveys as a routine maintenance tool. Also, highway agencies and research institutions can use the device as a high-level research tool for better understanding the behavior of pavements. The SPA provides comprehensive and accurate information at each test point.

Some of the unique and significant practical features of the system are

1. Almost all the data reduction is carried out in the field; minimal data reduction is required in the office.

2. The flexible structure of the software allows easy upgrade of the data reduction or interpretive capabilities of the device by either the manufacturer or the potential owner.

3. Rapid graphical presentation of all the pavement parameters allows the testing program to be modified or extended in the field. The data can be transmitted over a cellular telephone to an experienced engineer in the headquarters, while a technician collects data in the field.

4. All the measured pavement parameters are archived in a format that can be exported to a commercially available database or spreadsheet software; therefore, data reports can be produced quickly.

5. The SPA can be diagnosed, and recommendations for its repair can be given, over any cellular or public phone, minimizing down time of the equipment.

Plans for the commercialization of the SPA are being pursued at this time. It should be on the market in one year. The anticipated cost is substantially less than the cost of current state-of-the-art equipment.

References

1. Ameri-Gaznon, M., and D. N.Little. 1988. "Permanent Deformation Potential in Asphalt Concrete Overlay Over Portland Cement Concrete Pavements." Research Report 452-3F, Texas Transportation Institute, College Station, TX.

2. Bell, C. A. 1989. "Summary Report on the Aging of Asphalt-Aggregate Systems." Report SHRP-A-305. Strategic Highway Research Program, National Research Council, Washington, DC.

3. Carpenter, S. H., M. I. Darter, and B. J. Dempsey. 1981. "A Pavement Moisture Accelerated Distress Identification System. Volume 2: Users Manual." Research Report FHWA-RD-81-080. Federal Highway Administration, U.S. DOT, Washington, DC.

4. Cedergren, H. R. 1974. *Drainage of Highway and Airfield Pavements*. New York: John Wiley and Sons.

5. Darter, M. I. 1977. "Design of Zero-Maintenance Plain Jointed Pavement. Volume II: Design Manual." Report FHWA-RD-77-112, Federal Highway Administration, US DOT, Washington, DC.

6. Dempsey, B. J. 1982. "Laboratory and Field Studies of Channeling and Pumping." *Transportation Research Record* (National Research Council, Washington, DC) 849:1-12.

7. Dobry, R., and G. Gazetas. 1986. "Dynamic Response of Arbitrary Shaped Foundations." *Journal of Geotechnical Engineering* (American Society of Civil Engineers, New York) 112, no. 2, 2:109-35.

8. Goodrich, J. L. 1988. "Asphalt and Polymer Modified Asphalt Properties Related to Performance of Asphalt Concrete Mixtures." In *Proceedings*, Association of Asphalt Paving Technologists (Minneapolis, MN) 57:116-75.

9. Markow, M. J. 1982. "Simulating Pavement Performance under Various Moisture Conditions." *Transportation Research Record* (National Research Council, Washington, DC) 849:24-9.

10. Maser, K. R. and M. J. Markow. 1990. "Measuring Systems and Instrumentation for Evaluating the Effectiveness of Preventive Maintenance." Report SHRP-MIUWP-91-513. Strategic Highway Research Program, National Research Council, Washington, DC.

11. Miller, G. F., and H. Pursey. 1955. "On the Partition of Energy between Elastic Waves in a Semi-Infinite Solid." In *Proceedings*, International Conference on Microzonation for Safer Construction: Research and Application (Society of Exploration Geophysicists, Seattle, WA) Vol. 2, 545-58.

12. Nazarian, S., R. D. Baker and R. E. Smith. 1991. "Measurement Concepts and Technical Specification of Seismic Pavement Analyzer Device," Strategic Highway Research Program, National Research Council, Washington, DC (unpublished report).

13. Nazarian S. and M. Desai. 1993. "Automated Surface Wave Testing: Field Testing," *Journal of Geotechnical Engineering* (American Society of Civil Engineers, New York) 119, no. GT7:1094-112.

14. Nazarian, S., S. Reddy, and M. Baker. 1993. "Determination of Voids in Rigid Pavements Using the Impulse Response Method." STP 1198, American Society for Testing and Materials, Philadelphia, PA.

15. Nazarian, S., and K. H. Stokoe. 1989. "Nondestructive Evaluation of Pavements by Surface Wave Method." STP 1026, American Society for Testing and Materials, Philadelphia, PA.

16. Qian X. 1990. "Dynamic Behavior of Unsaturated Cohesionless Soil." Dissertation, The University of Michigan, Ann Arbor.

17. Raad, L. 1982. "Pumping Mechanism of Foundation Soils under Rigid Pavements." *Transportation Research Record* (National Research Council, Washington, DC) 849:29-47.

18. Reddy, S. 1992. "Determination of Voids in Rigid Pavements Using the Impulse Response Method." M.S. thesis, The University of Texas at El Paso, El Paso.

19. Richardson, M. H., and D. L. Formenti. 1982. "Parameter Estimation from Frequency Response Measurements Using Rational Fraction Polynomials." In *Proceedings*, First International Modal Analysis Conference (Society for Experimental Mechanics, Orlando, FL), 167-81.

20. Rodhe, G. T., W. Yang, C. P. Henry, M. Kartsounis, and R. E. Smith. 1990. "Users Guide to the Texas Flexible Pavement System (TFPS) Program." Texas Transportation Institute, College Station, TX.

21. Sansalone, M., and N. J. Carino. 1986. "Impact-Echo: A Method for Flaw Detection in Concrete Using Transient Stress Waves." Report NBSIR 86-3452. National Bureau of Standards, Gaithersburg, MD.

22. Smith, K. T., M. I. Mueller, M. I. Darter, and D. G. Peshkin. 1990. "Performance of Jointed Concrete Pavements. Volume II: Evaluation and Modification of Concrete Pavement Design and Analysis Models." Report FHWA-RD-89-137, Federal Highway Administration, US DOT, Washington, DC.

23. Tia, M., B. E. Ruth, C. T. Charai, J. M. Shiau, D. Richardson, and J. Williams. 1988. "Investigation of Original and In-Service Properties for Development of Improved Specifications: Final Phase of Testing and Analysis." Final Report. Engineering and Industrial Experiment Station, University of Florida, Gainsville, FL.

24. Torres, F., and B. F. McCullough. 1983. "Void Detection and Grouting Process." Research Report 249-3, Center for Transportation Research, The University of Texas, Austin, TX.

25. Uzan, J., and R. E. Smith. 1988. "TFPS Technical Report." Draft Report for Research Project 455, Texas Transportation Institute, Texas A&M University, College Station, TX.

26. Von Quintus, H., J. Scherocman, T. Kennedy, and C. S. Hughes. 1991. "Asphalt Aggregate Mixture Analysis System." Report 338 (National Cooperative Highway Research Program, National Research Council, Washington, DC).

27. Willis, M. E., and M. N. Toksoz. 1983. "Automatic P and S Velocity Determination from Full Wave form Digital Acoustic Logs." *Geophysics* 48, no. 12: 1631-44.

28. Wu, S., D. H. Gray, and F. E. Richart. 1984. "Capillary Effects on Dynamic Modulus of Sands and Silts." *Journal of Geotechnical Engineering* (American Society of Civil Engineers, New York) 110, no. GT9:1188-1203.

29. Yuan, D., and S. Nazarian. 1993. "Automated Surface Wave Testing: Inversion Technique." *Journal of Geotechnical Engineering* (American Society of Civil Engineers, New York) 119, no. GT7:1112-26.

Appendix A

Wave Propagation Theory

This appendix introduces the principle of wave propagation and clarifies the relationships between wave velocities and moduli.

For engineering purposes, profiles of most pavement sections can be reasonably approximated by a layered half-space. With this approximation, the profiles are assumed to be homogeneous and to extend to infinity in two horizontal directions. They are assumed to be heterogenous in the vertical direction, often modeled by a number of layers with constant properties within each layer. In addition, it is assumed that the material in each layer is elastic and isotropic.

Seismic Body Waves

Wave motion created by a disturbance within an ideal whole-space can be described by two kinds of waves: compression waves and shear waves. Collectively, these waves are called body waves, as they travel within the body of the medium. Compression and shear waves can be distinguished by the direction of particle motion relative to the direction of wave propagation.

Compression waves (also called dilatational waves, primary waves, or P-waves) exhibit a push-pull motion. As a result, wave propagation and particle motion are in the same

direction. Compression waves travel faster than the other types of waves, and therefore appear first in a direct travel-time record.

Shear waves (also called distortional waves, secondary waves, or S-waves) generate a shearing motion, causing particle motion to occur perpendicular to the direction of wave propagation. Shear waves can be polarized. If the directions of propagation and particle motion are contained in a vertical plane, the wave is "vertically polarized." This wave is called an SV-wave. However, if the direction of particle motion is perpendicular to a vertical plane containing the direction of propagation, the wave is "horizontally polarized." This wave is termed an SH-wave. Shear waves travel more slowly than P-waves and thus appear as the second major wave type in a direct travel-time record.

Seismic Surface Waves

In a half-space, other types of waves occur in addition to body waves. These waves are called surface waves. Many different types of surface waves have been identified and described. The two major types are Rayleigh waves and Love waves.

Surface waves propagate near the surface of the half-space. Rayleigh waves (R-waves) propagate at a speed of approximately 90 percent of S-waves. Particle motion associated with R-waves is composed of both vertical and horizontal components, that, when combined, form a retrograde ellipse close to the surface. However, with increasing depth, R-wave particle motion changes to a pure vertical and, finally, to a prograde ellipse. The amplitude of motion attenuates quite rapidly with depth. At a depth equal to about 1.5 times the wavelength, the vertical component of the amplitude is about 10 percent of that at the ground surface.

Particle motion associated with Love waves is confined to a horizontal plane and is perpendicular to the direction of wave propagation. This type of surface wave can exist only when low-velocity layers are underlain by higher velocity layers, because the waves are generated by total multiple reflections between the top and bottom surfaces of the low-velocity layer. As such, Love waves are not generated in pavement sections.

The propagation of body waves (shear and compression waves) and surface waves (Rayleigh waves) are away from a vertically vibrating circular source at the surface of a homogeneous, isotropic, elastic half-space. Miller and Pursey (1955) found that approximately 67 percent of the input energy propagates in the form of R-waves. Shear and compression waves carry

and compression waves carry 26 and 7 percent of the energy, respectively. Compression and shear waves propagate radically outward from the source. R-waves propagate along a cylindrical wave front near the surface. Although, body waves travel faster than surface waves, body waves attenuate in proportion to $1/r^2$, where r is the distance from the source. Surface wave amplitude decreases in proportion to $1/r^{0.5}$.

Seismic Wave Velocities

Seismic wave velocity is defined as the speed at which a wave advances in the medium. Wave velocity is a direct indication of the stiffness of the material; higher wave velocities are associated with higher stiffness. By employing elastic theory, compression wave velocity can be defined as

$$V_p = [(\lambda + 2G)/\rho]^{0.5} \tag{A.1}$$

where

V_p = compression wave velocity,
λ = Lame's constant,
G = shear modulus, and
ρ = mass density.

Shear wave velocity, V_s, is equal to

$$V_s = (G/\rho)^{0.5} \tag{A.2}$$

Compression and shear wave velocities are theoretically interrelated by Poisson's ratio

$$V_p/V_s = [(1 - \nu)/(0.5 - \nu)]^{0.5} \tag{A.3}$$

where ν is the Poisson's ratio. For a constant shear wave velocity, compression wave velocity increases with an increase in Poisson's ratio. For a ν of 0.0, the ratio of V_p to V_s is equal to $\sqrt{2}$; for a ν of 0.5 (an incompressible material), this ratio is to infinity.

For a layer with constant properties, R-wave velocity and shear wave velocity are also related by Poisson's ratio. Although, the ratio of R-wave to S-wave velocities increases as Poisson's ratio increases, the change in this ratio is not significant. For Poisson's ratio of

0.0 and 0.5, this ratio changes from approximately 0.86 to 0.95, respectively. Therefore, it can be assumed that the ratio is equal to 0.90 without introducing an error larger than about 5 percent.

Equation A.3 can be rewritten as

$$\nu = [0.5(V_p/V_s)^2 - 1]/[(V_p/V_s)^2 - 1] \quad (A.4)$$

This equation can then be used to calculate Poisson's ratio once V_s and V_p are known.

Elastic Constants

Propagation velocities per se have limited use in engineering applications. In pavement engineering, Young's moduli of the different layers should be measured. Therefore, calculating the elastic moduli from propagation velocities is important.

Shear wave velocity, V_s, is used to calculate the shear modulus, G, by

$$G = \rho V_s^2 \quad (A.5)$$

in which ρ is the mass density. Mass density is equal to Υ_t/g, where Υ_t is the total unit weight of the material, and g is gravitational acceleration. If Poisson's ratio (or compression wave velocity) is known, other moduli can be calculated for a given V_s. Young's and shear moduli are related by

$$E = 2G(1 + \nu) \quad (A.6)$$

or

$$E = 2\rho V_s^2(1 + \nu) \quad (A.7)$$

In a medium where the material is restricted from deformation in two lateral directions, the ratio of axial stress to axial strain is called constrained modulus. Constrained modulus, M, is defined as

$$M = \rho V_p^2 \quad (A.8)$$

or in terms of Young's modulus and Poisson's ratio

$$M = [(1 - \nu)E]/[(1 + \nu)(1 - 2\nu)] \tag{A.9}$$

The Bulk modulus, B, is the ratio of hydrostatic stress to volumetric strain and can be determined by

$$B = M - (4/3)G \tag{A.10}$$

Appendix B

Additional Information from Texas Sites

As indicated in Chapter 10, more information than required for diagnosing pavement distress was collected at each site. The results from these extra tests at Texas sites are summarized in this appendix.

Tomball, Texas

The measurements of the shear modulus of the asphalt concrete (AC) layer are shown in figure B.1. Substantial variation in the modulus of the AC layer is evident. The modulus values vary from a minimum of 3.5 GPa to a high of about 9 GPa. The mean and the standard deviation are also shown in the figure. The mean value of the AC shear modulus is about 6.3 GPa, corresponding to an average-quality material. As shown in the figure with the three horizontal lines, the level of precision associated with the method is rather high. Repeated tests resulted in a coefficient of variation approximately 5 percent.

The below-average values can be attributed to minor cracking at the site. To prove this, a series of tests was carried out at 6-m spacing in the 150-m to 180-m range. At the beginning of this section (around 150 m), minor tight cracks could be observed only under the right lighting. However, beyond 160 m (before core 2), the cracks could not be detected. As reflected in the results, the two data points around 150 m were tested on minor cracked sections. The data points around 250 m were also on mostly cracked pavements.

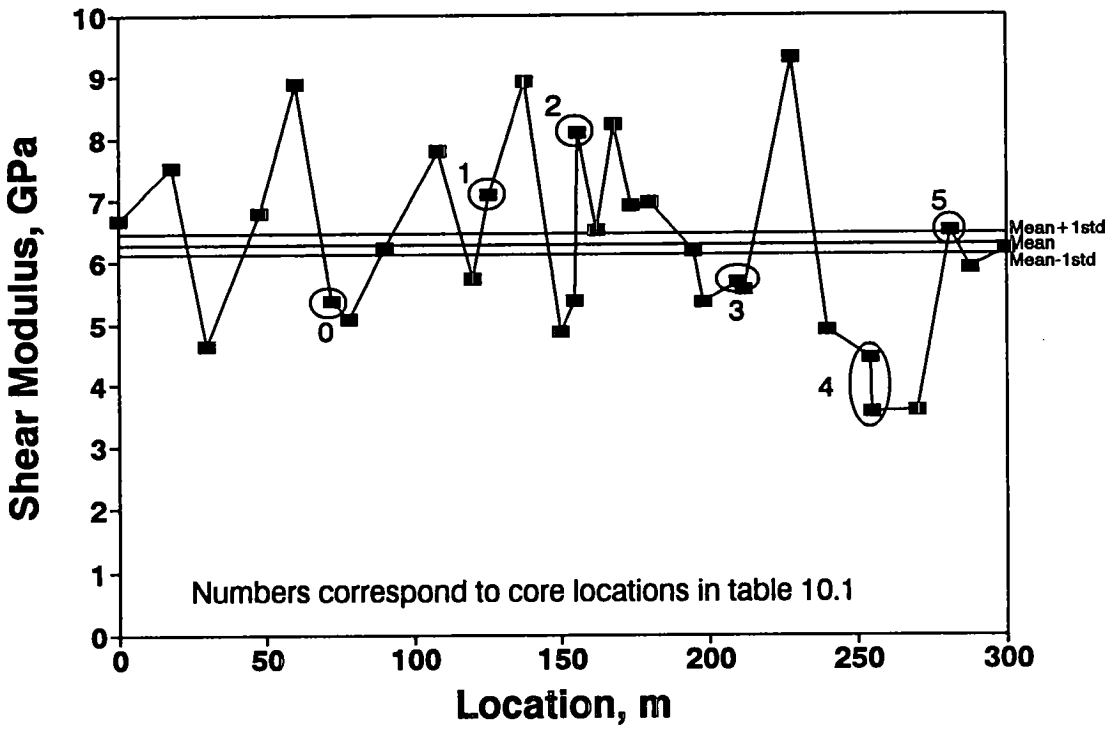

Figure B.1 - Variation in shear modulus of AC from ultrasonic-surface-wave tests at Tomball site

No plausible reason can be given for the points with high moduli, except that the material was actually stiffer.

The two points marked as core 4 were within 30 cm of each other. In the first case, a minor crack was located between the source and the two receivers (the point with the higher modulus), and in the second case the minor crack was between the two receivers (the point with the lower modulus). The modulus of the AC layer at the core locations cannot be compared with those of the FWD results, because of a lack of reasonable basin-fitting as discussed in Chapter 10.

Young's modulus values as determined from the ultrasonic-body-wave tests are shown in figure B.2. The mean Young's modulus at the section is about 13.5 GPa, corresponding to an average-quality AC layer. However, the coefficient of variation of the measurement is about 25 percent, which is rather large. Because of such a large coefficient of variation, the algorithm used to reduce ultrasonic body waves was significantly modified for tests in Georgia.

Even with such a large coefficient of variation, the pattern observed in this case is quite similar to that obtained for the more reliable ultrasonic-surface-wave test (see figure B.1). In other words, most of the points with low shear moduli in figure B.1 exhibit low Young's moduli with this technique.

The thickness of the AC layer as determined by the impact-echo tests is shown in figure B.3. The thickness of the layer varies significantly throughout the section. Even though the nominal thickness of the AC was 100 mm, the measured thicknesses varied between a minimum of 60 mm and a maximum of 180 mm. The figure also shows the actual thickness of the pavement at six core holes (labeled as points 0 through 5). The actual and predicted thicknesses are not in good agreement. The differences between the actual and measured values vary from about 60 percent to less than 3 percent. There are several reasons for this disagreement.

First, the coefficient of variation associated with the compression wave velocities (or Young's moduli) obtained from the ultrasonic-body-wave technique is rather large. As indicated above, the ultrasonic-body-wave technique at the site yielded large coefficients of variation (about 25 percent in moduli, which translates to 16 percent for compression wave velocities). Therefore, even if the peak frequency is determined perfectly the thickness would be estimated with a precision of about 16 percent.

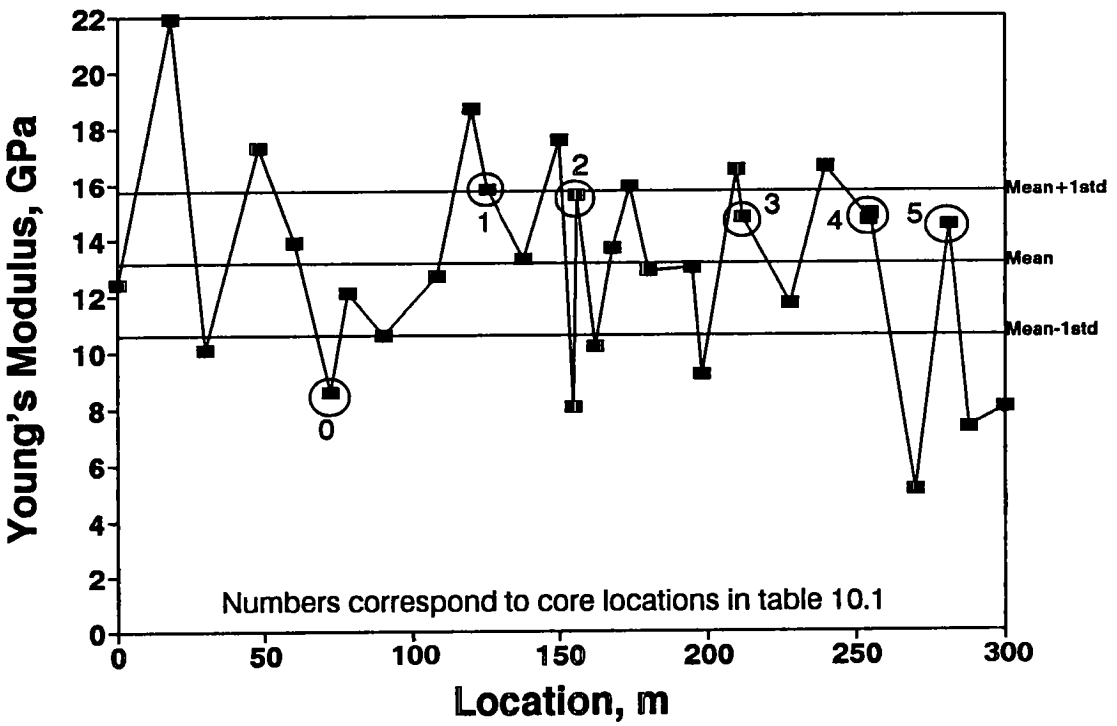

Figure B.2 - Variation in Young's modulus from ultrasonic-body-wave tests at Tomball site

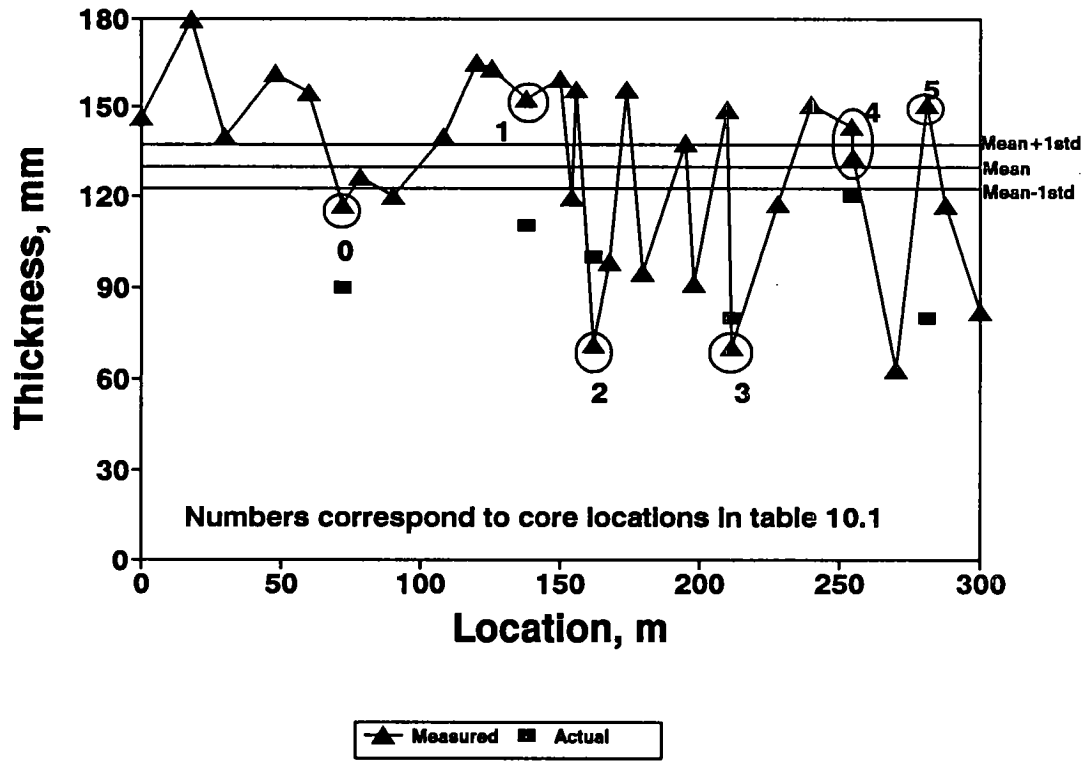

Figure B.3 - Variation in thickness of AC layer from impact-echo tests at Tomball site

The second problem has to do with the fact that several resonant peaks should be expected for such a composite pavement section (i.e., an AC layer over a rigid layer)—one from the vibration of waves trapped in the AC layer (the desirable peak), and one from the trapped waves in the composite layer. If the right spectral peak is not selected, then the thickness would be in error. For example, for core points 0 and 1 the program selected the wrong peaks therefore the thicknesses were grossly in error. However, for the remaining points the correct peaks were calculated, and the measured and actual thicknesses are within the expected variation of 15 to 20 percent, corresponding with the errors in determining the compression wave velocities.

It should be mentioned that for the two cases where the thicknesses were poorly estimated, the visual inspection of the IE tests would clearly reveal the existence of the desirable peak. However, the software did not pick the correct peaks because of the complexity of the problem. After this exercise, the software performing the IE test was extensively modified.

Houston, Texas

The measurements of Young's Modulus of the portland cement concrete layer are shown in figure B.4. Considering that the coefficient of variation associated with the version of the software used was about 16.5 percent, the compression wave velocities measured are more or less constant at about 35 GPa, corresponding to an average-quality concrete.

Some outliers are apparent in the results. Some of these points (such as those on slabs 3, 4 and 9) were due to the existence of a large crack between the source and the receivers. Typically one should expect a lower modulus at these points. However, our experience shows that if the cracks are significantly wide and deep, an unrealistically large modulus value may be obtained. Some other points (such as those on slabs 10 and 12) were caused by lack of robustness in the software. Again, the software was modified shortly after tests in Texas to remedy such problems.

Young's moduli are only reported for the approach side of each joint. For the leave side of the joint, most of the sensors of the SPA and the sources were on the opposite side of the joint. Propagation of waves across the joints for ultrasonic-body-wave tests was not practical.

The values of the shear modulus are shown in fig. B.5. In general, the shear moduli of the layer fall in a narrow range, with an average of about 16 GPa. This average modulus corresponds to an average quality concrete. The coefficient of variation was established as

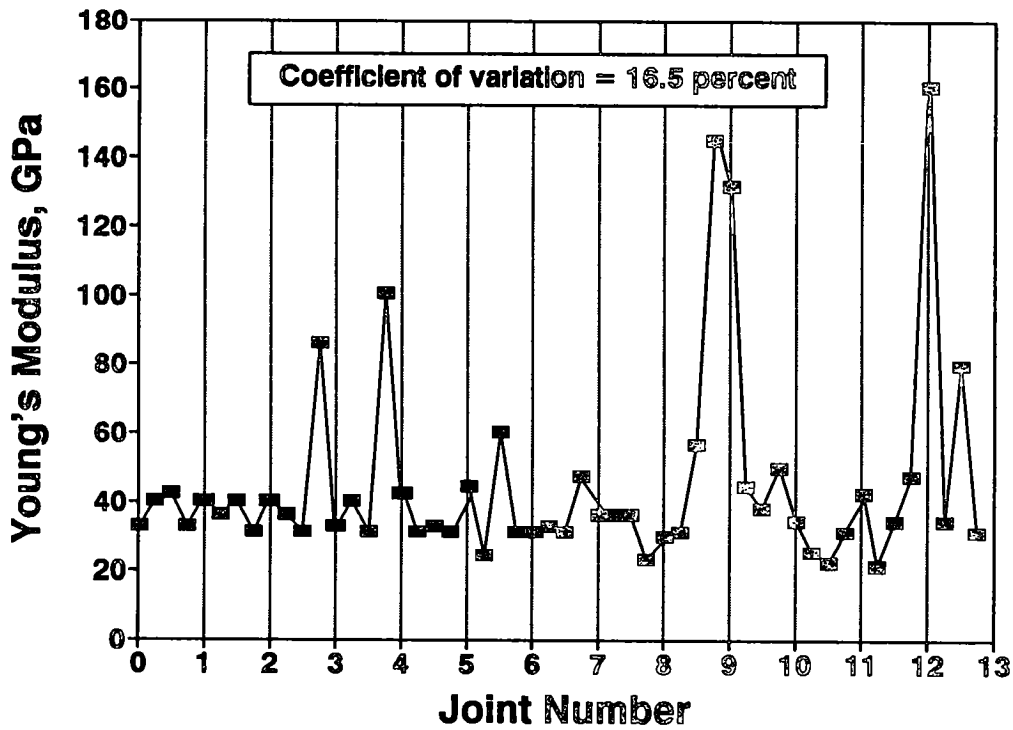

Figure B.4 - Variation in Young's modulus from ultrasonic body wave at Houston site

6.7 percent. Thus, as for the other test cases, the method is repeatable. In this case, all the anomalous test points correspond to the cracked pavement section, and the moduli of the cracked sections are all quite small. As with the ultrasonic-body-wave method, the modulus values are reported only for the approach side of the joints. Some of the anomalies do not occur concurrently between the two methods because different sensors are used to measure the shear and Young's moduli, as described in Chapter 6.

Poisson's ratio can be determined with the shear modulus (about 16 GPa) and Young's modulus (about 35 GPa). The average Poisson's ratio is about 0.13. This is slightly lower than expected for such a material; the typical Poisson's ratio for concrete is about 0.15.

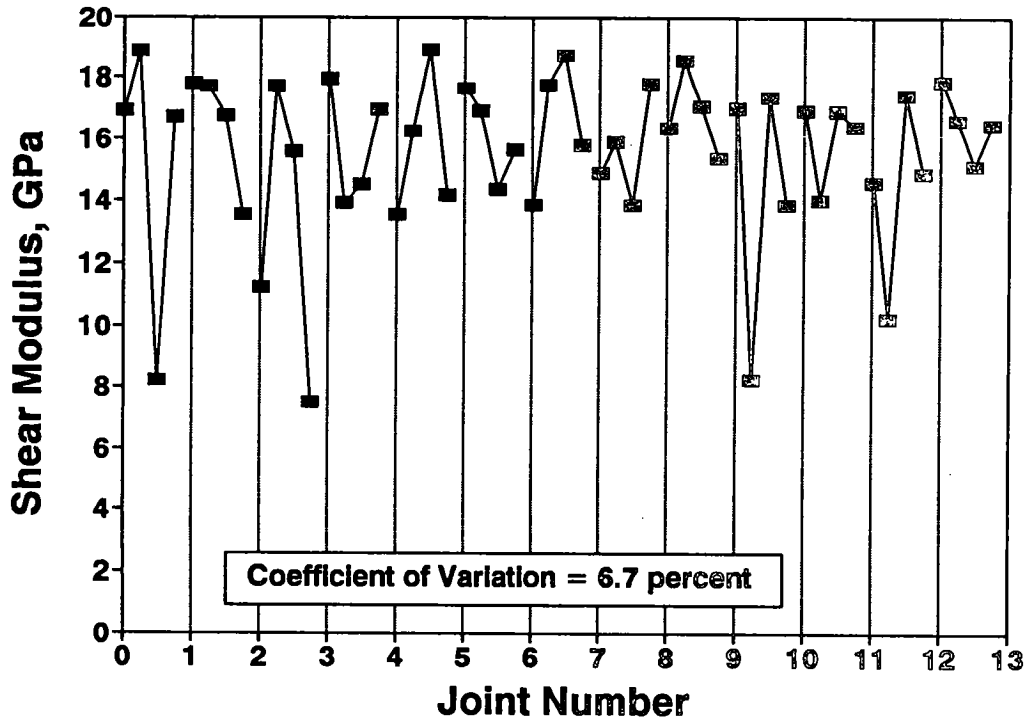

Figure B.5 - Variation in shear modulus from ultrasonic-surface-wave tests at Houston site

Appendix C

Additional Information from Georgia Sites

As indicated in Chapter 11, more information than required for diagnosing pavement distress was gathered at each site. The extra information for each site in Georgia is presented in this Appendix.

Gwinett County, Georgia—I-85

Thin Continuously-Reinforced-Concrete-Pavement Overlay

The shear and Young's moduli of the concrete layer are reported in figure C.1. A large variation in the moduli can be seen. A significant portion of the original section had been replaced, and numerous patches existed at the site; therefore, the quality of the concrete varied from point to point. However, tests were repeated at several points. As seen in the figure, some small variations in the moduli occurred in the repeat tests.

Thick Continuously-Reinforced-Concrete-Pavement Overlay

The values of the shear and Young's moduli for the thick layer are shown in figure C.2. Both moduli vary somewhat with the test location. This is reasonable because of extensive repairs done at the joints. The anomalous data point on slab 1 corresponds to severely

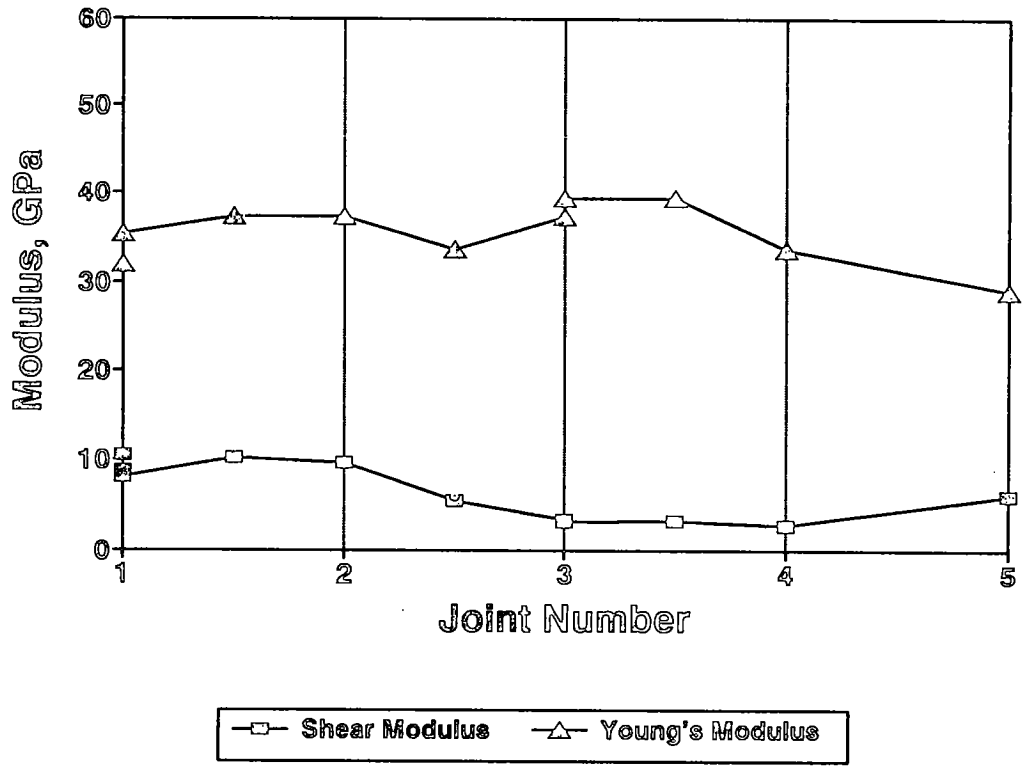

Figure C.1 - Variations in shear and Young's moduli of overlay at thin CRCP section tested on I-85

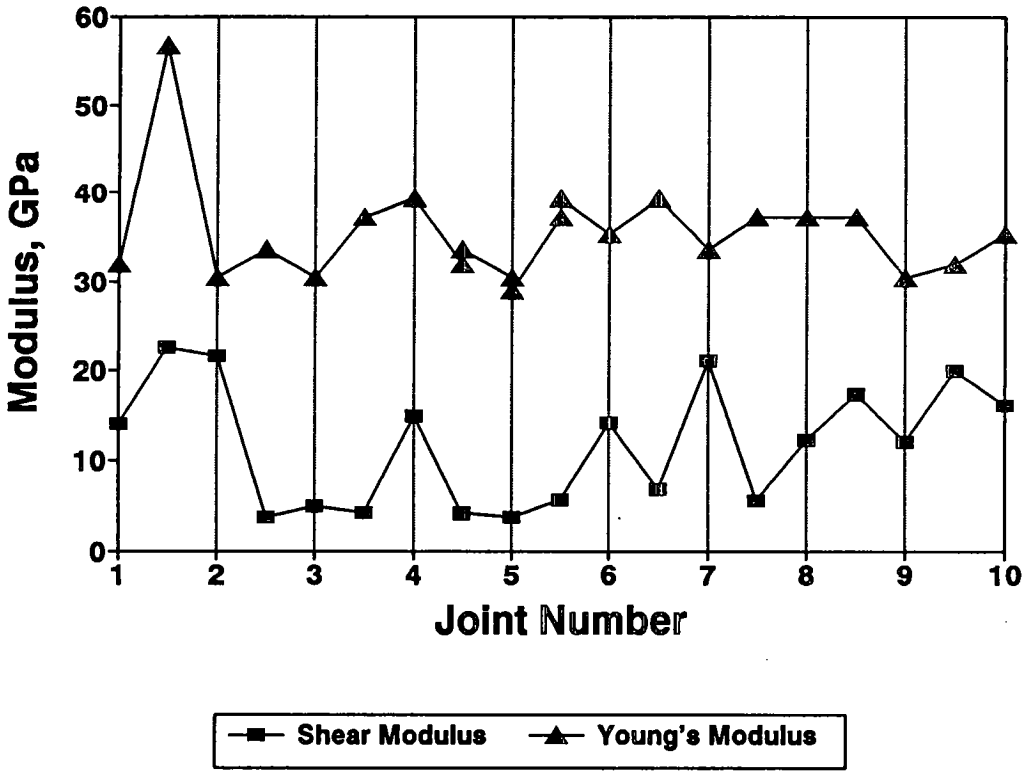

Figure C.2 - Variation in shear and Young's moduli of overlay at thick CRCP section tested on I-85

cracked concrete at the test point. In general, based upon the average shear and Young's moduli, the concrete condition at this site can be considered below average.

The measurements of thickness are shown in figure C.3. along with, the actual thickness of two points. Again, the nominal thickness and the expected range of the thickness are indicated with three horizontal lines. Most data points are within or close to the these limits.

Two points, marked in figure C.3, were cored to verify the thicknesses determined by the Seismic Pavement Analyzer. The actual and predicted thicknesses are within 15 percent of each other. Again, the dominant response has been from the interface of the two concrete layers, indicating debonding.

Jointed-Reinforced-Concrete-Pavement Overlay

This section had also been extensively repaired. Our condition survey sheet revealed that many of the test points were on or very close to actual or repaired cracks. This is reflected in the SPA's inability to determine the moduli with consistency (see figure C.4). Large variations in the data can be seen. Given the difficulty in determining the modulus values of concrete, one should not expect to determine thickness accurately. When a highly cracked section is tested, the compression wave velocity is affected by these cracks. The measured compression wave velocity is therefore not representative of the concrete tested. To obtain thickness, the "true" compression wave velocity of a concrete layer must be known.

The measurements of thickness for this section are shown in figure C.5. As expected, much variation in thickness is observed. In this case, most data points are outside the range of expected values. The actual thicknesses of two core locations are also shown. In one case (joint 8) the thickness is reasonably predicted. At the second point (joint 10), the thickness is greatly underpredicted. The raw data indicate that the resonance frequency corresponding to the actual thickness existed in the data. However, a peak corresponding to reflections from other sources (probably from the cracks) was slightly more dominant. These tests indicate that the current prototype may not be able to determine accurately the thickness of highly deteriorated concrete.

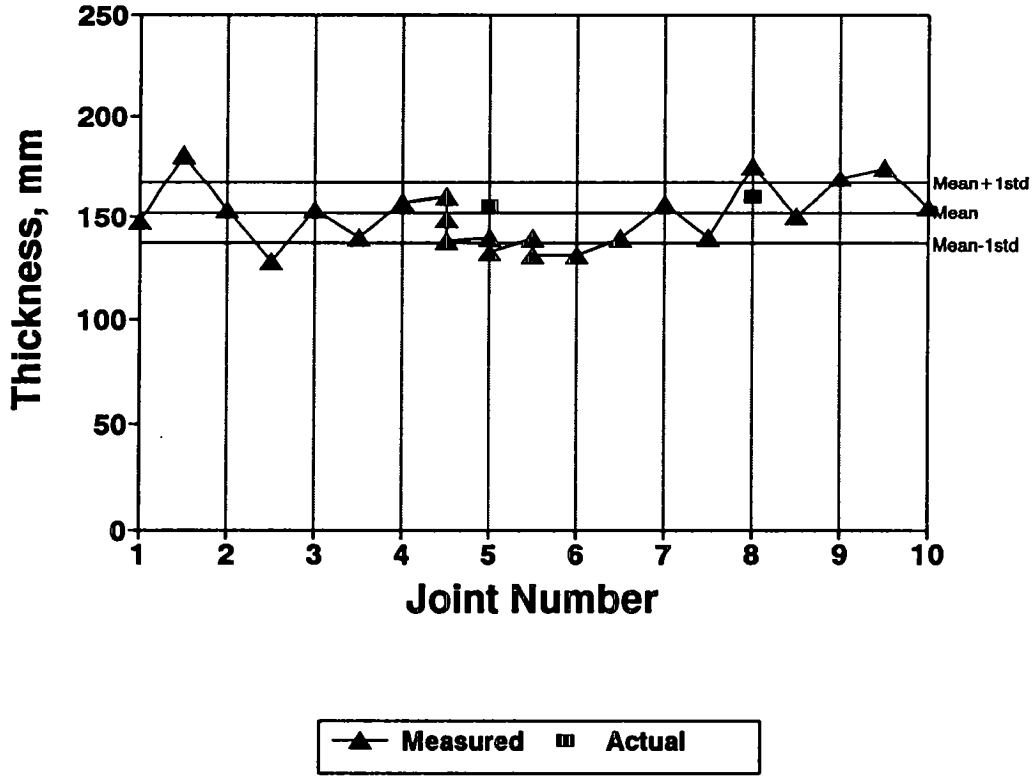

Figure C.3 - Variation in thickness of overlay at thick CRCP section tested on I-85

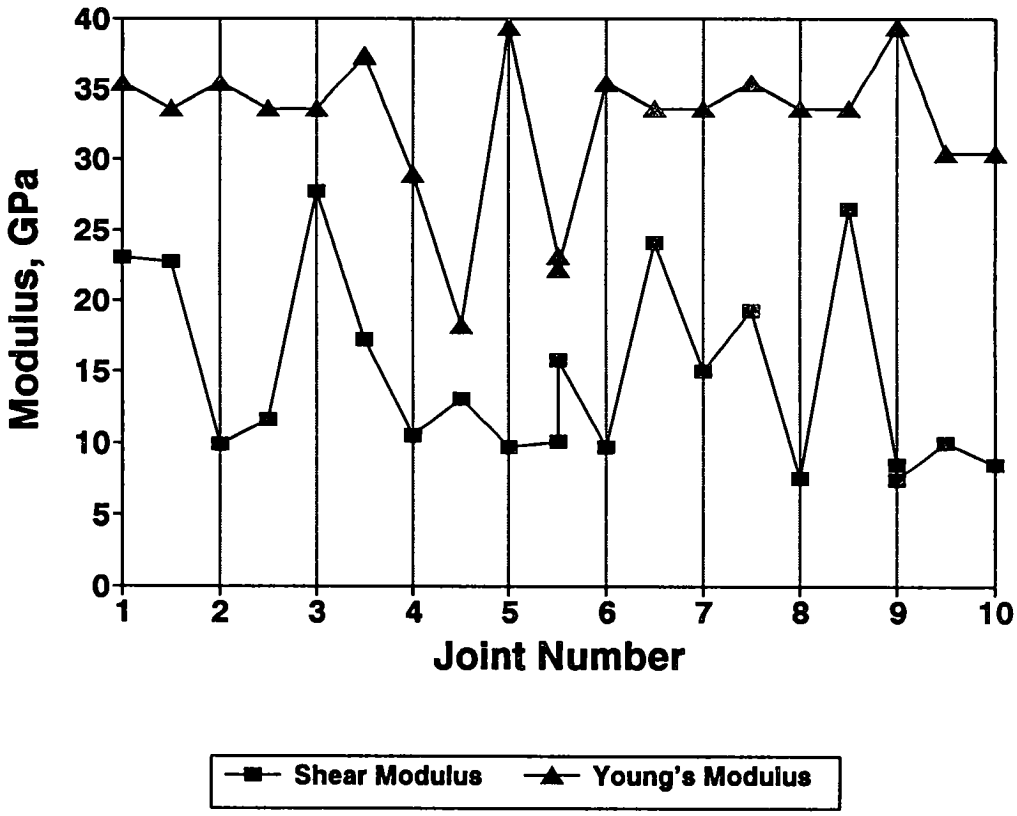

Figure C.4 - Variations in shear and Young's moduli of overlay at JRCP section tested on I-85

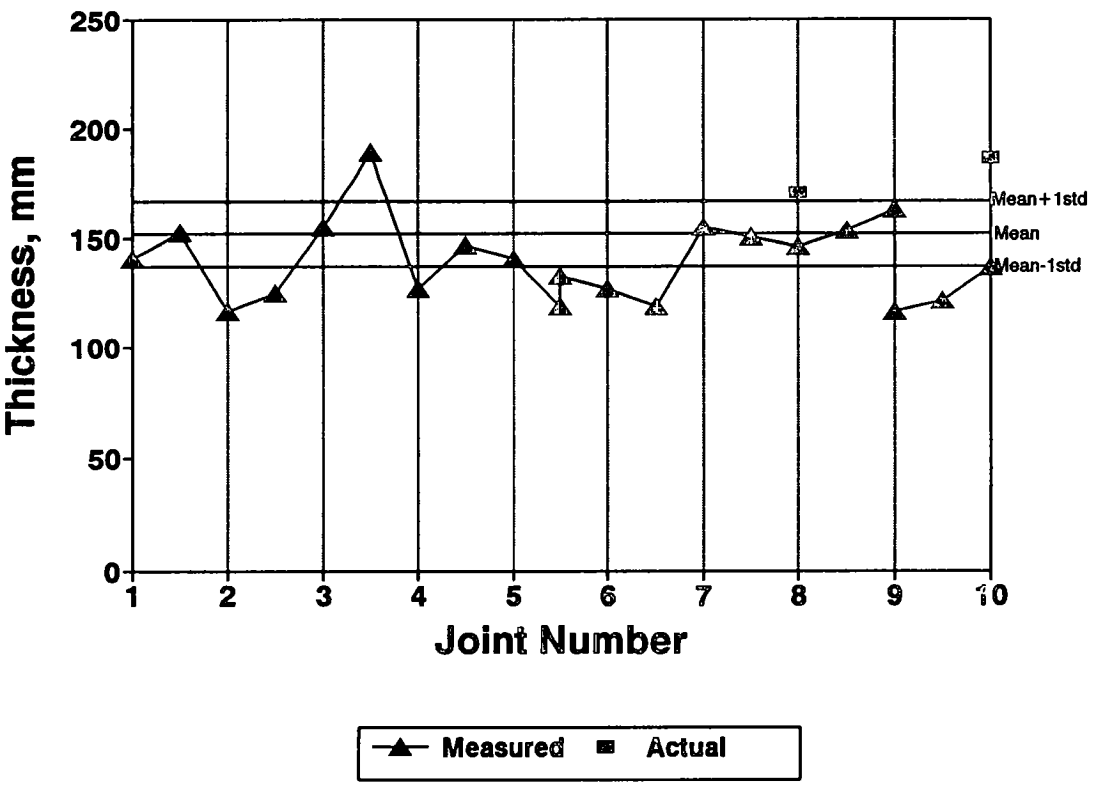

Figure C.5 - Variation in thickness of overlay at JRCP section tested on I-85

Augusta, Georgia—I-20

The values of Young's and shear moduli are shown in figure C.6. Only the properties from the middle of the slab are shown here. Some variation in the results can be attributed to the variability in the material properties and also to some variability in data interpretation. In most cases, the material properties vary because both methods measure consistently lower or higher for the same points. In the middle of slab 3, similar values for the shear and Young's moduli are reported; the reason for this discrepancy is not known. One possible explanation, aside from interpretation error, is the existence of a crack between the source and the accelerometer used to measure the compression wave velocity.

In general, the average Young's and shear moduli are 33 GPa and 15 GPa, respectively. These values represent average-quality concrete. From the average shear and Young's moduli, the average Poisson's ratio is about 0.14. This is an acceptable value for Poisson's ratio of concrete.

The measurements of the thickness of the portland cement concrete are shown in figure C.7. At the two core holes, the actual thicknesses of concrete is about 230 mm. The two points on slabs 11 and 12 that exhibit smaller thickness are in the area where the concrete requires repair. The reason for the thinness of slab 8 is not known.

Augusta, Georgia—River Watch Parkway

The values of the shear modulus of the asphalt concrete layer are shown in figure C.8. The pavement in locations around 600 m was not tested because there was a bridge. Moduli are clustered at two levels. Between locations 0 m and 600 m, the moduli are higher than the rest of the section, because of the temperature sensitivity of the AC layer. The 600-m section (between 0 m and 600 m) was tested in the early morning when the pavement was cold; the other sections were tested later, when the sun had been out, raising ambient temperature.

The variation in modulus with temperature for the entire section is shown in figure C.9. A smooth trend of reduction in modulus with increase in temperature is obvious. The pavement temperature varied between 2° and 22°C on that day.

This test demonstrated that the AC layer is more or less uniform. Based upon the average shear modulus of about 6 GPa at 20°C, the AC layer is considered of high quality.

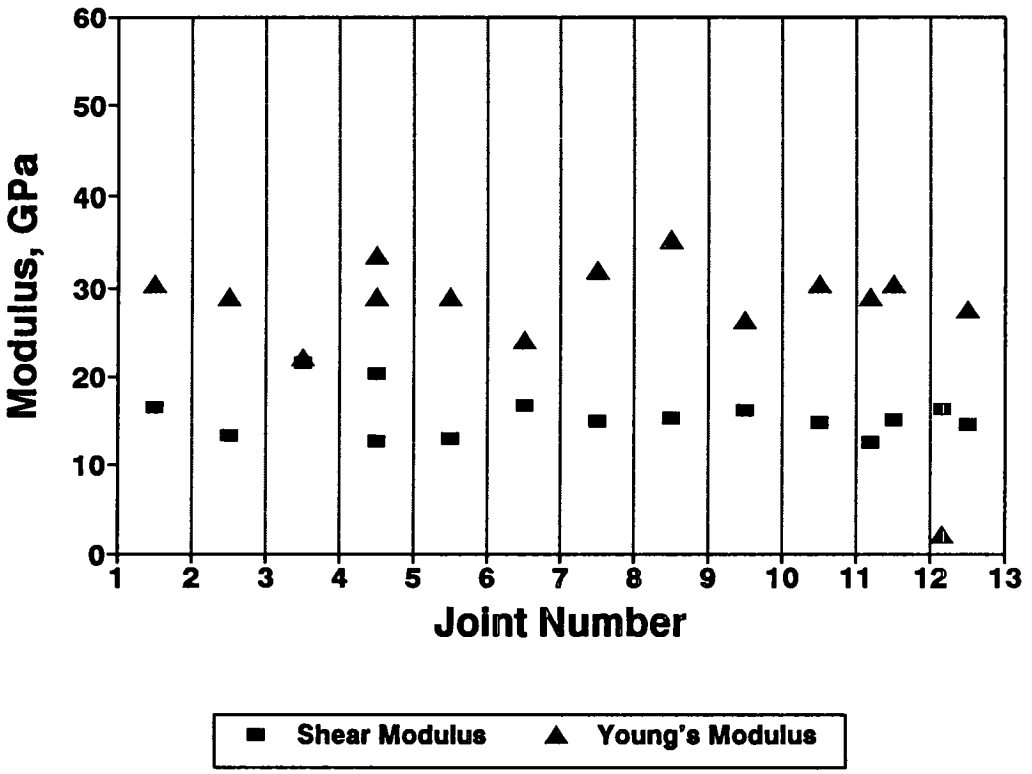

Figure C.6 - Variations in shear and Young's moduli of PCC layer at I-20 site

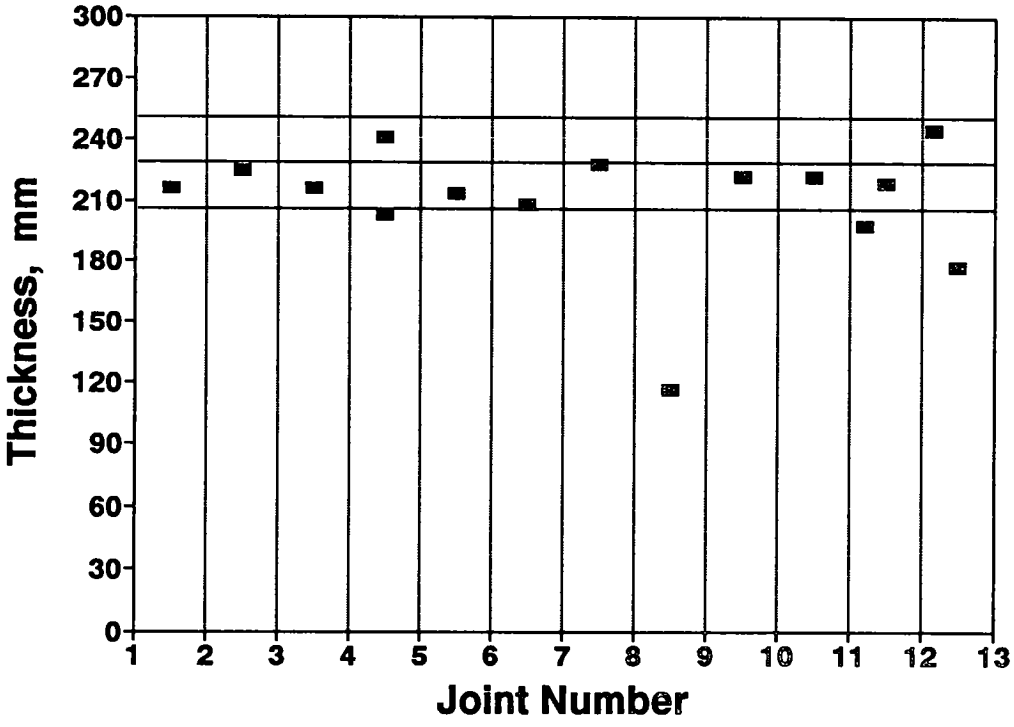

Figure C.7 - Variation in thickness of PCC layer at I-20 site

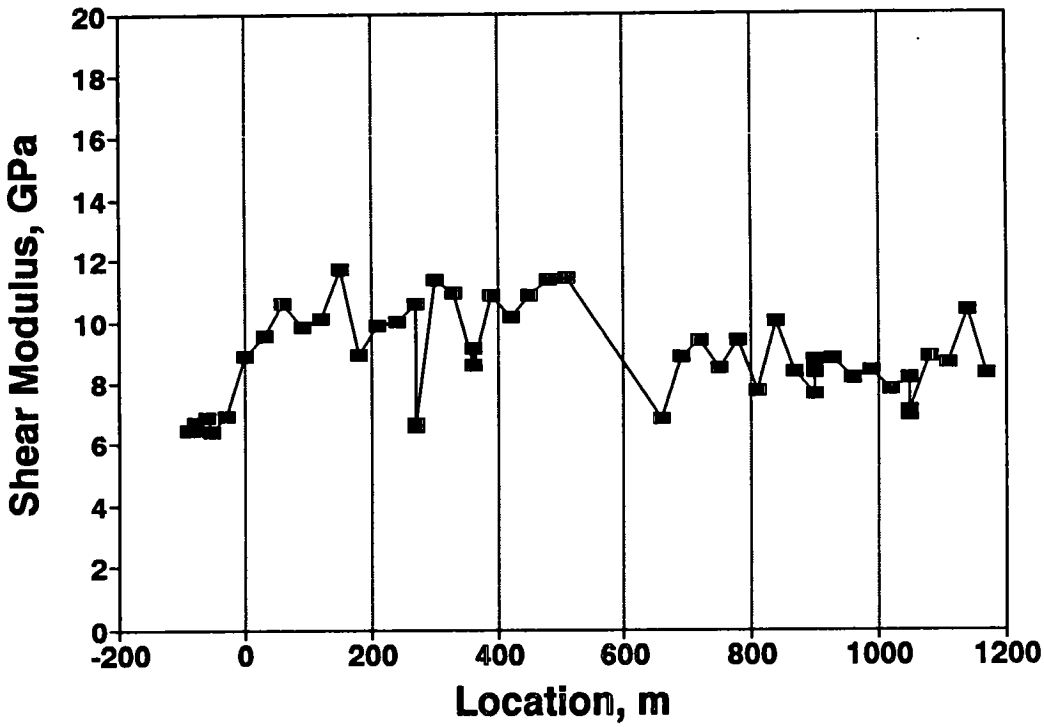

Figure C.8 - Variation in shear modulus at River Watch Parkway

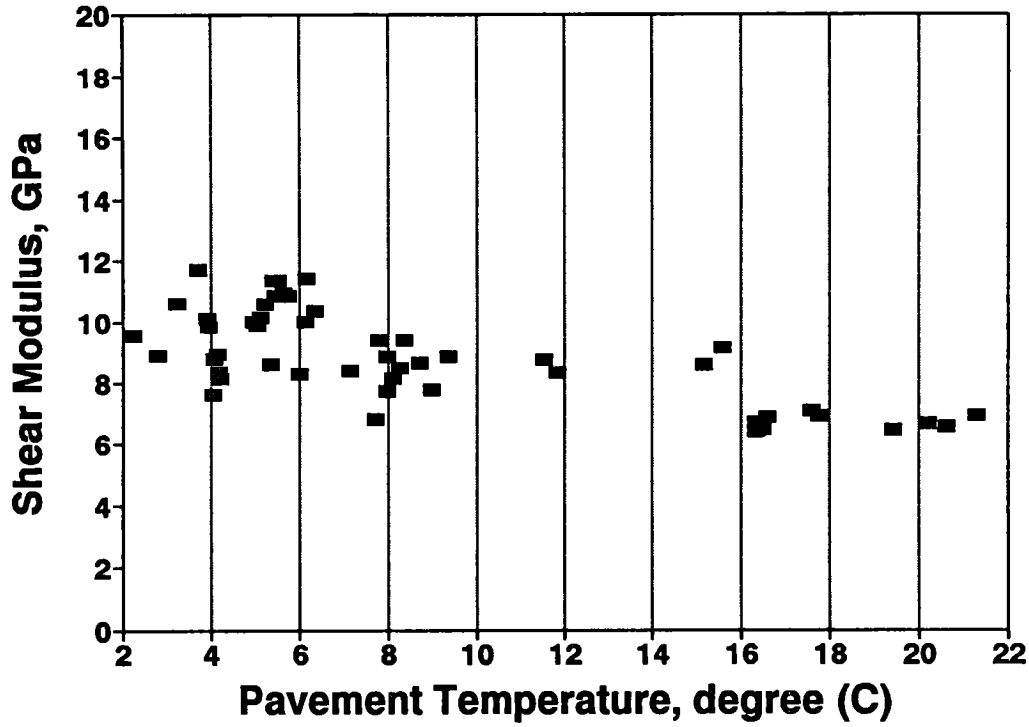

Figure C.9 - Variation in modulus with temperature at River Watch Parkway

The values of Young's modulus as determined from the ultrasonic-body-wave tests are shown in figure C.10. The same clustering of moduli can be seen in the results of this test as well; the two independent testing methodologies yield relatively similar results. From the shear and Young's moduli, Poisson's ratio is in the range of 0.29 to 0.35, which is quite reasonable.

The measurements of thickness of the AC layer as determined by the impact-echo tests are shown in figure C.11. The thickness of the layer does not vary significantly throughout the section. The nominal thickness of the AC was 225 mm $\pm$ 12 mm; the measured thicknesses varied between a minimum of 180 mm and a maximum of 235 mm. The figure also shows the actual thickness of the pavement at seven core holes. The actual and predicted thicknesses are typically in good agreement, except for the two cores installed at -54 m and -84 m. The difference between the actual and measured values is at worst 20 percent and is typically within 10 percent. Such good measurements of the AC thickness with IE tests were possible because the layer was quite thick and stiff. For thinner and less stiff AC layers such good measurements are not expected.

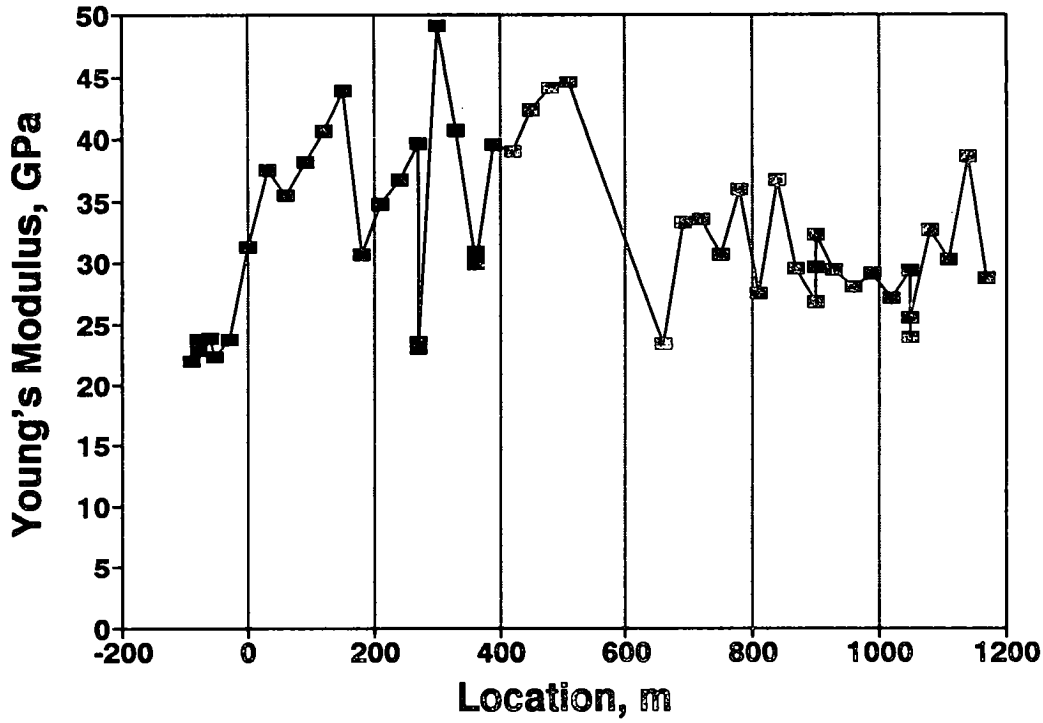

Figure C.10 - Variation in Young's modulus at River Watch Parkway

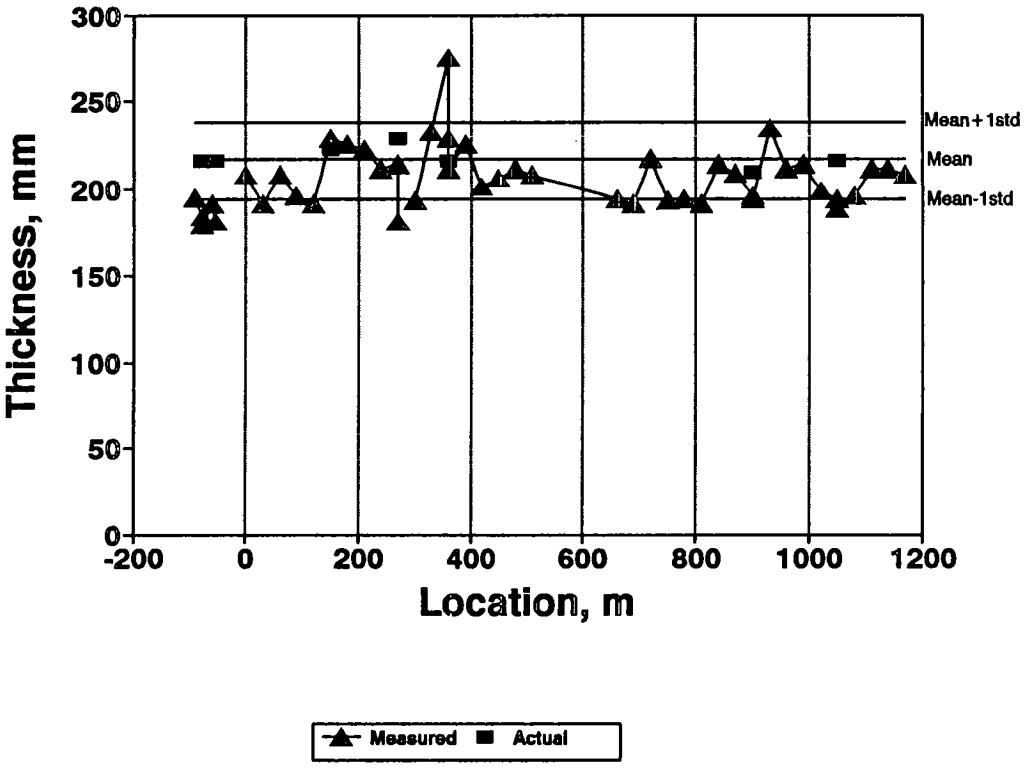

Figure C.11 - Variation in thickness at River Watch Parkway

Highway Operations Advisory Committee

Dean M. Testa, *chairman*
Kansas Department of Transportation

Clayton L. Sullivan, *vice-chairman*
Idaho Transportation Department

Ross B. Dindio
The Commonwealth of Massachusetts Highway Department

Richard L. Hanneman
The Salt Institute

Rita Knorr
American Public Works Association

David A. Kuemmel
Marquette University

Magdalena M. Majesky
Ministry of Transportation of Ontario

Michael J. Markow
Cambridge Systematics, Inc.

Gerald M. (Jiggs) Miner
Consultant

Richard J. Nelson
Nevada Department of Transportation

Rodney A. Pletan
Minnesota Department of Transportation

Michel P. Ray
The World Bank

Michael M. Ryan
Pennsylvania Department of Transportation

Bo H. Simonsson
Swedish Road and Traffic Research Institute

Leland Smithson
Iowa Department of Transportation

Arlen T. Swenson
John Deere

Anwar E.Z. Wissa
Ardaman and Associates, Inc.

John P. Zaniewski
Arizona State University

Liaisons

Ted Ferragut
Federal Highway Administration

Joseph J. Lasek
Federal Highway Administration

Frank N. Lisle
Transportation Research Board

Byron N. Lord
Federal Highway Administration

Mohamed Y. Shahin
U.S. Army Corps of Engineers

Harry Siedentopf
Federal Aviation Administration

Jesse Story
Federal Highway Administration

Expert Task Group

Gary Demich
Washington State Department of Transportation

Wouter Gulden
Georgia Department of Transportation

Rudy Hegmon
Federal Highway Administration

Dwight Hixon
Oklahoma Department of Transportation

Frank N. Lisle
Transportation Research Board

Gerald (Jiggs) Miner
Consultant

Michael M. Ryan
Pennsylvania Department of Transportation